UNIVERSITY OF KWAZULU-NATAL ™

INYUVESI YAKWAZULU-NATALI

Increase in live infected cell number with drug and generation of a quasispecies are consequences of multiply HIV infected cells

Laurelle Jackson

Submitted in fulfilment of the requirements for the degree of Doctor of Philosophy (Medicine) in the School of Laboratory Medicine and Medical Sciences, College of Health Sciences, University of KwaZulu-Natal

October 2018

DECLARATION

I, Miss **Laurelle Jackson**, declare as follows:

(i) The research proposed in this dissertation, except where otherwise indicated, is my original work.

(ii) This thesis has not been submitted for any degree or examination at any other university.

(iii) This thesis does not contain other persons' data, pictures, graphs or other information, unless specifically acknowledged as being sourced from other persons.

(iv) This thesis does not contain other persons' writing, unless specifically acknowledged as being sourced from other researchers. Where other written sources have been quoted, then:

a.) their words have been re-written but the general information attributed to them has been referenced;

b.) where their exact words have been used, their writing has been placed inside quotation marks, and referenced.

(v) Parts of this thesis was published in a publication titled 'Incomplete inhibition of HIV infection results in more HIV infected lymph node cells by reducing cell death', with myself and Jessica Hunter as the primary authors.

(vi) This dissertation does not contain text, graphics or tables copied and pasted from the internet, unless specifically acknowledged, and the source being detailed in the dissertation and in the References sections.

Signed: 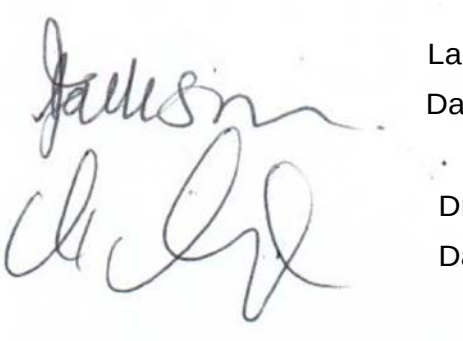 Laurelle Jackson (student)
Date: 10/09/2018

Signed: Dr. Alex Sigal (supervisor)
Date: 10/09/2018

LIST OF PUBLICATIONS

1. **Jackson L**, Hunter J, Cele S, Markham Ferreira I, Young A, Karim F, Madansein R, Dullabh KJ, Chen C, Buckels NJ, Ganga Y, Khan K, Boullé M, Lustig G, Neher RA, Sigal A (2017) Incomplete inhibition of HIV infection results in more HIV infected lymph node cells by reducing cell death. *Elife*. 7:e30134. 10.7554/eLife.30134

2. Boullé M, Müller TG, Dähling S, Ganga Y, **Jackson L**, Mahamed D, Oom L, Lustig G, Neher RA, Sigal A (2016) HIV Cell-to-Cell Spread Results in Earlier Onset of Viral Gene Expression by Multiple Infections per Cell. *PLoS Pathog* 12: e1005964. https://doi.org/10.1371/journal.ppat.1005964

ACKNOWLEDMENTS

In the past 5 years, conducting the work in this thesis, would not have been possible without the help and support from many individuals, who I would like to acknowledge and thank:

My supervisor, Dr. Alex Sigal for all his time and effort in helping design projects that are unique and significant to the field of HIV infection biology.

All the members in the lab. Jess Hunter for her input, hard work and effort for the eLife publication. Sandile Cele, Dr. Gil Lustig, Andrew Young, Isabella Markham Ferrriera, Yashica Ganga, Shi-Hsia Hwa, Mikael Boullè and Vivienne Clarence for their assistance with administration, guidance on project design as well as technical help.

The collaborators of the Sigal lab. These include Dr. Richard Neher (Biozentrum and SIB Swiss Institute of Bioinformatics, University of Basel, Basel, Switzerland) and Prof. Tulio de Oliveira (KwaZulu-Natal Research and Innovation Sequencing Platform, UKZN, Durban, South Africa).

The clinical core team, Farina Karim and Khadija Khan, for your efforts in managing the clinical samples required for the studies.

The cardiothoracic surgeons Rajhmun Madansein, Kaylesh J Dullabh, Chih-Yuan Chen and Noel J Buckels for the lymph nodes obtained from a field of surgery of participants undergoing surgery for diagnostic purposes and/or complications of inflammatory lung disease.

Lastly, the National Research Foundation (NRF) in South Africa for providing me with funding for my PhD.

TABLE OF CONTENTS

LIST OF FIGURES AND TABLES

Chapter 1: Literature Review

Chapter 2: Incomplete inhibition of HIV infection results in more HIV infected lymph node cells by reducing cell death

Chapter 3: HIV complementation creates a quasispecies of wildtype and mutant virus in the face of selection

Chapter 4: Determination of the number of HIV infections per cell in lymph nodes from HIV infected individuals

ACRONYMS

HIV.....Human Immunodeficiency virus
ARV .....Antiretroviral therapy
RNA.....Ribonucleic acid
DNA.....Deoxyribonucleic acid
RT.....Reverse Transcriptase
MOI.....Multiplicity of infection
ICAM-1 .....Intercellular adhesion molecule 1
ICAM-3 .....Intercellular adhesion molecule 3
LFA-1.....Leukocyte function-associated antigen 1
DCs.....Dendritic cells
DC-SIGN.....DC-specific intercellular adhesion molecule-3-grabbing non-integrin
FISH .....Fluorescence in situ hybridization
LTR.....Long terminal repeat
MSW.....Mutant selection window
WGW.....Wildtype growth window
V1/V2.....Variable region 1/Variable region 2
ART .....Antiretroviral therapy
PCR.....Polymerase chain reaction
GFP .....Green fluorescent protein
CFP .....Cyan fluorescent protein
YFP.....Yellow fluorescent protein
CTFR.....Cell Trace Far Red
PBMC .....Peripheral blood mononuclear cell
RevCEM .....Rev dependent indicator CEM T cell line
LN.....Lymph node
p24.....Anti-HIV Gag
FRISCR .....Fixed and Recovered Intact Single-cell RNA
TB.....Tuberculosis
XDR.....Extremely drug resistant
MDR .....Multiple drug resistant
EFV.....Efavirenz
FTC.....Emtricitabine

TDF.....Tenofovir

RTV .....Ritonavir

LPV.....Lopinavir

ABC .....Abacavir

ABSTRACT

HIV may form reservoirs in anatomical compartments and evolve a quasispecies in order to survive under selective pressures such as antiretroviral drugs. Lymph nodes and lymphoid tissue - critical sites for reservoir formation - are environments conducive to cell-to-cell spread, an efficient mode of HIV transmission. Cell-to-cell spread can lead to multiple infections per cell which in turn profoundly changes how the virus responds to selective pressure.

In this thesis, my goal was to understand the consequences of multiple infections per cell on how the infection responds to and evolves in the face of inhibitors. The specific aims were to: (1) model and experimentally examine the effect of attenuating cell-to-cell spread by using antiretrovirals (ARVs) on infected cell viability; (2) test whether a stable quasispecies can be formed and maintained by complementation– a process where virions derived from different HIV genotypes infecting the same cell share components; (3) test the feasibility of new single-cell RNA-Seq methodology that can be applied to quantify the frequency of multiply infected cells *in vivo*.

These studies showed that: (1) partially attenuating infection involving multiple virions per cell with drug resulted in an increase in the number of live infected cells in both cell line and lymph nodes at suboptimal drug strengths. The increase in live infected cells was a result of fewer HIV DNA copies per cell, relative to no drug; (2) under the selective pressure of efavirenz (EFV), when drug-resistant and drug sensitive HIV co-infect the same cell during drug resistant evolution, complementation takes place, driving the formation and maintenance of a quasispecies; (3) Novel single-cell RNA-Seq approaches are feasible to quantify the number of cells that are multiply infected *in vivo*. Inhibiting mechanisms such as cell-to-cell spread may therefore reduce infection in the face of ARVs and limit viral diversity and hence the ability of HIV to evolve resistance.

INTRODUCTION

Both the development of HIV anatomical reservoirs and the generation of a robust HIV quasispecies are constraints to a successful cure. Critical anatomical reservoirs are lymph nodes and lymphoid tissue. These environments are conducive to infection due to the presence of infectible cells [1-3] and the lack of flow of cells which enables cell-to-cell-spread of HIV [4-15].

Although cell-to-cell spread is an efficient means of transmitting HIV and assists in the development of a reservoir, it causes CD4+ T cell death [16,17]. Cell death occurs by several mechanisms, which are either directly or indirectly mediated by HIV infection. Accumulation of incompletely reverse transcribed HIV transcripts is sensed by interferon-γ–inducible protein 16 [17] and leads to pyroptotic death of incompletely infected cells by initiating a cellular defense program involving the activation of caspase 1 [16,17,20]. HIV proteins Tat and Env have also been shown to lead to cell death of infected cells through CD95 mediated apoptosis following T cell activation [21-23]. Finally, double strand breaks in the host DNA caused by integration of the reverse transcribed virus results in cell death by the DNA-PK mediated activation of the p53 response [18].

Cell-to-cell spread is thought to be the main cause of multiple infections per cell [9]. Several studies have shown that multiple infections in lymph nodes cells is frequent [24-26] while another study demonstrated that this is not the case [30]. Multiple infection attempts may be enough to lead to cell death. Hence, multiply infected cells may die before being detected. One consequence of HIV mediated death may be that attenuation of cell-to-cell spread with ARVs may increase the number of live infected cells. Indeed, it has been suggested that more attenuated HIV strains result in more successful infections in terms of the ability of the virus to replicate in the infected individual [31-35]. An increase in the number of live infected cells as a result of attenuation of cell-to-cell spread by ARVs may not necessarily contribute to a bigger reservoir but may assist to the establishment of a reservoir after therapy initiation. Recently it was shown in outgrowth assays, 60 to 100% of the viruses from patients on prolonged ARV treatment were genetically related to virus circulating prior to treatment and only 0 to 22% were related to virus circulating during treatment, suggesting ART contribute to reservoir formation [36].

In addition to the number of infected cells in the face of drug, multiple infections per cell may influence HIV evolution. HIV evolves and exists as multiple genotypes in a single infected individual, referred to as a quasispecies. Evidence of an HIV quasispecies within a host comes

from: (1) ENV diversity, which allows HIV to evade immune pressures by escaping neutralizing antibodies [37,38]; (2) co-existence of drug resistant and drug sensitive HIV variants in treatment naïve patients [39-42]; (3) co-existence of drug resistant and drug sensitive HIV genomes in patients on antiretroviral therapy [43-45].

Due to the errors in reverse transcription, HIV replication generates a quasispecies where variants are at low frequencies around the main viral sequence [46-48]. However, how a stable quasispecies with variants at high frequencies is maintained is unclear. One possibility is that different anatomical environments apply different selective pressures, therefore leading to a diverse viral pool [49,50]. One mechanism to create a quasispecies that does not rely on the assumption of different environments is complementation [51,52]. In complementation, a virus of genotype 1 may contain proteins from virus of genotype 2 and vice versa. If one of the genotypes has a fitness cost relative to the other, the difference in fitness will be masked. Given that cells in lymph nodes are conducive to cell-to-cell spread and that this mode is thought to be the main cause of high multiplicity of infection (MOI), it may be possible that multiple genetic variants from contacts with different infected cells infect the same cell and “mix” their viral components frequently enough to sustain and maintain an HIV quasispecies under selective pressure.

The degree to which multiple successful infections occur per cell has been disputed. One challenge with quantifying the number of infections per cell is the limitations of established assays, since partial efficiency of detection would translate to decreased HIV copy number per cell. Therefore, multiple infections are extremely dependent on the sensitivity of the assay used. However, new technologies such as single-cell RNA Seq, which are designed to detect gene transcripts on the level of the individual cell, may offer a new perspective on the detection problem.

The aims of the studies below was to examine the effects of multiple infections per cell on HIV infection and evolution in presence of selective pressure.

Aim1: Determine the effects of multiple infection of cells on cell death.

Aim2: Determine the effects of multiply infected cells on the development of a quasispecies during evolution of drug resistance, via the mechanism of complementation.

Aim3: Review and test the feasibility to quantify the frequency of multiply infected cells *in vivo*

CHAPTER 1:

Literature Review

1.1 Origin of HIV

Human immunodeficiency virus (HIV) is a lentivirus as well as a subgroup of retroviruses. HIV causes acquired immunodeficiency syndrome (AIDS). A common property of lentiviruses is that they are transmitted as single-stranded positive-sense enveloped viruses. HIV is a parasitic virus and therefore requires a host cell in order to replicate and survive. HIV can be transmitted from person to person via blood, pre-ejaculate, semen and vaginal fluids. Non-sexual transmission from mother to child can occur during pregnancy, childbirth or breast milk.

HIV is believed to have originated in non-human primates in West-central Africa and transferred to humans in the early 20th century [53]. HIV is closely related to simian immunodeficiency virus (SIV). SIV has evolved many strains, classified by their natural host species. Many of the SIV strains have had a long history with their host. SIV hosts have adapted in the presence of the virus. Together with the genetic makeup of the virus, SIV has resulted in mild immune responses and SIV AIDS does not develop in the host [54]. Two types of HIV have been characterized, HIV-1 and HIV-2. HIV-1 is most widespread around the world, with HIV-2 being less prevalent and less pathogenic. HIV-2 is mostly confined to West Africa [55]. Three different groups of HIV-1 have been identified based on the difference in the envelope protein. These groups include, M, N and O [56]. Group M is the most prevalent and is subdivided into eight different subtypes or clades. The clades are based on the whole genome and are geographically distinct. Most HIV infections in Africa are caused by Clade C subtype [56].

1.2 Structure and Life cycle of HIV

The HIV genome is composed of nines genes; Gag, Pol Env, Tat, Rev, Nef, Vif, Vpr and Vpu (Figure 1). The genome is flanked by a 5' and 3' long terminal repeat (LTR). Gag, Pol and Env contain sequences required to make enzymes and structural proteins for the new virus particle [57]. Specifically, the Gag gene encodes for four smaller proteins, namely; matrix, capsid (p24), nucleocapsid and p6 [57]. Pol encodes for the viral protease, integrase and reverse transcriptase (RT) [57]. Env encodes for the glycoprotein gp160, which is a precursor to gp120 and gp41 [57]. Tat, Rev, Nef, Vif, Vpr and Vpu are regulatory genes that code for proteins that control the ability of HIV to infect a cell, import in to the host nucleus and produce new copies of virus (Figure 1).

Each HIV virion is composed of two positive sense single stranded RNAs that codes the viruses' nine genes (Figure 2). The RNAs are bound to the nucleocapsid (not shown in Figure 2). In turn, the nucleocapsid is enclosed by an outer p24 capsid. Enzymes required for the development of a new virion, such as RT, proteases and integrases are also enclosed within the capsid. The

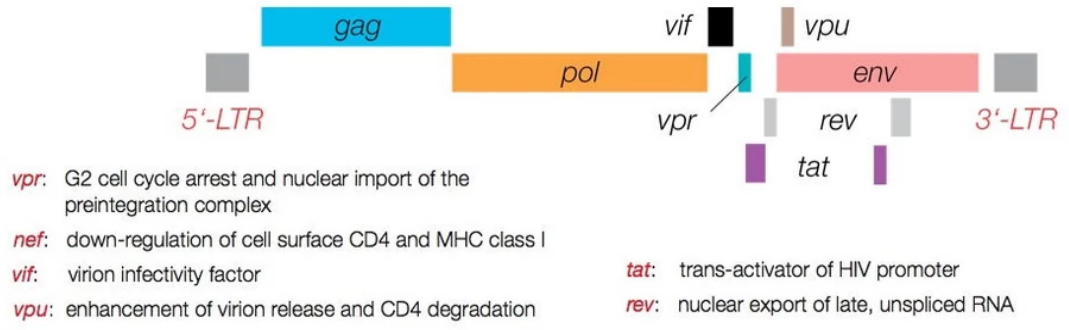

Figure 1. HIV genome structure. HIV genome consists of nine genes; Gag, Pol Env, Tat, Rev, Nef, Vif, Vpr and Vpu. The viral genomes are flanked by a 5' and 3' LTRs. Gag, Pol and Env contain information needed to make structural proteins and enzymes for the new virus particle. Tat, Rev, Nef, Vif, Vpr and Vpu are regulatory genes the code for proteins that control the ability of HIV to infect a cell, import in to the host nucleus and produce new copies of virus (functions shown above).

capsid is surrounded by a viral envelope, which is composed of a lipid bilayer taken from the host cell when it buds off it. The viral envelope consists of an Env-glycoprotein complex, which includes the gp160 spike (gp120 and gp41).

The first step in the HIV life cycle is entry into the host cell. This is mediated through the interaction of HIV gp120 and CD4 on the target cell membrane [58,59]. The interaction induces a conformational change in the envelope protein that in turn allows the binding of the virion to chemokine co-receptors on the surface of the host cell. Macrophage tropic (M-tropic) strains of HIV, generally called R5 HIV, use the CCR5 chemokine co-receptor, whereas T cell tropic (T tropic) strains of HIV, or X4 HIV, bind CXCR4 [60]. X4 strains are frequently found during later stages of disease[60]. HIV can also enter a host cell via a pH-independent endocytosis [61] (Figure 2).

The stable interaction between HIV and host cell surface allows for gp41 to penetrate the cell membrane, causing the virus and cell membrane close together and subsequent fusion of the membranes [62]. The HIV capsid is released into the cell, where the capsid is uncoated and viral proteins, (RT, integrase, proteases) as well as viral double stranded RNA is released into the cytoplasm. RT contains RNA-dependent DNA polymerase activity, DNA-dependent DNA polymerase activity and RNase H activity [63,64]. RT reverse transcribes a single positive sense viral RNA genome into a double stranded DNA copy [63,64]. The RNase H is used to remove the original RNA viral template from the first DNA strand. RT, together with the copy DNA, integrase and Vpr, form a pre-integration complex (PIC) [65]. The PIC is then transported to the nucleus. Vpr has been

implicated in mediating the nuclear import of PIC [66].

Integration of the viral copy DNA is facilitated by integrase. The integrated viral copy DNA, namely proviral DNA, can lead to transcriptionally active or latent forms of infection. In the host genome, the LTRs function as eukaryotic transcriptional elements, containing downstream and upstream transcriptional promoter elements [67]. These elements help position the RNA polymerase II [67]. This in turn, leads to transcription of the HIV genome. Some of the transcribed RNA created undergoes splicing to produce messenger RNA (mRNA). The mRNA is transported into the cytoplasm where it is translated into proteins. The translated regulatory protein, Rev, binds to the Rev response element (RRE), part of the second intron of HIV, in the nucleus [68]. This binding facilitates the export of unspliced and incompletely spliced transcribed viral RNA from the nucleus to the cytoplasm [68]. Some of the full-length transcribed viral RNAs function as new copies of the virus genome, while multiply spliced transcripts encode Nef, Tat and Rev. Other singly spliced or unspliced viral transcripts encode polyproteins, such as gp160 (later cleaved in gp120 and gp41), Gag and Gag-Pol polyproteins or precursor [69].

The cleavage products of gp160, gp120 and gp41, are transported to the plasma membrane of the infected cell. The Gag and Gag-Pol polyproteins also become associated with the plasma membrane of the infected cell and along with the HIV transcribed RNA and Vpr, form a virion that begins to bud. On average about 100 molecules of Gag-Pol and 1500 Gag polyproteins are packaged in the assembled genome [70]. The budded virion is considered immature as the Gag and Gag-Pol polyproteins still require cleavage. Cleavage of the Gag-Pol precursor results in the production of protease, integrase, RT. Cleavage of Gag results in the capsid (p24) and nucleocapsid. The cleavage is mediated by HIV protease.

Mature virions can infect new cells. Two known modes of infections of host cells have been described. These include cell-free and cell-to-cell mode of infection. Below, I will describe both modes as well as the implications of both.

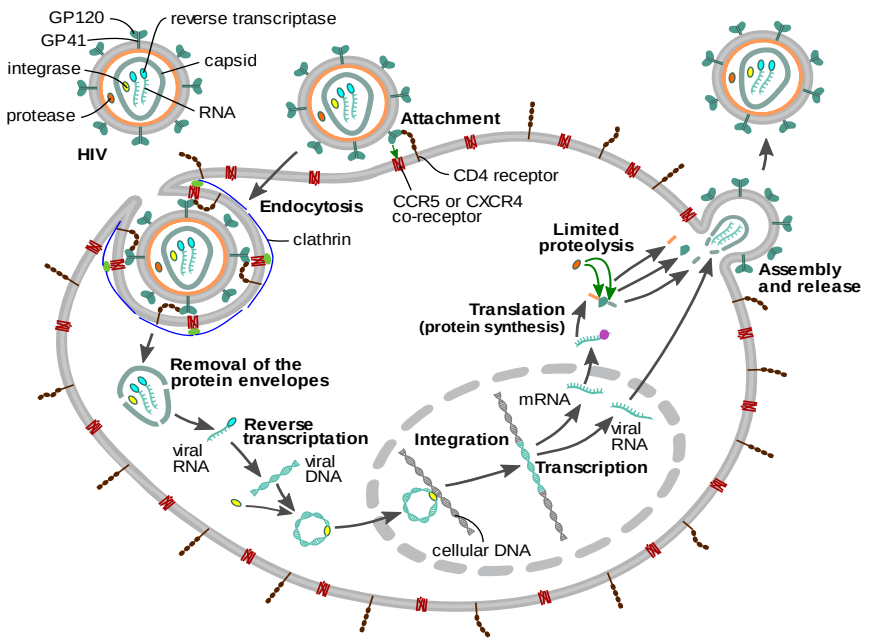

Figure 2. Life cycle of HIV. HIV enter a cell through either ENV and host cell receptor binding and subsequent fusion or through endocytosis. HIV capsid is released into the cell where viral RNA is reverse transcribed into viral DNA. Viral DNA is integrated into the host genome and following transcription, splicing and translation, new HIV proteins and viral RNA are produced that are then assembled at the host cell membrane and released from the host cell via budding.

1.3 Cell-to-cell infection

Cell-to-cell is a mode of infection, only described for enveloped viruses, whereby virus is spread from an infected cell to an uninfected target cell in close proximity. This is unlike a cell-free infection where free floating virus in the extracellular milieu infects a cell (Figure 3A). In cell-to-cell spread, this contact-dependent mode of transmission involves the formation of either a virological synapse[10,71,72] or an infectious synapse [73] between immune cells. Virological synapses are formed by HIV infected cells, where virus can bud from the plasma membrane and infect a target cell that is polarized and in close contact with the infected cell. Infectious synapses are formed by uninfected cells that capture free HIV on its surface and uninfected target cell in that are in close proximity. Both types of synapses enable a stable polarization after contact with other cells which are generally immobile in the tissue [9-11].

The virological synapse formed during cell-to-cell infection is initiated by the binding the HIV envelope protein (ENV), on the surface of an infected cell, with CD4 on the surface of an uninfected T cell [10] (Figure 3B). After stable adhesion is established, the viral protein Gag is

recruited to the cell contact in an actin-dependent manner [10]. Actin rearrangements

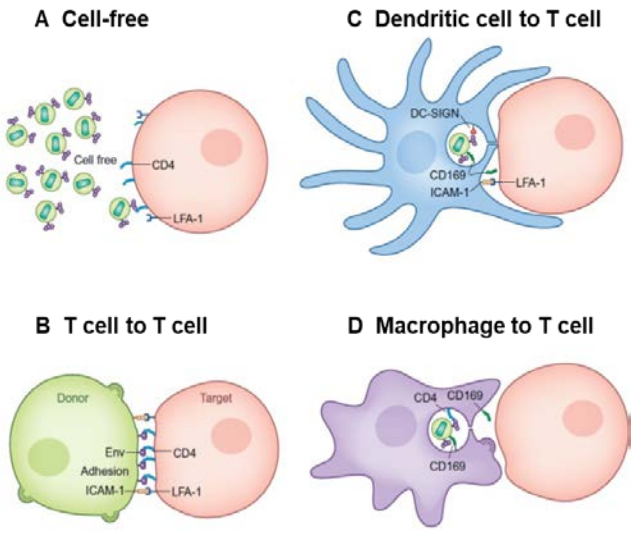

Figure 3. Modes of entry of HIV into targets cells. (A) Cell-free virus released into the extracellular milieu bind CD4 on the target cell surface via HIV ENV gp120. (B) Virological synapse and (C) Infectious synapses for different cell types. (B) Infected CD4 T cell binds to an uninfected T cell through engagement of HIV ENV. Adhesion molecules LFA-1 and ICAM-1 also facilitate in cell-to-cell contact. (C) Dendritic cell to T cell or CD4+ expressing cell involves capture of HIV through DC-SIGN and CD-169 for either internalisation into the DC or transient surface attachment until a cell-to-cell synapse has been made. Adhesion molecules LFA-1 and ICAM-1 facilitate in synapse formation. (D) Macrophage to T cell synapse-like interface. Macrophages can internalize HIV through CD4 and CD169 binding. HIV can be spread directly to uninfected T cells across a synapse-like interface (adapted from Law et al., 2016).

appear to be critical for the formation of a virological synapse on the infected donor cell side, where filamentous actin accumulates at the site of adhesion [74]. Several other adhesion molecules such as intercellular adhesion molecule 1 (ICAM-1), ICAM-3 and leukocyte function-associated antigen 1 (LFA-1) can promote the formation of a virological synapse [75-77]. The CD4-ENV interaction, along with the other adhesion molecules results in a stable binding that subsequently leads to the production of virus at the site of the cell-to-cell contact [9,11]. It is possible for one infected cell T cell to assemble multiple cell-to-cell contacts or virological synapses with several target simultaneously (polysynapse) [76].

The most well characterized infectious synapse with an antigen presenting donor are dendritic cells (DCs). DCs survey mucosal tissues and transport HIV to secondary lymphoid tissues [78,79]. In the lymphoid tissues, DCs can form an infectious synapse with the CD4+ T cells [73,80]. DC-

specific intercellular adhesion molecule-3-grabbing non-integrin (DC-SIGN), is a C-type lectin and mediates the capture and/or internalization of HIV, by interacting with gp120 [81] (Figure 3C). Other molecules such as CD169, on the surface of DCs can also help capture HIV [82]. Both LFA-1 and ICAM-1 adhesion molecules facilitate in the formation of the infectious synapse of a DC with an uninfected target cell [83]. A infectious synapse-like interface can also be formed with macrophages [84-86]. Here, HIV is captured on the surface of macrophages and subsequently internalized for infection. The efficient capture is mediated by CD169/CD4 [87] (Figure 3D).

It is well known that HIV replicates rapidly in target cells co-cultured with infected cells than with cell-free virus inoculation [88-90]. It has been demonstrated in an *in vitro* co-culture systems, where both cell-free and cell-to-cell HIV infection occured, cell-to-cell spread was the predominant mode of HIV dissemination [14]. The relative contribution of cell-to-cell spread via synapses is difficult to visualize *in vivo* and therefore difficult to quantify. Virus transmitted via cell-to-cell spread may overcome many of the barriers that the cell-free virus faces. Infected cells entering a new host can avoid mucosal epithelial barriers that would normally be impermeable to free virions. Virus spread by cell-to-cell transmission does not have to diffuse in the cellular milieu like cell-free virus [90]. This diffusion step can result in a progressive loss of infectivity for cell-free virus. HIV spreading directly from one cell to another cell can be more protected from the immune response that otherwise targets the virus. It has been shown that cell-associated virus exhibits greater resistance to neutralization by patient antisera as compared with a homologous cell-free viral challenge [89,91]. Possible reasons for the reduced efficiency of neutralization by antibodies in patient sera may include the Env conformation on HIV infected cells, kinetic barriers or the multiplicity of HIV infection per cell [92]. With regards to the latter, it has been shown that cell-to-cell spread leads to the transfer of a large amount of virus[4,9,11,26,27,84,93-100], resulting in multiple infection attempts (discussed below). Sigal et al. (2011) showed that multiple virions transmitted per cell can increase the probability that at least one virion escapes antiretroviral therapy and in doing so, continues to infect.

1.3.1 High multiplicity of infection

An important feature of HIV cell-to-cell spread is the transfer of large amounts of virus per infection event from an infected cell to an uninfected target cell [4,9,11,26,27,84,93-100]. Transmission electron micrographs (TEMs) depict many free virus particles in the space between the donor and target cells [11] (Figure 4). A study of the gut-associated lymphoid tissue (GALT) of HIV infected mice with humanized immune systems showed that the number of HIV virions in the intercellular pools in

the GALT region near the edge of a crypt ranged from 17 to 59 [100]. These HIV intercellular pools were seen as tight areas of free virus between cells and would require cell morphologies to change in order for virus to escape. TEMs from another study do not show free viral particles in the synaptic space but rather nascent, crescent viral buds that are directly apposed to the target cell membrane [9]. In either case, the large transfer of virus numbers is unique to cell-to-cell spread.

It has been shown in lymphoid tissues that the majority of trapped HIV (estimated at 1.5×10^8 copies of viral RNA per gram lymphoid tissues) exists on the surface of follicular dendritic cells (FDCs) in the germinal centers [101]. FDCs can retain a high concentration of infectious HIV in close proximity to susceptible CD4+ T cells. Earlier work demonstrated that CD57+CD4+ T cells in germinal centers intimately interact with FDCs in direct cell-to-cell contact [102]. More recent work has shown that T follicular helper cells - in direct contact with FDCs - are responsible for HIV replication in both viremic [103] and aviremic [104] HIV infected patients.

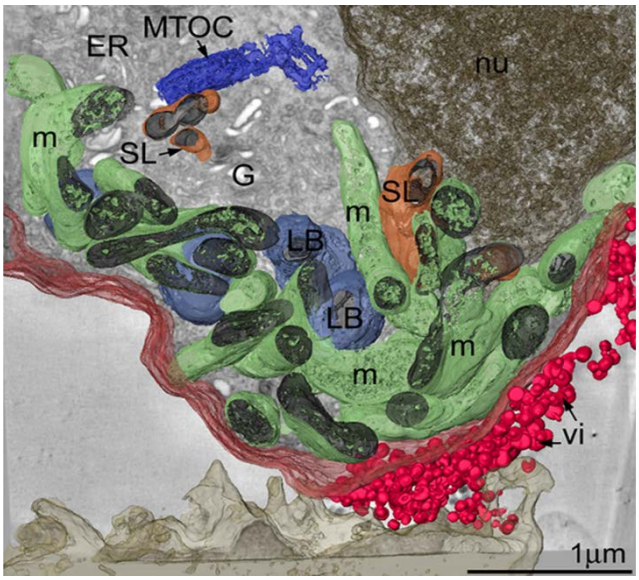

Figure 4. Transfer of large amounts of HIV from an infected cell to an uninfected cell at the site of a virological synapse. Infected Jurkat T cells were mixed with primary $CD4^+$ T cells, fixed and embedded. Secretory organelles (endoplasmic reticulum, ER, not pseudocoloured), secretory lysosomes (SL, orange), Golgi (G, not pseudocoloured), mitochondria (m, green) and lipid bodies (LB, pale blue) and microtubule organizing centre – MTOC - (blue), towards the site of virus particle (vi, red) release in the HIV-1 infected T cell (adapted from Jolly et al., 2011) [11].

A transfer of large amounts of virus during cell-to-cell spread increases the chances that cells will become multiply infected [27,93,98]. Del Portillo et al. (2011) showed, using fluorescence *in situ* hybridization (FISH), that the average copy number of proviral genomes per cell in cell-to-cell spread in *in vitro* PBMC infections is ~2.5-fold higher than that in cell-free infection (Figure 5). Multiple infections per cell, as measured by the number of proviral DNA copies, occurs frequently in the lymph nodes [24] but with lower rates (1-10%) in the peripheral blood [30,105]. Meyerhans

showed in two studies that a majority of *in vivo* infected splenocytes harbored a mean 3.2 proviral HIV copies/cell as detected by FISH (Figure 6A and B) [24] [28]. In contrast, Josefsson et al. (2011 and 2013) showed that only ~ 5-7% of CD4+ T cells circulating the blood and peripheral lymphoid tissues carry more than 1 provirus.

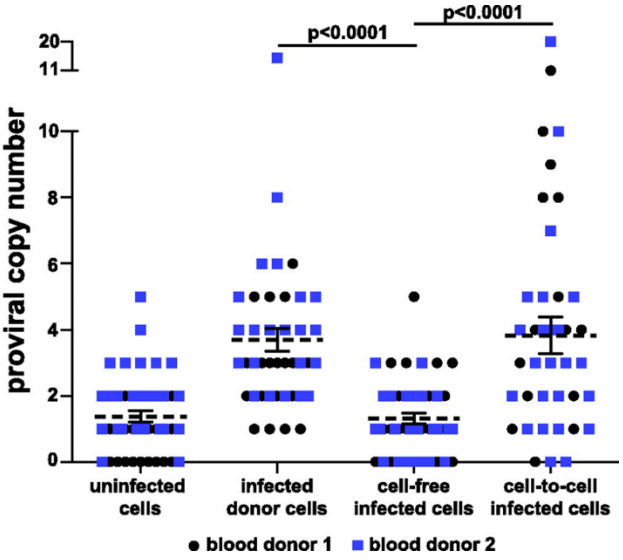

Figure 5. Increased number of proviral copies in cell-to-cell spread compared to cell-free infection. Distributions of nuclear HIV-1 proviral copies in an *in vitro* infection of $CD4^+$ cells isolated from two different blood donors. Combined means ± SEM are shown. Blood donor 1: cell-free mean = 1.11, n = 26; cell-to-cell mean = 3.72, n = 25, P = 0.0003. Blood donor 2: cell-free mean = 1.55, n = 20; cell-to-cell mean = 3.95, n = 20, P = 0.0138. Combined blood donors: donor cell mean = 3.71, n = 45, cell-free mean = 1.30, n = 46, cell-to-cell mean = 3.82, n = 45; P values are displayed. Significance was tested using the two-tailed Mann-Whitney U test with an alpha level of 0.05 (adapted from Del Portillo et al., 2011) [27].

There are two possible explanations for the variations in the number of proviral HIV copies per cell. Firstly, different cell subsets are infected to different degrees. Recent work investigating markers associated with HIV latency in the face of antiretroviral therapy (ART) found that the average number of HIV DNA copies per cell in blood samples is greater than one in 3 out of 12 individuals.

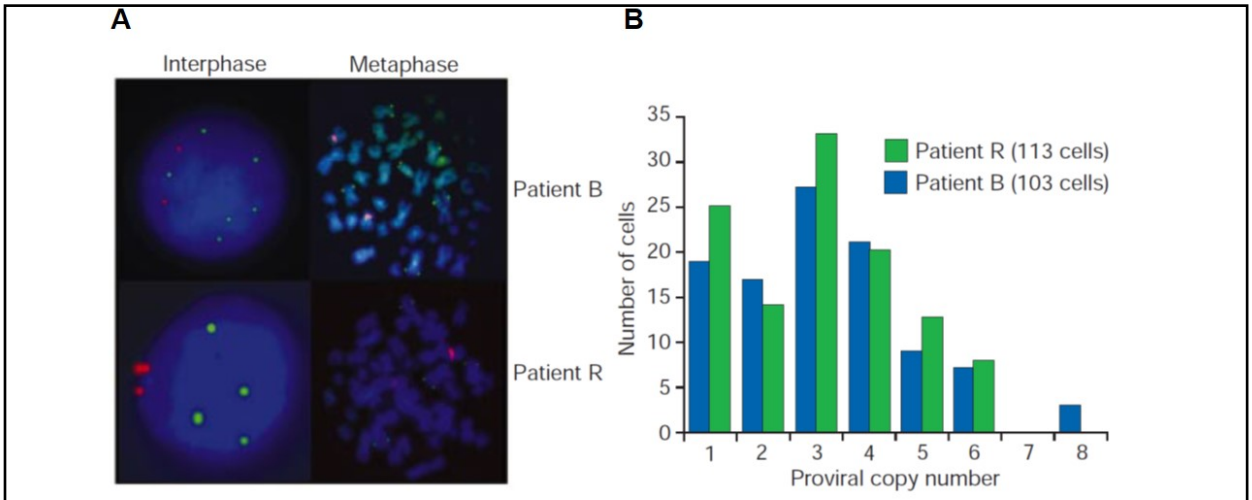

Figure 6. HIV-infected splenocytes harbour many proviruses. (A), FISH image of HIV-1 proviruses in interphase nuclei and metaphase chromosomes from splenocytes. Green, integrated HIV genomes, or proviruses; Red, centromeric region of chromosome 12. (B), Frequency distribution of the number of HIV-1 proviral copies per infected cell (adapted from Jung et al., 2002) [24].

This occurred in the CD3+ positive, CD32a high CD4+ T cell subset [106]. A second reason for the discrepancy in the results from the different studies is that multiply infected cells may die more frequently through cell-to-cell spread.

1.3.2 Cell Death in cell-to-cell spread

HIV infection is known to result in extensive T cell depletion in lymph node environments where the force of infection is high [16,17,20,107-109]. The mode of HIV infection can determine the pathway for cell-death. Cell-free infection can lead to caspase 3 apoptosis in small fraction of permissive CD4+ T cells in the lymphoid tissue [16] (Figure 7). For the remaining less permissive targets, cell-to-cell spread is required with the accumulation of incompletely reverse transcribed HIV transcripts being sensed by interferon-γ–inducible protein 16 (IFI16) [17], depleting cells via a caspase 1-depedent pyroptosis [16,17] (Figure 7).

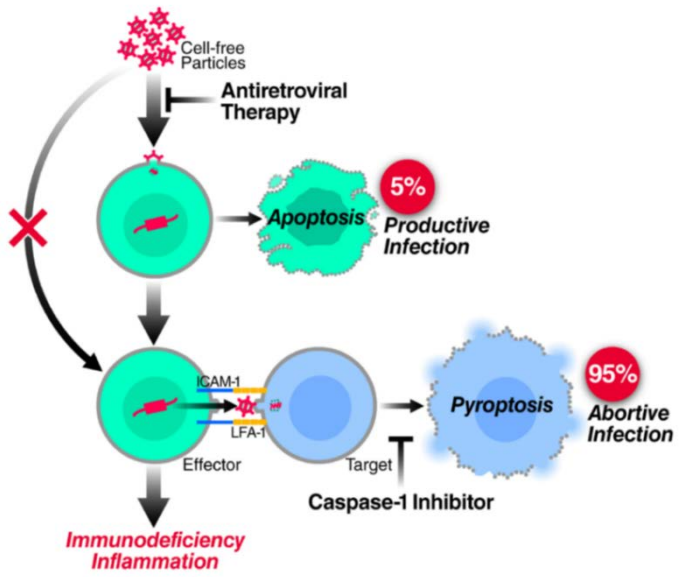

Figure 7. The mode of HIV spread determines the type of cell death. Cell-free HIV particles result in productive infection and caspase 3 apoptosis in a small fraction of permissive lymphoid CD4+ T cells. Cell-to-cell spread of HIV is required to deplete the non-permissive lymphoid CD4+ T cells, which represent 95% or more of the target cells in lymphoid tissues, via caspase 1-dependent pyroptosis. Free HIV particles, even at high quantities, cannot trigger innate immune recognition and produce this form of cell death (adapted from Galloway et al., 2015) [16].

Cooper et al. (2013) demonstrated that double strand breaks in the host DNA caused by integration of the reverse transcribed virus results in cell death (Figure 8A). The accumulation of unintegrated reverse transcripts as measured by the long terminal repeat (LTR) copy number has less of an effect of cell death (Figure 8A). Furthermore, these authors showed cell death can be reduced by reducing the amount proviral integration and that cell death was a DNA-PK mediated activation of the p53 response (Figure 8B and C). Other mechanisms of T cell death may or may

not be dependent on cell-to-cell infection. HIV proteins Tat and Env have also been shown to lead to cell death of infected cells through CD95 mediated apoptosis following T cell activation [21-23]. Therefore, counterintuitively, HIV cell-to-cell spread, a much more efficient infection mechanism, may act to limit the number of infected cells by promoting cell-death.

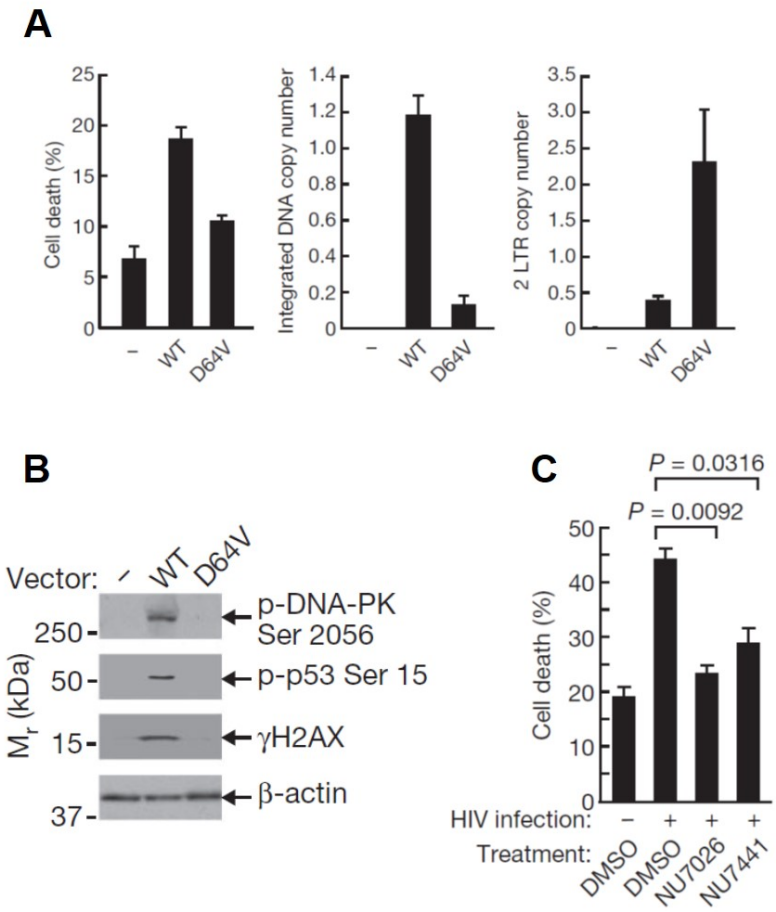

Figure 8. Proviral DNA integration triggers cell death through DNA-PK mediated activation of p53 during HIV infection. (A) Cell death and proviral DNA analyses of CD4⁺ lymphocytes infected with wild type HIV NL43 or with HIV NL43 D64V integrase mutant. (B) Western blot analysis showing phosphorylation of DNA-PK, p53 and H2AX following high MOI HIV infection with either wild type or mutant virus in primary CD4⁺ lymphocytes. (C) Cell death analysis gated on p24+ cells of primary CD4⁺ lymphocyte cultures either uninfected or infected with HIV-189.6 in the absence or presence of DNA-PK inhibitors NU7026 or NU7441 for 7 days. Data in panels A and C are representative of at least two independent experiments done in triplicate. Error bars represent the standard deviation of the mean of cell death (adapted from Cooper et al., 2013) [18].

1.2.3. Evolving a quasispecies

The evolution of a genetically diverse population of variants, or quasispecies, enables HIV to adapt and survive in ever changing environments. Evidence of an HIV quasispecies within a host includes: (1) ENV diversity, which has allowed for HIV to evade immune pressures by escaping neutralizing antibodies [37,38]; (2) co-existence of drug resistant and drug sensitive HIV variants in treatment naïve patients [39-42]; (3) co-existence of drug resistant and drug sensitive HIV genomes in patients on antiretroviral therapy [43-45]. Whether the outgrowth of wildtype (drug sensitive) virus after antiretroviral therapy interruption is a result of the latter quasispecies formation is still to be determined.

Predictions on when drug resistant and drug sensitive variants arise are based on a current model which describes drug resistant mutants arising in the mutant selection window (MSW), where at higher drug concentrations, the relative fitness of the mutant is higher than that of the wildtype virus [29,110] (Figure 9). This model cannot adequately account for the generation and maintenance of an HIV quasispecies as a counter-force to drug resistant evolution, where less fit and more fit variants to stably co-exist.

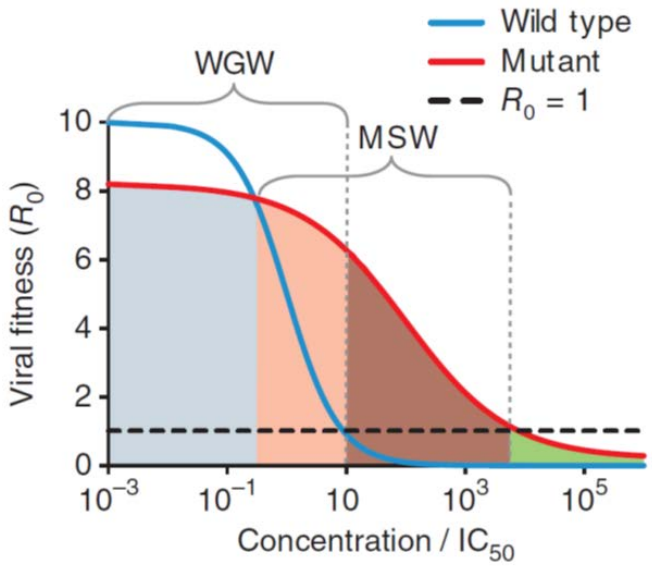

Figure 9. Drug concentrations determine the relative fitness of the wild type and drug resistant virus. (A) As measured by the replication ratio (R_0), the wild type (blue line) is most fit at low drug concentrations and dominates in the wild type growth window (WGW, grey area). A drug resistant mutant (red line) is less fit than the wild type at low concentrations but more fit at higher drug concentrations, out-competing wild type in the mutant selection window (MSW, brown area). In the overlapping windows (orange area), both mutant and wild type can grow but with decreasing replication. At very high drug concentrations (green area), the replication ratio of both wild type and mutant is <1 and the virus does not (adapted from Rosenbloom et al., 2012) [29].

Intracellular-cell selection of HIV in multiply infected cells introduces new evolutionary dynamics. Multiple infections per cell can result in the co-infection of genetically distinct HIV variants. Co-infection of genetically distinct HIV variants has been well documented [24,28,30,95,111-113]. For example, as depicted in Figure 10, a single splenocyte from an HIV infected individual can harbour multiple variants of the ENV region.

One mechanism to create a quasispecies that does not rely on the assumption of different environments is complementation, also called phenotypic mixing [51,52]. In this mechanism, co-infection and viral protein expression from two different viral genotypes in the same cell results in sharing of viral components. This is distinct from recombination, where two viral genomes co-packaged in the same cell recombine to form a new genome [114]. In complementation, a virus of genotype 1 may contain proteins from virus of genotype 2 and vice versa. If one of the genotypes has a fitness cost relative to the other, the difference in fitness will be masked [115]. This process has been shown to operate in viruses [116,117] including HIV [112,113]. There is no known mechanism which prevents one HIV strain packaging components such as reverse transcriptase from another HIV strain if both strains are in the same cell since RT molecules mix in the cell cytoplasm [118]. The first step in determining whether complementation is relevant, particularly in patients on antiretroviral therapy or harboring some level of drug resistant mutations, is quantifying how frequent multiple variants infect the same cell *in vivo*. This would include using novel, sensitive single cell techniques.

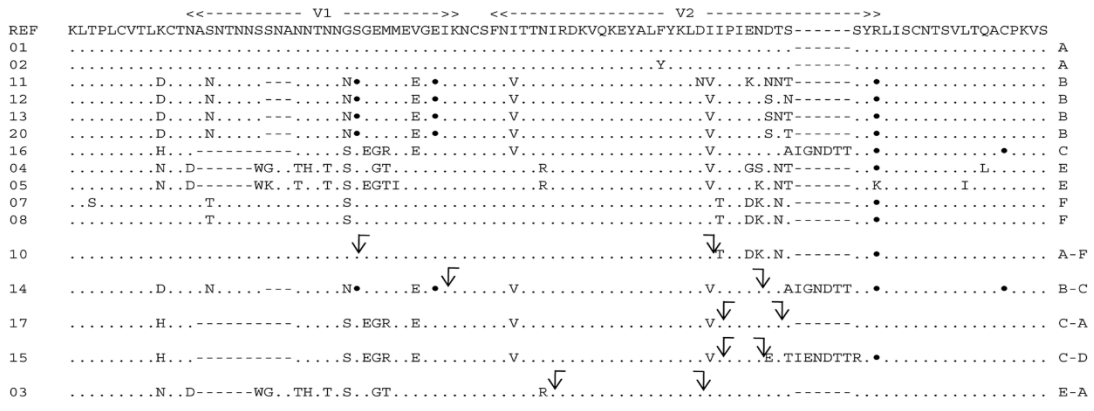

Figure 10. HIV ENV sequence diversity from a single splenocyte. HIV ENV V1/V2 amino acid sequences from a single splenocyte compared to reference sequence. The sequences are grouped and coded by capital letters to the right. Dots denote synonymous substitutions, while arrows correspond to recombination sites (adapted from Suspene et al., 2012) [28].

1.4 Single cell RNA-Seq methods to determine the number of HIV infections per cell

A novel approach to define the HIV cellular reservoir and associated sequences at the level of the single infected cell is the emerging technology of single cell RNA-Seq. This enables analysis of single-cell transcriptomes to discover cell type/state [119], and can also be used to detect HIV transcripts in individual cells. For example, Seq-Well is a microwell-based platform that enables high-throughput single cell RNA-Seq using ~86,000 subnanoliter wells pre-loaded with barcoded mRNA capture beads. Each cell is captured with a single bead in a single well using gravity.

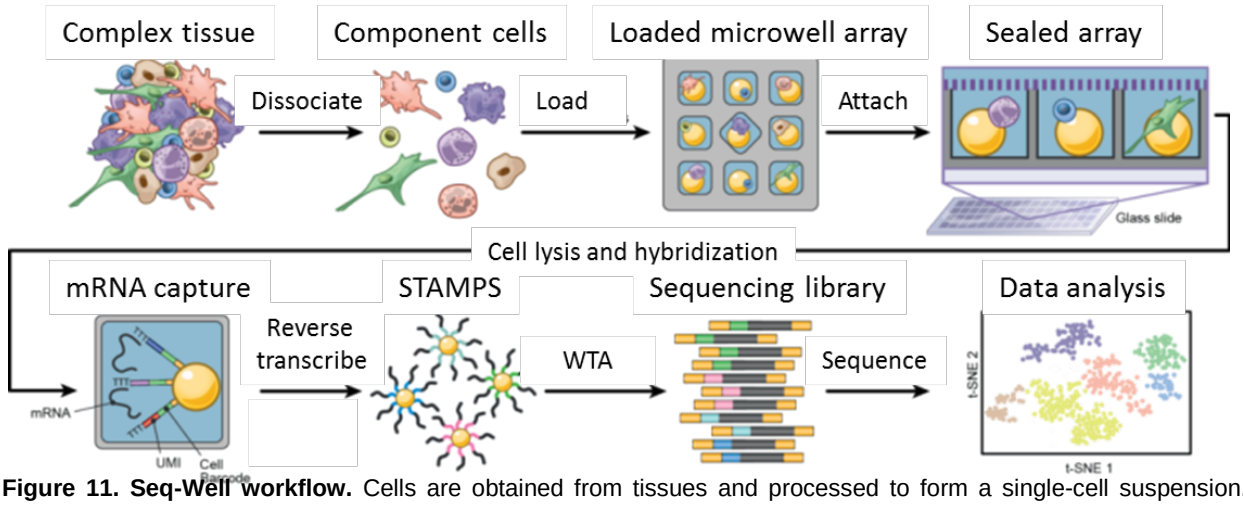

Figure 11. Seq-Well workflow. Cells are obtained from tissues and processed to form a single-cell suspension. Barcoded mRNA capture beads are added to the surface of the microwell device, settling into wells by gravity, and then the single-cell suspension is applied. The device is sealed using a semi-permeable membrane that, upon addition of a chemical lysis buffer, confines cellular mRNAs within wells while allowing efficient buffer exchange. Liberated cellular transcripts hybridize to the bead-bound barcoded poly(dT) primers that contain a cell barcode (shared by all probes on the same bead but different between beads) and a unique molecular identifier (UMI) for each transcript molecule. After hybridization, the beads are removed from the array and bulk reverse transcription is performed to generate single-cell cDNAs attached to beads. Libraries are then made by whole transcriptome amplification (WTA) and sequenced. After, single-cell transcriptomes are assembled in silico using cell barcodes and UMIs.

The wells are then sealed using a semi-permeable membrane, cells are lysed within the array, and cellular mRNAs are captured on barcoded beads (Figure 11). Reverse transcription, library preparation and paired-end sequencing is carried out [120-122]. Seq-Well enables transcriptomic profiling of thousands of cells in parallel, with each cell profiled individually by applying unfixed cells in suspension to the microwell chip [123].

In addition to Seq-Well, other single cell RNA-Seq approaches can be used to specifically detect and analyze the transcriptomes of HIV infected cells. These techniques sequence cells in a 96-well format and therefore rely on enrichment strategies of HIV infected cells. One such approach is using Fixed and Recovered Intact Single-cell RNA (FRISCR) [124] for HIV infected cells (Figure 12). HIV infected cells can be enriched using intracellular anti-HIV Gag (p24) staining. With the FRISCR approach, fixed HIV infected cells are single cell sorted into a Proteinase K digestion buffer (PKD). Each cell in the well is lysed and the RNA is reverse crosslinked by heating. FRISCR has been successfully applied to radial glia cells of the human neocortex, yielding expression data similar to that of unfixed cells [124]. If direct detection of HIV is not possible, an alternative is single cell RNA-Seq of cell types enriched for HIV infection. Here, cells are sorted based of cell-surface markers rather than fixing and using intracellular staining.

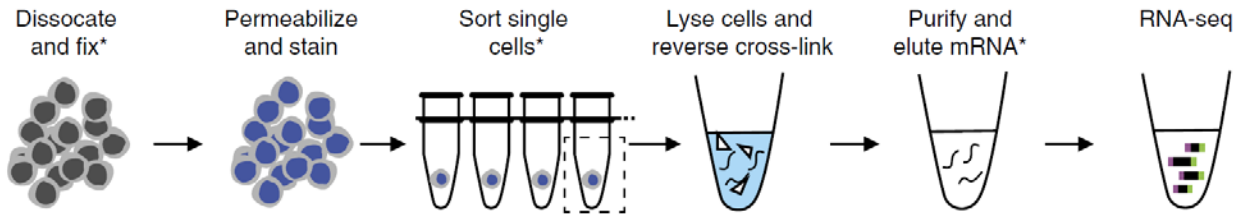

Figure 12. Steps in the FRSICR method. The first step of the process is to dissociate, fix, permeabilize and stain a population of cells. Cells are then single cell sorted based on staining markers. For HIV, this would be sorting on p24 positive cells. Single cells are sorted into a Proteinase K digestion buffer. Each cell is lysed and the mRNA is reverse cross-linked by heating. The mRNA is purified using Oligo dT25 beads and the sample is then applied to RNA sequencing (adapted from Thomsen et al., 2016) [124].

References

1 Deleage, C. *et al.* Defining HIV and SIV reservoirs in lymphoid tissues. *Pathogens & immunity* **1**, 68 (2016).

2 Embretson, J. *et al.* Massive covert infection of helper T lymphocytes and macrophages by HIV during the incubation period of AIDS. *Nature* **362**, 359 (1993).

3 Tenner-Racz, K. *et al.* The unenlarged lymph nodes of HIV-1–infected, asymptomatic patients with high CD4 T cell counts are sites for virus replication and CD4 T cell proliferation. The impact of highly active antiretroviral therapy. *Journal of Experimental Medicine* **187**, 949-959 (1998).

4 Baxter, A. E. *et al.* Macrophage infection via selective capture of HIV-1-infected CD4+ T cells. *Cell Host Microbe* **16**, 711-721 (2014).

5 Dale, B. M. *et al.* Cell-to-cell transfer of HIV-1 via virological synapses leads to endosomal virion maturation that activates viral membrane fusion. *Cell Host Microbe* **10**, 551-562 (2011).

6 Groot, F., Welsch, S. & Sattentau, Q. J. Efficient HIV-1 transmission from macrophages to T cells across transient virological synapses. *Blood* **111**, 4660-4663 (2008).

7 Groppelli, E., Starling, S. & Jolly, C. Contact-induced mitochondrial polarization supports HIV-1 virological synapse formation. *J Virol* **89**, 14-24 (2015).

8 Gummuluru, S., KewalRamani, V. N. & Emerman, M. Dendritic cell-mediated viral transfer to T cells is required for human immunodeficiency virus type 1 persistence in the face of rapid cell turnover. *J Virol* **76**, 10692-10701 (2002).

9 Hubner, W. *et al.* Quantitative 3D video microscopy of HIV transfer across T cell virological synapses. *Science* **323**, 1743-1747 (2009).

10 Jolly, C., Kashefi, K., Hollinshead, M. & Sattentau, Q. J. HIV-1 cell to cell transfer across an Env-induced, actin-dependent synapse. *J Exp Med* **199**, 283-293 (2004).

11 Jolly, C., Welsch, S., Michor, S. & Sattentau, Q. J. The regulated secretory pathway in CD4(+) T cells contributes to human immunodeficiency virus type-1 cell-to-cell spread at the virological synapse. *PLoS Pathog* **7**, e1002226 (2011).

12 Munch, J. *et al.* Semen-derived amyloid fibrils drastically enhance HIV infection. *Cell* **131**, 1059-1071 (2007).

13 Sherer, N. M. *et al.* Retroviruses can establish filopodial bridges for efficient cell-to-cell transmission. *Nat Cell Biol* **9**, 310-315 (2007).

14 Sourisseau, M., Sol-Foulon, N., Porrot, F., Blanchet, F. & Schwartz, O. Inefficient human immunodeficiency virus replication in mobile lymphocytes. *Journal of virology* **81**, 1000-1012 (2007).

15 Sowinski, S. *et al.* Membrane nanotubes physically connect T cells over long distances presenting a novel route for HIV-1 transmission. *Nat Cell Biol* **10**, 211-219 (2008).

16 Galloway, N. L. *et al.* Cell-to-Cell Transmission of HIV-1 Is Required to Trigger Pyroptotic Death of Lymphoid-Tissue-Derived CD4 T Cells. *Cell Rep* **12**, 1555-1563 (2015).

17 Doitsh, G. *et al.* Cell death by pyroptosis drives CD4 T-cell depletion in HIV-1 infection. *Nature* **505**, 509-514 (2014).

18 Cooper, A. *et al.* HIV-1 causes CD4 cell death through DNA-dependent protein kinase during viral integration. *Nature* **498**, 376-379, doi:10.1038/nature12274 (2013).

19 Law, K. M., Satija, N., Esposito, A. M. & Chen, B. K. Cell-to-Cell Spread of HIV and Viral Pathogenesis. *Adv Virus Res* **95**, 43-85, doi:10.1016/bs.aivir.2016.03.001 (2016).

20 Doitsh, G. *et al.* Abortive HIV infection mediates CD4 T cell depletion and inflammation in human lymphoid tissue. *Cell* **143**, 789-801 (2010).

21 Westendorp, M. O. *et al.* HIV-1 Tat potentiates TNF-induced NF-kappa B activation and cytotoxicity by altering the cellular redox state. *EMBO J* **14**, 546-554 (1995).

22 Westendorp, M. O., Frank, R., Ochsenbauer, C. & Stricker, K. Sensitization of T cells to CD95-mediated apoptosis by HIV-1 Tat and gp120. *Nature* **375**, 497 (1995).
23 Banda, N. K. *et al.* Crosslinking CD4 by human immunodeficiency virus gp120 primes T cells for activation-induced apoptosis. *J Exp Med* **176**, 1099-1106 (1992).
24 Jung, A. *et al.* Recombination: Multiply infected spleen cells in HIV patients. *Nature* **418**, 144 (2002).
25 Gratton, S., Cheynier, R., Dumaurier, M.-J., Oksenhendler, E. & Wain-Hobson, S. Highly restricted spread of HIV-1 and multiply infected cells within splenic germinal centers. *Proceedings of the National Academy of Sciences* **97**, 14566-14571 (2000).
26 Law, K. M. *et al.* In Vivo HIV-1 Cell-to-Cell Transmission Promotes Multicopy Micro-compartmentalized Infection. *Cell Rep* **15**, 2771-2783 (2016).
27 Del Portillo, A. *et al.* Multiploid inheritance of HIV-1 during cell-to-cell infection. *J Virol* (2011).
28 Suspene, R. & Meyerhans, A. Quantification of unintegrated HIV-1 DNA at the single cell level in vivo. *PLoS One* **7**, e36246, doi:10.1371/journal.pone.0036246 (2012).
29 Rosenbloom, D. I., Hill, A. L., Rabi, S. A., Siliciano, R. F. & Nowak, M. A. Antiretroviral dynamics determines HIV evolution and predicts therapy outcome. *Nat Med* **18**, 1378-1385, doi:10.1038/nm.2892 (2012).
30 Josefsson, L. *et al.* Single cell analysis of lymph node tissue from HIV-1 infected patients reveals that the majority of CD4+ T-cells contain one HIV-1 DNA molecule. *PLoS Pathog* **9**, e1003432 (2013).
31 Payne, R. *et al.* Impact of HLA-driven HIV adaptation on virulence in populations of high HIV seroprevalence. *Proc Natl Acad Sci U S A* **111**, E5393-5400 (2014).
32 Arien, K. K. *et al.* Replicative fitness of historical and recent HIV-1 isolates suggests HIV-1 attenuation over time. *AIDS* **19**, 1555-1564, doi:00002030-200510140-00001 [pii] (2005).
33 Nowak, M. & May, R. M. *Virus dynamics: mathematical principles of immunology and virology: mathematical principles of immunology and virology*. (Oxford University Press, UK, 2000).
34 Quinones-Mateu, M. E. & Arts, E. J. Virus fitness: concept, quantification, and application to HIV population dynamics. *Curr Top Microbiol Immunol* **299**, 83-140 (2006).
35 Wodarz, D. & Levy, D. N. Human immunodeficiency virus evolution towards reduced replicative fitness in vivo and the development of AIDS. *Proc Biol Sci* **274**, 2481-2490 (2007).
36 Joseph, S. B. *et al.* in *XXII International AIDS Conference, 2018* (Amsterdam, Netherlands, 2018).
37 Frost, S. D. *et al.* Neutralizing antibody responses drive the evolution of human immunodeficiency virus type 1 envelope during recent HIV infection. *Proceedings of the National Academy of Sciences* **102**, 18514-18519 (2005).
38 Rong, R. *et al.* Escape from autologous neutralizing antibodies in acute/early subtype C HIV-1 infection requires multiple pathways. *PLoS pathogens* **5**, e1000594 (2009).
39 Bonhoeffer, S., May, R. M., Shaw, G. M. & Nowak, M. A. Virus dynamics and drug therapy. *Proc Natl Acad Sci U S A* **94**, 6971-6976 (1997).
40 Bonhoeffer, S. & Nowak, M. A. Mutation and the evolution of virulence. *Proceedings of the Royal Society of London B: Biological Sciences* **258**, 133-140 (1994).
41 Ribeiro, R. M. & Bonhoeffer, S. Production of resistant HIV mutants during antiretroviral therapy. *Proc Natl Acad Sci U S A* **97**, 7681-7686 (2000).
42 Ribeiro, R. M., Bonhoeffer, S. & Nowak, M. A. The frequency of resistant mutant virus before antiviral therapy. *AIDS* **12**, 461-465 (1998).
43 Bansode, V. *et al.* Characterizing the emergence and persistence of drug resistant mutations in HIV-1 subtype C infections using 454 ultra deep pyrosequencing. *BMC Infect*

Dis **13**, 52, doi:10.1186/1471-2334-13-52 (2013).
44 Allers, K. *et al.* Persistence of lamivudine-sensitive HIV-1 quasispecies in the presence of lamivudine in vitro and in vivo. *JAIDS Journal of Acquired Immune Deficiency Syndromes* **44**, 377-385 (2007).
45 Brenner, B. G. *et al.* Persistence and fitness of multidrug-resistant human immunodeficiency virus type 1 acquired in primary infection. *J Virol* **76**, 1753-1761 (2002).
46 Coffin, J. M. Genetic diversity and evolution of retroviruses. *Curr Top Microbiol Immunol* **176**, 143-164 (1992).
47 Katz, R. A. & Skalka, A. M. Generation of diversity in retroviruses. *Annu Rev Genet* **24**, 409-445, doi:10.1146/annurev.ge.24.120190.002205 (1990).
48 Pathak, V. K. & Temin, H. M. Broad spectrum of in vivo forward mutations, hypermutations, and mutational hotspots in a retroviral shuttle vector after a single replication cycle: deletions and deletions with insertions. *Proc Natl Acad Sci U S A* **87**, 6024-6028 (1990).
49 Paranjpe, S. *et al.* Subcompartmentalization of HIV-1 quasispecies between seminal cells and seminal plasma indicates their origin in distinct genital tissues. *AIDS research and human retroviruses* **18**, 1271-1280 (2002).
50 Schnell, G., Price, R. W., Swanstrom, R. & Spudich, S. Compartmentalization and clonal amplification of HIV-1 variants in the cerebrospinal fluid during primary infection. *Journal of virology* **84**, 2395-2407 (2010).
51 Hill, A. L., Rosenbloom, D. I. & Nowak, M. A. Evolutionary dynamics of HIV at multiple spatial and temporal scales. *Journal of molecular medicine* **90**, 543-561 (2012).
52 Domingo, E., Sheldon, J. & Perales, C. Viral quasispecies evolution. *Microbiology and Molecular Biology Reviews* **76**, 159-216 (2012).
53 Faria, N. R. *et al.* HIV epidemiology. The early spread and epidemic ignition of HIV-1 in human populations. *Science* **346**, 56-61, doi:10.1126/science.1256739 (2014).
54 Holzammer, S., Holznagel, E., Kaul, A., Kurth, R. & Norley, S. High virus loads in naturally and experimentally SIVagm-infected African green monkeys. *Virology* **283**, 324-331, doi:10.1006/viro.2001.0870 (2001).
55 Reeves, J. D. & Doms, R. W. Human immunodeficiency virus type 2. *J Gen Virol* **83**, 1253-1265, doi:10.1099/0022-1317-83-6-1253 (2002).
56 Thomson, M. M., Perez-Alvarez, L. & Najera, R. Molecular epidemiology of HIV-1 genetic forms and its significance for vaccine development and therapy. *Lancet Infect Dis* **2**, 461-471 (2002).
57 Kuiken, C. *et al. HIV Sequence Compendium 2008*. (Theoretical Biology and Biophysics, 2008).
58 Chan, D. C., Fass, D., Berger, J. M. & Kim, P. S. Core structure of gp41 from the HIV envelope glycoprotein. *Cell* **89**, 263-273 (1997).
59 Arrildt, K. T., Joseph, S. B. & Swanstrom, R. The HIV-1 env protein: a coat of many colors. *Curr HIV/AIDS Rep* **9**, 52-63, doi:10.1007/s11904-011-0107-3 (2012).
60 Berger, E. A. *et al.* A new classification for HIV-1. *Nature* **391**, 240, doi:10.1038/34571 (1998).
61 Daecke, J., Fackler, O. T., Dittmar, M. T. & Krausslich, H. G. Involvement of clathrin-mediated endocytosis in human immunodeficiency virus type 1 entry. *J Virol* **79**, 1581-1594, doi:10.1128/JVI.79.3.1581-1594.2005 (2005).
62 Chan, D. C. & Kim, P. S. HIV entry and its inhibition. *Cell* **93**, 681-684 (1998).
63 Baltimore, D. RNA-dependent DNA polymerase in virions of RNA tumour viruses. *Nature* **226**, 1209-1211 (1970).
64 Temin, H. M. & Mizutani, S. RNA-dependent DNA polymerase in virions of Rous sarcoma virus. *Nature* **226**, 1211-1213 (1970).
65 Miller, M. D., Farnet, C. M. & Bushman, F. D. Human immunodeficiency virus type 1 preintegration complexes: studies of organization and composition. *J Virol* **71**, 5382-5390

(1997).
66 Sherman, M. P., de Noronha, C. M., Heusch, M. I., Greene, S. & Greene, W. C. Nucleocytoplasmic shuttling by human immunodeficiency virus type 1 Vpr. *J Virol* **75**, 1522-1532, doi:10.1128/JVI.75.3.1522-1532.2001 (2001).
67 Taube, R., Fujinaga, K., Wimmer, J., Barboric, M. & Peterlin, B. M. Tat transactivation: a model for the regulation of eukaryotic transcriptional elongation. *Virology* **264**, 245-253, doi:10.1006/viro.1999.9944 (1999).
68 Pollard, V. W. & Malim, M. H. The HIV-1 Rev protein. *Annu Rev Microbiol* **52**, 491-532, doi:10.1146/annurev.micro.52.1.491 (1998).
69 Butsch, M. & Boris-Lawrie, K. Destiny of unspliced retroviral RNA: ribosome and/or virion? *J Virol* **76**, 3089-3094 (2002).
70 Zimmerman, C. *et al.* Identification of a host protein essential for assembly of immature HIV-1 capsids. *Nature* **415**, 88-92, doi:10.1038/415088a (2002).
71 Bangham, C. R. The immune control and cell-to-cell spread of human T-lymphotropic virus type 1. *J Gen Virol* **84**, 3177-3189, doi:10.1099/vir.0.19334-0 (2003).
72 Piguet, V. & Sattentau, Q. Dangerous liaisons at the virological synapse. *J Clin Invest* **114**, 605-610, doi:10.1172/JCI22812 (2004).
73 McDonald, D. *et al.* Recruitment of HIV and its receptors to dendritic cell-T cell junctions. *Science* **300**, 1295-1297, doi:10.1126/science.1084238 (2003).
74 Chen, B. K. T cell virological synapses and HIV-1 pathogenesis. *Immunol Res* **54**, 133-139, doi:10.1007/s12026-012-8320-8 (2012).
75 Jolly, C., Mitar, I. & Sattentau, Q. J. Adhesion molecule interactions facilitate human immunodeficiency virus type 1-induced virological synapse formation between T cells. *J Virol* **81**, 13916-13921, doi:10.1128/JVI.01585-07 (2007).
76 Rudnicka, D. *et al.* Simultaneous cell-to-cell transmission of human immunodeficiency virus to multiple targets through polysynapses. *J Virol* **83**, 6234-6246, doi:10.1128/JVI.00282-09 (2009).
77 Vasiliver-Shamis, G. *et al.* Human immunodeficiency virus type 1 envelope gp120 induces a stop signal and virological synapse formation in noninfected CD4+ T cells. *J Virol* **82**, 9445-9457, doi:10.1128/JVI.00835-08 (2008).
78 Lekkerkerker, A. N., van Kooyk, Y. & Geijtenbeek, T. B. Viral piracy: HIV-1 targets dendritic cells for transmission. *Curr HIV Res* **4**, 169-176 (2006).
79 Piguet, V. & Steinman, R. M. The interaction of HIV with dendritic cells: outcomes and pathways. *Trends Immunol* **28**, 503-510, doi:10.1016/j.it.2007.07.010 (2007).
80 Arrighi, J. F. *et al.* DC-SIGN-mediated infectious synapse formation enhances X4 HIV-1 transmission from dendritic cells to T cells. *J Exp Med* **200**, 1279-1288, doi:10.1084/jem.20041356 (2004).
81 Geijtenbeek, T. B. *et al.* DC-SIGN, a dendritic cell-specific HIV-1-binding protein that enhances trans-infection of T cells. *Cell* **100**, 587-597 (2000).
82 Izquierdo-Useros, N. *et al.* HIV-1 capture and transmission by dendritic cells: the role of viral glycolipids and the cellular receptor Siglec-1. *PLoS Pathog* **10**, e1004146, doi:10.1371/journal.ppat.1004146 (2014).
83 Geijtenbeek, T. B. *et al.* DC-SIGN-ICAM-2 interaction mediates dendritic cell trafficking. *Nat Immunol* **1**, 353-357, doi:10.1038/79815 (2000).
84 Duncan, C. J., Russell, R. A. & Sattentau, Q. J. High multiplicity HIV-1 cell-to-cell transmission from macrophages to CD4+ T cells limits antiretroviral efficacy. *AIDS* **27**, 2201-2206 (2013).
85 Duncan, C. J. *et al.* High-multiplicity HIV-1 infection and neutralizing antibody evasion mediated by the macrophage-T cell virological synapse. *J Virol* **88**, 2025-2034, doi:10.1128/JVI.03245-13 (2014).
86 Phillips, D. M. The role of cell-to-cell transmission in HIV infection. *AIDS* **8**, 719-731 (1994).

87 Sewald, X. *et al.* Retroviruses use CD169-mediated trans-infection of permissive lymphocytes to establish infection. *Science* **350**, 563-567, doi:10.1126/science.aab2749 (2015).
88 Boulle, M. *et al.* HIV Cell-to-Cell Spread Results in Earlier Onset of Viral Gene Expression by Multiple Infections per Cell. *PLoS Pathog* **12**, e1005964, doi:10.1371/journal.ppat.1005964 (2016).
89 Gupta, P., Balachandran, R., Ho, M., Enrico, A. & Rinaldo, C. Cell-to-cell transmission of human immunodeficiency virus type 1 in the presence of azidothymidine and neutralizing antibody. *J Virol* **63**, 2361-2365 (1989).
90 Sattentau, Q. Avoiding the void: cell-to-cell spread of human viruses. *Nat Rev Microbiol* **6**, 815-826, doi:10.1038/nrmicro1972 (2008).
91 Chen, P., Hubner, W., Spinelli, M. A. & Chen, B. K. Predominant mode of human immunodeficiency virus transfer between T cells is mediated by sustained Env-dependent neutralization-resistant virological synapses. *J Virol* **81**, 12582-12595, doi:10.1128/JVI.00381-07 (2007).
92 Schiffner, T., Sattentau, Q. J. & Duncan, C. J. Cell-to-cell spread of HIV-1 and evasion of neutralizing antibodies. *Vaccine* **31**, 5789-5797, doi:10.1016/j.vaccine.2013.10.020 (2013).
93 Boullé, M. *et al.* HIV Cell-to-Cell Spread Results in Earlier Onset of Viral Gene Expression by Multiple Infections per Cell. *PLoS Pathog* **12**, e1005964 (2016).
94 Dang, Q. *et al.* Nonrandom HIV-1 infection and double infection via direct and cell-mediated pathways. *Proc Natl Acad Sci U S A* **101**, 632-637, doi:10.1073/pnas.0307636100 (2004).
95 Dixit, N. M. & Perelson, A. S. Multiplicity of human immunodeficiency virus infections in lymphoid tissue. *J Virol* **78**, 8942-8945, doi:10.1128/JVI.78.16.8942-8945.2004 (2004).
96 Reh, L. *et al.* Capacity of Broadly Neutralizing Antibodies to Inhibit HIV-1 Cell-Cell Transmission Is Strain- and Epitope-Dependent. *PLoS Pathog* **11**, e1004966 (2015).
97 Russell, R. A., Martin, N., Mitar, I., Jones, E. & Sattentau, Q. J. Multiple proviral integration events after virological synapse-mediated HIV-1 spread. *Virology* **443**, 143-149 (2013).
98 Sigal, A. *et al.* Cell-to-cell spread of HIV permits ongoing replication despite antiretroviral therapy. *Nature* **477**, 95-98 (2011).
99 Zhong, P. *et al.* Cell-to-cell transmission can overcome multiple donor and target cell barriers imposed on cell-free HIV. *PLoS One* **8**, e53138 (2013).
100 Ladinsky, M. S. *et al.* Electron tomography of HIV-1 infection in gut-associated lymphoid tissue. *PLoS Pathog* **10**, e1003899, doi:10.1371/journal.ppat.1003899 (2014).
101 Cavert, W. *et al.* Kinetics of response in lymphoid tissues to antiretroviral therapy of HIV-1 infection. *Science* **276**, 960-964 (1997).
102 Yuda, F., Terashima, K., Dobashi, M., Ishikawa, M. & Imai, Y. Ultrastructural analysis of HNK-1+ cells in human peripheral blood and lymph nodes. *Histol Histopathol* **4**, 137-152 (1989).
103 Perreau, M. *et al.* Follicular helper T cells serve as the major CD4 T cell compartment for HIV-1 infection, replication, and production. *J Exp Med* **210**, 143-156, doi:10.1084/jem.20121932 (2013).
104 Banga, R. *et al.* PD-1(+) and follicular helper T cells are responsible for persistent HIV-1 transcription in treated aviremic individuals. *Nat Med* **22**, 754-761, doi:10.1038/nm.4113 (2016).
105 Josefsson, L. *et al.* Majority of CD4+ T cells from peripheral blood of HIV-1–infected individuals contain only one HIV DNA molecule. *Proceedings of the National Academy of Sciences* **108**, 11199-11204 (2011).
106 Descours, B. *et al.* CD32a is a marker of a CD4 T-cell HIV reservoir harbouring replication-competent proviruses. *Nature* **543**, 564-567 (2017).

107 Brenchley, J. M. *et al.* CD4+ T cell depletion during all stages of HIV disease occurs predominantly in the gastrointestinal tract. *J Exp Med* **200**, 749-759 (2004).
108 Finkel, T. H. *et al.* Apoptosis occurs predominantly in bystander cells and not in productively infected cells of HIV- and SIV-infected lymph nodes. *Nat Med* **1**, 129-134 (1995).
109 Mattapallil, J. J. *et al.* Massive infection and loss of memory CD4+ T cells in multiple tissues during acute SIV infection. *Nature* **434**, 1093-1097 (2005).
110 Hill, A. L., Rosenbloom, D. I., Fu, F., Nowak, M. A. & Siliciano, R. F. Predicting the outcomes of treatment to eradicate the latent reservoir for HIV-1. *Proceedings of the National Academy of Sciences* **111**, 13475-13480 (2014).
111 Charpentier, C., Nora, T., Tenaillon, O., Clavel, F. & Hance, A. J. Extensive recombination among human immunodeficiency virus type 1 quasispecies makes an important contribution to viral diversity in individual patients. *J Virol* **80**, 2472-2482, doi:10.1128/JVI.80.5.2472-2482.2006 (2006).
112 Gelderblom, H. C. *et al.* Viral complementation allows HIV-1 replication without integration. *Retrovirology* **5**, 60, doi:10.1186/1742-4690-5-60 (2008).
113 Mo, H., Lu, L., Pithawalla, R., Kempf, D. J. & Molla, A. Complementation in cells cotransfected with a mixture of wild-type and mutant human immunodeficiency virus (HIV) influences the replication capacities and phenotypes of mutant variants in a single-cycle HIV resistance assay. *J Clin Microbiol* **42**, 4169-4174, doi:10.1128/JCM.42.9.4169-4174.2004 (2004).
114 Levy, D. N., Aldrovandi, G. M., Kutsch, O. & Shaw, G. M. Dynamics of HIV-1 recombination in its natural target cells. *Proceedings of the National Academy of Sciences* **101**, 4204-4209 (2004).
115 Andino, R. & Domingo, E. Viral quasispecies. *Virology* **479-480**, 46-51, doi:10.1016/j.virol.2015.03.022 (2015).
116 Vignuzzi, M., Stone, J. K., Arnold, J. J., Cameron, C. E. & Andino, R. Quasispecies diversity determines pathogenesis through cooperative interactions in a viral population. *Nature* **439**, 344-348, doi:10.1038/nature04388 (2006).
117 Froissart, R. *et al.* Co-infection weakens selection against epistatic mutations in RNA viruses. *Genetics* **168**, 9-19, doi:10.1534/genetics.104.030205 (2004).
118 Freed, E. O. HIV-1 replication. *Somatic cell and molecular genetics* **26**, 13-33 (2001).
119 Patel, A. P. *et al.* Single-cell RNA-seq highlights intratumoral heterogeneity in primary glioblastoma. *Science* **344**, 1396-1401 (2014).
120 Gaublomme, J. T. *et al.* Single-Cell Genomics Unveils Critical Regulators of Th17 Cell Pathogenicity. *Cell* **163**, 1400-1412, doi:10.1016/j.cell.2015.11.009
S0092-8674(15)01489-0 [pii] (2015).
121 Kimmerling, R. J. *et al.* A microfluidic platform enabling single-cell RNA-seq of multigenerational lineages. *Nat Commun* **7**, 10220, doi:10.1038/ncomms10220
ncomms10220 [pii] (2016).
122 Tirosh, I. *et al.* Dissecting the multicellular ecosystem of metastatic melanoma by single-cell RNA-seq. *Science* **352**, 189-196, doi:10.1126/science.aad0501
352/6282/189 [pii] (2016).
123 Macosko, E. Z. *et al.* Highly Parallel Genome-wide Expression Profiling of Individual Cells Using Nanoliter Droplets. *Cell* **161**, 1202-1214, doi:10.1016/j.cell.2015.05.002
S0092-8674(15)00549-8 [pii] (2015).
124 Thomsen, E. R. *et al.* Fixed single-cell transcriptomic characterization of human radial glial diversity. *Nat Methods* **13**, 87-93, doi:10.1038/nmeth.3629 (2016).

eLIFE elifesciences.org

RESEARCH ARTICLE

Incomplete inhibition of HIV infection results in more HIV infected lymph node cells by reducing cell death

Laurelle Jackson[1,2†], Jessica Hunter[1,2†], Sandile Cele[1], Isabella Markham Ferreira[1,2], Andrew C Young[1,3], Farina Karim[1], Rajhmun Madansein[4,5], Kaylesh J Dullabh[4], Chih-Yuan Chen[4], Noel J Buckels[4], Yashica Ganga[1], Khadija Khan[1], Mikael Boulle[1], Gila Lustig[1], Richard A Neher[6,7], Alex Sigal[1,2,8*]

[1]Africa Health Research Institute, Durban, South Africa; [2]School of Laboratory Medicine and Medical Sciences, University of KwaZulu-Natal, Durban, South Africa; [3]Department of Neurology, Massachusetts General Hospital and Harvard Medical School, Boston, United States; [4]Department of Cardiothoracic Surgery, University of KwaZulu-Natal, Durban, South Africa; [5]Centre for the AIDS Programme of Research in South Africa, Durban, South Africa; [6]Biozentrum, University of Basel, Basel, Switzerland; [7]SIB Swiss Institute of Bioinformatics, Basel, Switzerland; [8]Max Planck Institute for Infection Biology, Berlin, Germany

Abstract HIV has been reported to be cytotoxic in vitro and in lymph node infection models. Using a computational approach, we found that partial inhibition of transmissions of multiple virions per cell could lead to increased numbers of live infected cells. If the number of viral DNA copies remains above one after inhibition, then eliminating the surplus viral copies reduces cell death. Using a cell line, we observed increased numbers of live infected cells when infection was partially inhibited with the antiretroviral efavirenz or neutralizing antibody. We then used efavirenz at concentrations reported in lymph nodes to inhibit lymph node infection by partially resistant HIV mutants. We observed more live infected lymph node cells, but with fewer HIV DNA copies per cell, relative to no drug. Hence, counterintuitively, limited attenuation of HIV transmission per cell may increase live infected cell numbers in environments where the force of infection is high.
DOI: https://doi.org/10.7554/eLife.30134.001

***For correspondence:** alex.sigal@k-rith.org

[†]These authors contributed equally to this work

Competing interest: See page 17

Funding: See page 17

Received: 18 July 2017
Accepted: 08 March 2018
Published: 20 March 2018

Reviewing editor: Wenying Shou, Fred Hutchinson Cancer Research Center, United States

Introduction

HIV infection is known to result in extensive T cell depletion in lymph node environments (***Sanchez et al., 2015***), where infection is most robust (***Brenchley et al., 2004***; ***Doitsh et al., 2010***; ***Doitsh et al., 2014***; ***Finkel et al., 1995***; ***Galloway et al., 2015***; ***Mattapallil et al., 2005***). Depletion of HIV infectable target cells, in addition to onset of immune control, is thought to account for the decreased replication ratio of HIV from an initial peak in early infection (***Bonhoeffer et al., 1997***; ***Nowak and May, 2000***; ***Perelson, 2002***; ***Phillips, 1996***; ***Quiñones-Mateu and Arts, 2006***; ***Ribeiro et al., 2010***; ***Wodarz and Levy, 2007***). This is consistent with observations that individuals are most infectious in the initial, acute stage of infection, where the target cell population is relatively intact and produces high viral loads (***Hollingsworth et al., 2008***; ***Wawer et al., 2005***).

T-cell death occurs by several mechanisms, which are either directly or indirectly mediated by HIV infection. Accumulation of incompletely reverse transcribed HIV transcripts is sensed by interferon-γ–inducible protein 16 (***Monroe et al., 2014***) and leads to pyroptotic death of incompletely infected

eLife digest The HIVvirus infects cells of the immune system. Once inside, it hijacks the cellular molecular machineries to make more copies of itself, which are then transmitted to new host cells. HIV eventually kills most cells it infects, either in the steps leading to the infection of the cell, or after the cell is already producing virus. HIV can spread between cells in two ways, known as cell-free or cell-to-cell. In the first, individual viruses are released from infected cells and move randomly through the body in the hope of finding new cells to infect. In the second, infected cells interact directly with uninfected cells. The second method is often much more successful at infecting new cells since they are exposed to multiple virus particles.

HIV infections can be controlled by using combinations of antiretroviral drugs, such as efavirenz, to prevent the virus from making more of itself. With a high enough dose, the drugs can in theory completely stop HIV infections, unless the virus becomes resistant to treatment. However, some patients continue to use these drugs even after the virus they are infected with develops resistance. It is not clear what effect taking ineffective, or partially effective, drugs has on how HIV progresses.

Using efavirenz, Jackson, Hunter et al. partially limited the spread of HIV between human cells grown in the laboratory. The experiments mirrored the situation where a partially resistant HIV strain spreads through the body. The results show that the success of cell-free infection is reduced as drug dose increases. Yet paradoxically, in cell-to-cell infection, the presence of drug caused more cells to become infected. This can be explained by the fact that, in cell-to-cell spread, each cell is exposed to multiple copies of the virus. The drug dose reduced the number of viral copies per cell without stopping the virus from infecting completely. The reduced number of viral copies per cell made it more likely that infected cells would survive the infection long enough to produce virus particles themselves.

Viruses that can kill cells, such as HIV, must balance the need to make more of themselves against the speed that they kill their host cell to maximize the number of infected cells. If transmission between cells is too effective and too many virus particles are delivered to the new cell, the virus may not manage to infect new hosts before killing the old ones. These findings highlight this delicate balance. They also indicate a potential issue in using drugs to treat partially resistant virus strains. Without care, these treatments could increase the number of infected cells in the body, potentially worsening the effects of living with HIV.

DOI: https://doi.org/10.7554/eLife.30134.002

cells by initiating a cellular defence program involving the activation of caspase 1 (***Doitsh et al., 2010***; ***Doitsh et al., 2014***; ***Galloway et al., 2015***). HIV proteins Tat and Env have also been shown to lead to cell death of infected cells through CD95-mediated apoptosis following T-cell activation (***Banda et al., 1992***; ***Westendorp et al., 1995a***; ***Westendorp et al., 1995b1995***). Using SIV infection, it has been shown that damage to lymph nodes due to chronic immune activation leads to an environment less conducive to T-cell survival (***Zeng et al., 2012***). Finally, double strand breaks in the host DNA caused by integration of the reverse transcribed virus results in cell death by the DNA-PK-mediated activation of the p53 response (***Cooper et al., 2013***).

The lymph node environment is conducive to HIV infection due to: (1) presence of infectable cells (***Deleage et al., 2016***; ***Embretson et al., 1993***; ***Tenner-Racz et al., 1998***); (2) proximity of cells to each other and lack of flow which should enable cell-to-cell HIV spread (***Baxter et al., 2014***; ***Dale et al., 2011***; ***Groot et al., 2008***; ***Groppelli et al., 2015***; ***Gummuluru et al., 2002***; ***Hübner et al., 2009***; ***Jolly et al., 2004***; ***Jolly et al., 2011***; ***Münch et al., 2007***; ***Sherer et al., 2007***; ***Sourisseau et al., 2007***; ***Sowinski et al., 2008***); (3) decreased penetration of antiretroviral therapy (ART) (***Fletcher et al., 2014a***). Multiple infections per cell have been reported in cell-to-cell spread of HIV (***Baxter et al., 2014***; ***Boullé et al., 2016***; ***Dang et al., 2004***; ***Del Portillo et al., 2011***; ***Dixit and Perelson, 2004***; ***Duncan et al., 2013***; ***Law et al., 2016***; ***Reh et al., 2015***; ***Russell et al., 2013***; ***Sigal et al., 2011***; ***Zhong et al., 2013***). In this mode of HIV transmission, an interaction between the infected donor cell and the uninfected target results in directed transmission of large numbers of virions (***Baxter et al., 2014***; ***Groppelli et al., 2015***; ***Hübner et al., 2009***; ***Sowinski et al., 2008***). This is in contrast to cell-free infection, where free-floating virus finds target

cells through diffusion. Both modes occur simultaneously when infected donor cells are cocultured with targets. However, the cell-to-cell route is thought to be the main cause of multiple infections per cell (**Hübner et al., 2009**). In the lymph nodes, several studies showed multiple infections (**Gratton et al., 2000**; **Jung et al., 2002**; **Law et al., 2016**) while another study did not (**Josefsson et al., 2013**). One explanation for the divergent results is that different cell subsets are infected to different degrees. For example, T cells were shown not to be multiply infected in the peripheral blood compartment (**Josefsson et al., 2011**). However, more recent work investigating markers associated with HIV latency in the face of ART found that the average number of HIV DNA copies per cell is greater than one in 3 out of 12 individuals. This occurred in the face of ART in the CD3-positive, CD32a high CD4 T-cell subset (**Descours et al., 2017**). In the absence of suppressive ART, it would be expected that the number of HIV DNA copies per cell would be higher.

Multiple viral integration attempts per cell may increase the probability of death. One consequence of HIV-mediated death may be that attenuation of infection may increase viral replication by increasing the number of live targets. Indeed, it has been suggested that more attenuated HIV strains result in more successful infections in terms of the ability of the virus to replicate in the infected individual (**Ariën et al., 2005**; **Nowak and May, 2000**; **Payne et al., 2014**; **Quiñones-Mateu and Arts, 2006**; **Wodarz and Levy, 2007**).

Here, we experimentally examined the effect of attenuating cell-to-cell spread by using HIV inhibitors. We observed that partially inhibiting infection with drug or antibody resulted in an increase in the number of live infected cells in both a cell line and in lymph node cells. This is, to our knowledge, the first experimental demonstration at the cellular level that attenuation of HIV infection can result in an increase in live infected cells under specific infection conditions.

Results

We introduce a model of infection where each donor to target transmission leads to an infection probability r and death probability q per infection attempt. In our experimental system, one infection attempt is measured as one HIV DNA copy, whether integrated or unintegrated. The probability of successful infection of a target cell given n infection attempts is $1-(1-r)^n$ (**Sigal et al., 2011**). We define L_n as the probability of a cell to survive infection in the face of n infection attempts. Assuming infection attempts act independently, $L_n=(1-q)^n$. The probability of a cell to be infected and not die after it has been exposed to n infection attempts is therefore:

$$P_n = (1-(1-r)^n)(1-q)^n \tag{1}$$

This model makes several simplifying assumptions: (1) all infection attempts have equal probabilities to infect targets. (2) The probability for a cell to die from each transmission is equal between transmissions. (3) Infection attempts act independently, and productive infection and death are independent events. In this model, r and q capture the probabilities for a cell to be infected or die post-reverse transcription. For example, mutations which reduce viral fitness by decreasing the probability of HIV to integrate would reduce r, while mutations which reduce the probability of successful reverse transcription would reduce n.

If the number of infection attempts n is Poisson distributed with mean λ, the probability for a cell to be infected is $1-e^{-r\lambda}$ and the probability of a cell to live is $L_n = e^{-q\lambda}$ (see **Supplementary file 1** for parameters and definitions). As derived in Appendix 1, the probability that a cell is productively infected will be:

$$P_\lambda = e^{-\lambda q}\left(1-e^{-\lambda r(1-q)}\right) \tag{2}$$

Since antiretroviral drugs lead to a reduction in the number of infection attempts by, for example, decreasing the probability of reverse transcription in the case of reverse transcriptase inhibitors, we introduced a drug strength value d, where $d = 1$ in the absence of drug and $d > 1$ in the presence of drug. In the presence of drug, λ is decreased to λ/d. The drug therefore tunes λ, and if the antiretroviral regimen is fully suppressive, λ/d is expected to be below what is required for ongoing replication. The probability of a cell to be infected and live given drug strength d is therefore:

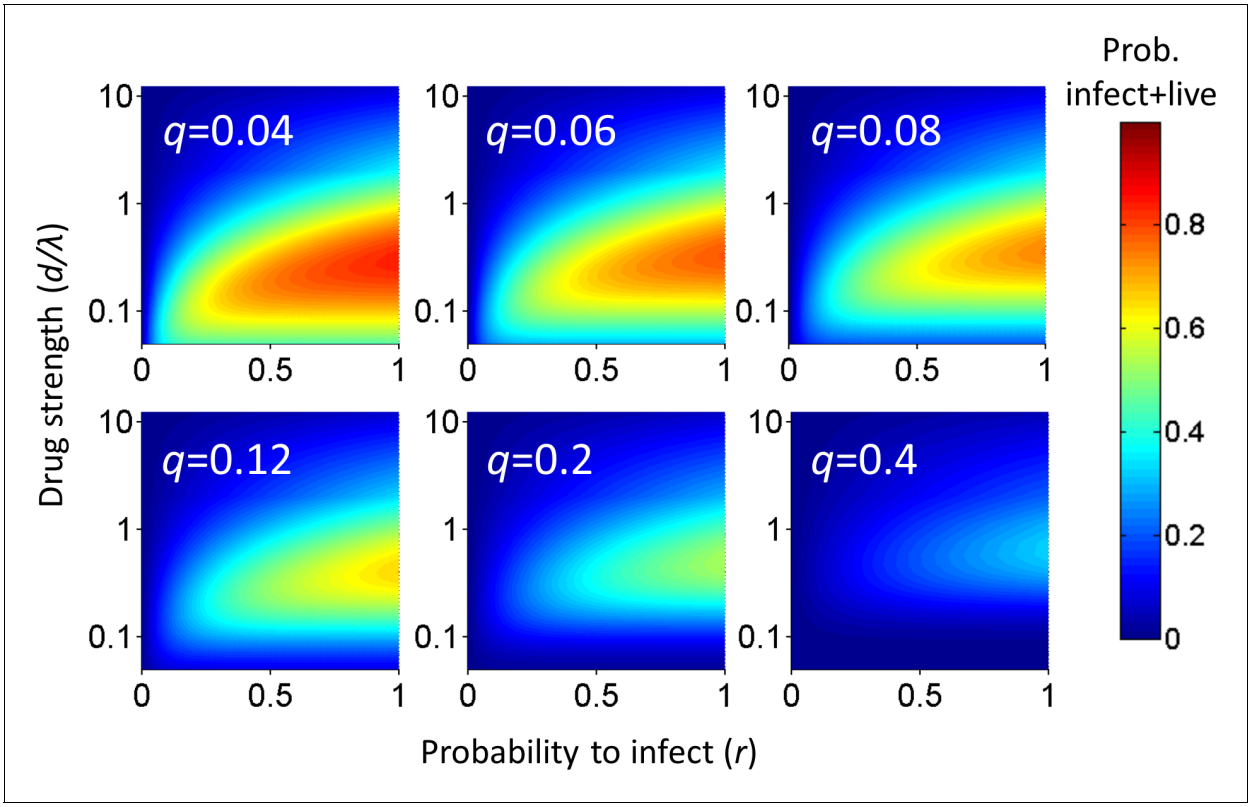

Figure 1. Probability for a cell to be infected and live as a function of inhibitor. Probability for a cell to be infected and live was calculated for 20 infection attempts (λ) and represented as a heat map. Drug strength (*d/λ)* is on the y-axis, and the probability per infection attempt to infect (r) is on the x-axis. Each plot is the calculation for one value of the probability per infection attempt to die (q) denoted in white in the top left corner.
DOI: https://doi.org/10.7554/eLife.30134.003

$$P_{\lambda/d} = e^{-\lambda q/d}\left(1 - e^{-\lambda r(1-q)/d}\right) \quad (3)$$

Analysis of the probability of a cell to survive and be infected as a function of *r* and *q* shows that at each drug strength *d/λ*, P_λ increases as the probability of infection *r* increases (***Figure 1***). Hence, the value of *r* strongly influences the amplitude of P_λ. How P_λ behaves when drug strength *d/λ* increases depends on the parameter values of *r* and *q*. A subset of parameter values results in a peak in the number of infected cells at intermediate *d/λ*, decreasing as drug strength increases further (***Figure 1***). We refer to such a peak in infected numbers as an infection optimum. As *q* increases, the cost of multiple infections per cell increases, and the infection optimum shifts to higher *d/λ* values. A fall from the infection optimum at decreasing *d/λ* is driven by increasing cell death as a result of increasing infection attempts per cell. This slope is therefore shallower, and peaks broader, at low *q* values (***Figure 1***).

Our model assumes that cellular infection and death due to an HIV infection attempt are independent processes. This is based on observations that support a role for cell death as a cellular defence mechanism which may occur before productive infection, such as programmed cell death triggered by HIV integration induced DNA damage (***Cooper et al., 2013***). An alternative model is that HIV-mediated cell death depends on productive infection. This would be consistent with cell death due to, for example, expression of viral proteins (***Westendorp et al., 1995b1995***). Since the concentration of viral proteins may also scale with the number of infections per cell, we derived the mathematical model for such a process in the supplementary mathematical analysis. The models are equivalent, showing that independence of cell death and infection is not a necessary condition for an infection optimum to occur in the presence of inhibitor.

Given that an infection optimum is dependent on parameter values, we next examined whether these parameter values occur experimentally in HIV infection. We therefore first tested for an infection optimum in the RevCEM cell line engineered to express GFP upon HIV Rev protein expression (**Wu et al., 2007**). We subcloned the cell line to maximize the frequency of GFP-positive cells upon infection (**Boullé et al., 2016**). We needed to detect the number of infection attempts per cell λ. To estimate this, we used PCR to detect the number of reverse transcribed copies of viral DNA in the cell by splitting each individual infected cell over multiple wells. We then detected the number of wells with HIV DNA by PCR amplification of the reverse transcriptase gene. Hence, the number of positive wells indicated the minimum number of viral DNA copies per cell, since more than one copy can be contained within the same well (**Josefsson et al., 2011**; **Josefsson et al., 2013**). We first measured the number of viral DNA copies in ACH-2 cells, reported to contain a single inactive HIV integration per genome (**Chun et al., 1997**; **O'Doherty et al., 2002**). We sorted a total of 166 ACH-2 cells at one cell per well into lysis buffer and subdivided single-cell lysates into four wells (**Figure 2—figure supplement 1A**). About one quarter of cells showed a PCR product of the expected size. Cells with more than one HIV copy per cell were very rare and may reflect either errors in cell sorting or dividing cells (**Figure 2—figure supplement 1B**). Similar frequencies were obtained when the ACH-2 cell line was subcloned or split over 10 wells (**Figure 2—figure supplement 1C**). Given that each ACH-2 cell contains one HIV DNA copy, the frequency of detection indicated our detection efficiency per HIV DNA copy.

To investigate the effect of multiple infection attempts per cell, we used coculture infection, where infected (donor) cells are co-incubated with uninfected (target) cells and lead to cell-to-cell spread. We used approximately 2% infected donor cells as our input, and detected the number of HIV DNA copies per cell by flow cytometric sorting of individual GFP-positive cells followed by splitting each cell lysate over 10 wells. Wells were then amplified by PCR and visualized on an agarose gel (**Figure 2A**). We assayed 60 cells and obtained a wide distribution of viral DNA copies per cell, which ranged from 0 to 9 copies (**Figure 2B**). The range of HIV DNA copies per cell fit a Poisson distribution with two means better than either a single mean Gaussian or Poisson distribution. However, the fit of the two mean Poisson distribution did not show two obvious peaks, and instead seemed to fit the data better due to the addition of fit parameters (**Figure 2—figure supplement 2**). Hence we cannot conclude that the distribution is bimodal. We also detected the HIV copy number in 30 GFP-positive cells infected by cell-free HIV. HIV in cell-free form was obtained by filtering supernatant from HIV producing cells to exclude cells or cell fragments, then infecting target cells with the filtered virus. Infection with this virus is defined here as cell-free infection. In this case, we detected either zero or one HIV copy per cell (**Figure 2B** inset). The frequency of single HIV DNA copies was 0.23, identical to the measured result in the ACH-2 cell line. We computationally corrected the detected number of DNA copies in coculture infection for the sensitivity of our PCR reaction as determined by the ACH-2 results (Materials and methods). On average we obtained 15 ± 3 copies per cell after correction.

To tune λ, we added the HIV reverse transcriptase inhibitor efavirenz (EFV) to infections. To calculate d, we used cell-free infection (**Figure 2C**, see **Figure 2—figure supplement 3** for logarithmic y-axis plot), which as verified above, results in single HIV copies per cell. For cell-free infection, we approximate $d = 1/Tx$, where Tx is defined as the number of infected cells with drug divided by the number of infected cells without drug with single infection attempts (see Materials and methods and [(**Sigal et al., 2011**]). This is equivalent to 1-ε in a commonly used model describing the effect of inhibitors on infection. In this model, ε is drug effectiveness, with the 50% inhibitory drug concentration (IC_{50}) and the Hill coefficient for drug action as parameter values (**Canini and Perelson, 2014**; **Shen et al., 2008**). We fit the observed response of infection to EFV using this approach to estimate d across a range of EFV concentrations. Fit of the model to the cell-free data using wild type, EFV-sensitive HIV showed a monotonic decrease with IC_{50} = 2.9 nM and Hill coefficient of 2.1 (**Figure 2C**, black line).

We next dialed in EFV to tune λ/d in coculture infection. To obtain the number of infected target cells, and specifically exclude donor cells or donor-target cell fusions, target cells were marked by the expression of mCherry. Donor cells were stained with the vital stain Cell Trace Far Red (CTFR). The concentration of live infected cells was determined after 2 days in coculture with infected donors. Live infected cells were identified based on the absence of cell death indicator dye DAPI fluorescence, and presence of GFP. The input of infected donor cells was excluded from the count

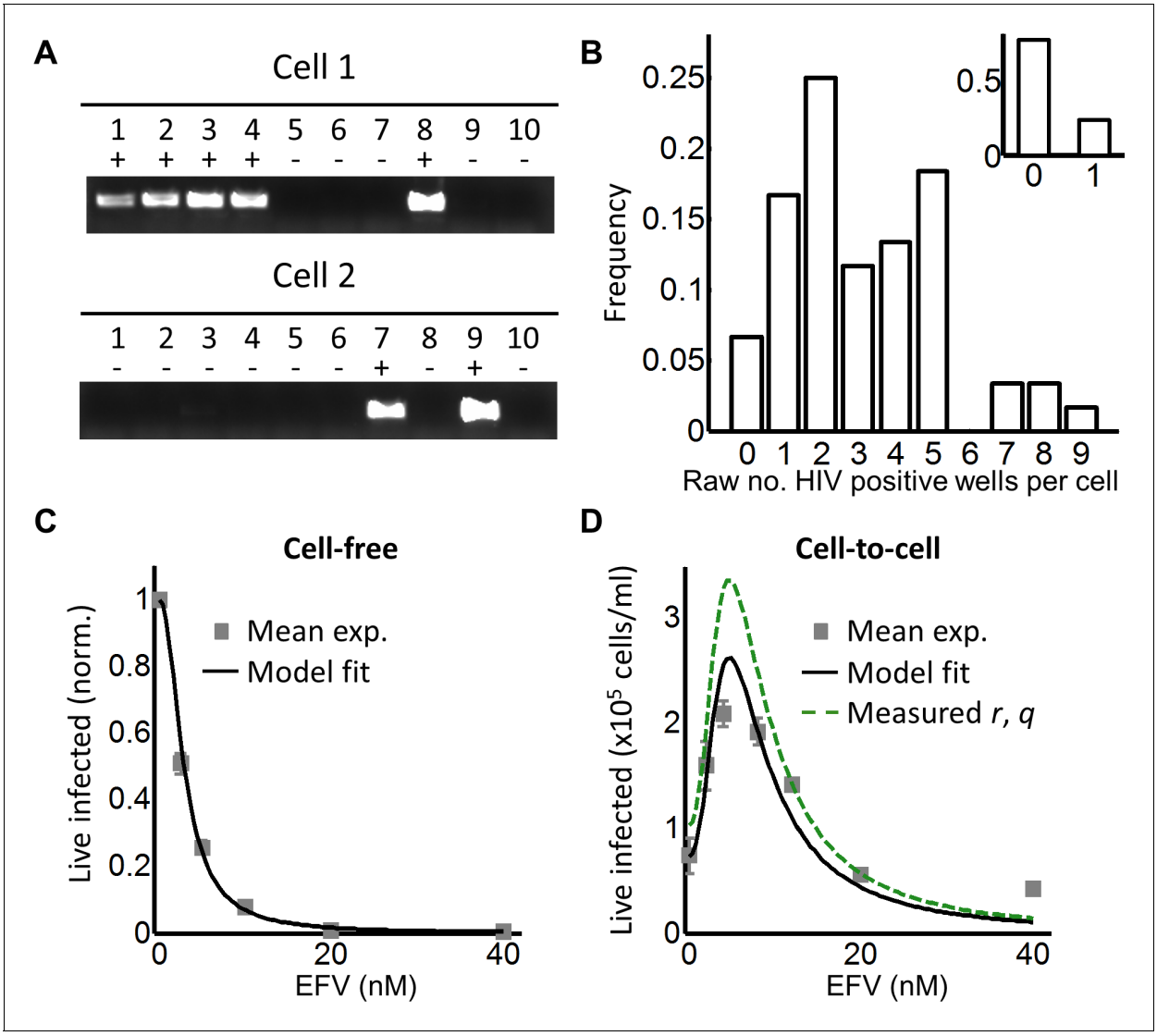

Figure 2. Partial inhibition increases the number of live infected cells. (**A**) To quantify HIV DNA copy number per cell, GFP-positive cells were sorted into individual wells and lysed. Each lysate was subdivided into 10 wells and PCR performed to detect HIV DNA, with the sum of positive wells being the raw HIV copy number for that cell. (**B**) Histogram of raw HIV DNA copies per cell in coculture infection (n = 60 cells, four independent experiments). Inset shows raw HIV DNA copies per cell in cell-free infection (n = 30, two independent experiments) (**C**) Number of live infected cells normalized by maximum number of live infected cells in cell-free infection with EFV. Black line is best-fit for EFV suppression of cell-free infection (IC_{50} = 2.9 nM, h = 2.1). Means and standard errors for three independent experiments. (**D**) Number of live infected cells/ml 2 days post-infection resulting from coculture infection of 10^6 cells/ml in the presence of EFV. Means and standard errors for three independent experiments. Black line is best-fit of ***Equation (3)*** with r = 0.22 and q = 0.17. Dashed green line is the result of ***Equation (3)*** with experimentally measured r = 0.28, q = 0.15.

DOI: https://doi.org/10.7554/eLife.30134.004

The following figure supplements are available for figure 2:

Figure supplement 1. Detected integrations in ACH-2 cells.

DOI: https://doi.org/10.7554/eLife.30134.005

Figure supplement 2. Fitting of different distributions to the frequency of HIV DNA copies per cell.

DOI: https://doi.org/10.7554/eLife.30134.006

Figure supplement 3. The number of live infected cells in cell-free infection with wild-type HIV.

DOI: https://doi.org/10.7554/eLife.30134.007

Figure supplement 4. Gating strategy for coculture infection with wild type HIV.

DOI: https://doi.org/10.7554/eLife.30134.008

Figure supplement 5. Experimental measurement of r and q.

DOI: https://doi.org/10.7554/eLife.30134.009

Figure 2 continued on next page

Figure 2 continued

Figure supplement 6. Time-lapse microscopy of HIV infection in the absence and presence of EFV.
DOI: https://doi.org/10.7554/eLife.30134.010

of infected cells based on the absence of mCherry fluorescence. Donor-target cell fusions were excluded by excluding CTFR-positive cells (see ***Figure 2—figure supplement 4*** for gating strategy).

While the percent of infected cells was reduced with drug, the concentration of live infected cells increased (***Figure 2—figure supplement 4***). We observed a peak in the number of live infected target cells at 4 nM EFV (***Figure 2D***). We then fit the number of live infected cells using ***Equation (3)***, where P_λ was multiplied by the input number of target cells per ml (10^6 cells/ml) to obtain the predicted number of live infected cells per ml of culture. This was done to constrain r in the model, which strongly determines the amplitude of $P_{\lambda/d}$ as described above. ***Equation (3)*** best fit the behaviour of infection when r = 0.22 *and* q = 0.17, resulting in a peak at 4.8 nM EFV (***Figure 2D***, black line). Hence an infection optimum is present in the cell line infection system.

In order to determine whether the fitted r and q values were within a reasonable range, we measured these values experimentally. To measure r, we infected with cell-free HIV to avoid the broad distribution of HIV copy numbers observed in cell-to-cell spread, and determined the fraction of live infected cells P_λ (***Figure 2—figure supplement 5A***). We then determined the mean number of HIV copies per cell λ for the same set of experiments corrected by the efficiency of detection (***Figure 2—figure supplement 5B***). The parameter r was calculated as $-ln(1-P_\lambda)/\lambda$ (***Supplementary file 2***). To measure q, we blocked cell division using serum starvation to measure differences in cell concentration due to cell death only, and not due to proliferation of uninfected cells (***Figure 2—figure supplement 5C***). We then infected with cell-free HIV and measured L_λ, defined as the fraction of live cells remaining upon infection with λ HIV DNA copies relative to infection blocked with EFV (see below). To specifically detect the decrease in live cells as a result of events downstream of reverse transcription, we compared infected cells to cells exposed to the same virus concentration but treated with 40 nM EFV, a drug concentration where infection by cell-free virus is negligible (***Figure 2—figure supplement 3***). q was then calculated as $-ln(L_\lambda)/\lambda$, where L_λ was the probability of a cell to live given transmission with λ copies (***Supplementary file 2***). Measured r and q values were 0.28 ± 0.08 and 0.15 ± 0.07 (mean ±standard deviation), respectively. The solution to ***Equation (3)*** using these values showed similar behavior to the solution with the fitted values for wild-type HIV infection, indicating that the fitted values gave a reasonable approximation of the behavior of the system (***Figure 2D***, dashed green line).

In order to investigate the dynamics of cell depletion due to cell-to-cell HIV spread and its modulation by the addition of an inhibitor, we performed time-lapse microscopy over a two day infection window. While infection parameters were different due to the constraints of visualizing cells (Materials and methods), the general trend from the data was deterioration in the number of live cells in the time-lapse culture starting at 1 day post-infection when no drug was added. The deterioration in live cell numbers was averted by the addition of EFV (***Figure 2—figure supplement 6***).

We next investigated whether an infection optimum occurs with EFV-resistant HIV. To derive the resistant mutant, we cultured wild-type HIV in our reporter cell line in the presence of EFV. We obtained the L100I partially resistant mutant. We then replaced the reverse transcriptase of the wild-type molecular clone with the mutant reverse transcriptase gene (Materials and methods). We derived d_{mut} for the L100I mutant using cell-free mutant infection (***Figure 3A***, see ***Figure 3—figure supplement 1*** for logarithmic y-axis plot). The L100I mutant was found to have an IC_{50} = 29 nM EFV and a Hill coefficient of 2.0 (***Figure 3A***, black line).

We next performed coculture infection (see ***Figure 3—figure supplement 2*** for gating strategy). Similarly to wild-type HIV coculture infection, there was a peak in the number of live infected target cells for the L100I mutant infection. However, the peak in live infected cells was shifted to 40 nM EFV (***Figure 3B***). Fits were obtained to ***Equation (3)*** using d_{mut} values and λ measured for wild-type infection. The fits recapitulated the experimental results when r = 0.29 and q = 0.13, with a fitted peak at 45 nM EFV (***Figure 3B***, black line). The solution to ***Equation (3)*** using the measured values for r and q showed a similar pattern to that obtained with the fitted values (***Figure 3B***, dashed green line). We note that both wild type and mutant coculture infection has data points above the fit line at the highest drug concentrations. This may be a limitation of our model at drug values much higher

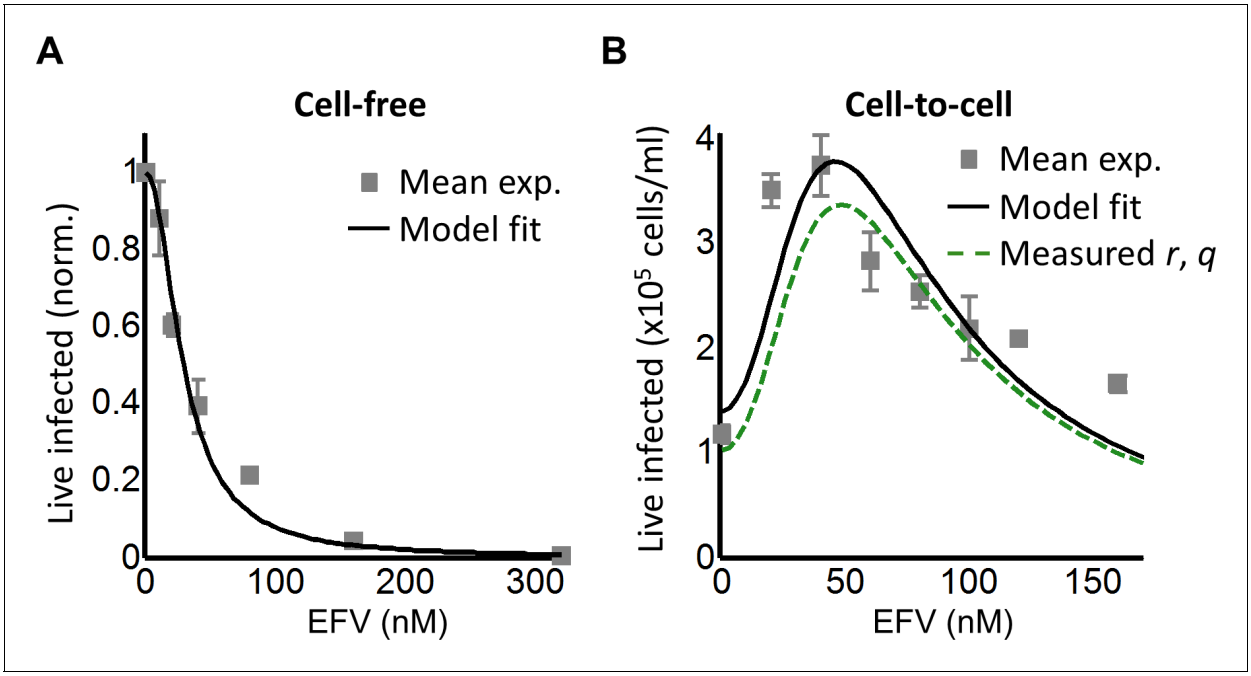

Figure 3. Partial inhibition of the EFV-resistant L100I mutant shifts the peak of live infected cells to higher EFV concentrations. (**A**) The number of live infected cells normalized by the maximum number of live infected cells in cell-free infection as a function of EFV for the L100I mutant. Black line is best-fit for EFV suppression of cell-free infection (IC_{50} = 29 nM, h = 2.0). Shown are means and standard errors for three independent experiments. (**B**) Number of live infected cells/ml 2 days post-infection resulting from coculture infection of 10^6 cells/ml in the presence of EFV. Means and standard errors for three independent experiments. Black line is best-fit of ***Equation (3)*** with r = 0.29 and q = 0.13. Dashed green line is the result of ***Equation (3)*** with the experimentally measured r = 0.28 and q = 0.15 for wild-type HIV infection.

DOI: https://doi.org/10.7554/eLife.30134.011

The following figure supplements are available for figure 3:

Figure supplement 1. The number of live infected cells in cell-free infection with the L100I mutant.

DOI: https://doi.org/10.7554/eLife.30134.012

Figure supplement 2. Gating strategy for coculture infection with mutant HIV.

DOI: https://doi.org/10.7554/eLife.30134.013

than observed at the infection optimum. In this range of drug values, our model predicts a more pronounced decline in the number of infected cells than is observed experimentally.

In order to examine whether a peak in live infected targets can be obtained with an unrelated inhibitor, we used the HIV neutralizing antibody b12. This antibody is effective against cell-to-cell spread of HIV (***Baxter et al., 2014***; ***Reh et al., 2015***). We obtained a peak in live infected cells at 5 ug/ml b12 (***Figure 4***). The b12 concentration that resulted in a peak number of live infected cells was the same for wild-type virus and the L100I mutant, showing that L100I mutant fitness gain was EFV specific. In contrast, cell-free infection in the face of b12 showed a sharp and monotonic drop in live infected cells for both wild type and mutant virus (***Figure 4—figure supplement 1***).

While the RevCEM cell line is a useful tool to illustrate the principles governing the formation of an infection optimum, the sensitivity of such an optimum to parameter values would make its presence in primary HIV target cells speculative. We therefore investigated whether a fitness optimum occurs in primary human lymph node cells, the anatomical site which would be most likely to have a high force of infection. We derived human lymph nodes from HIV-negative individuals from indicated lung resections (***Supplementary file 3***), cellularized the lymph node tissue using mechanical separation, and infected the resulting lymph node cells with HIV. A fraction of the cells was infected by cell-free virus and used as infected donor cells. We added these to uninfected target cells from the same lymph node to test coculture infection, and detected the number of live infected cells 4 days post-infection with the L100I EFV-resistant mutant in the face of EFV. We detected the number of

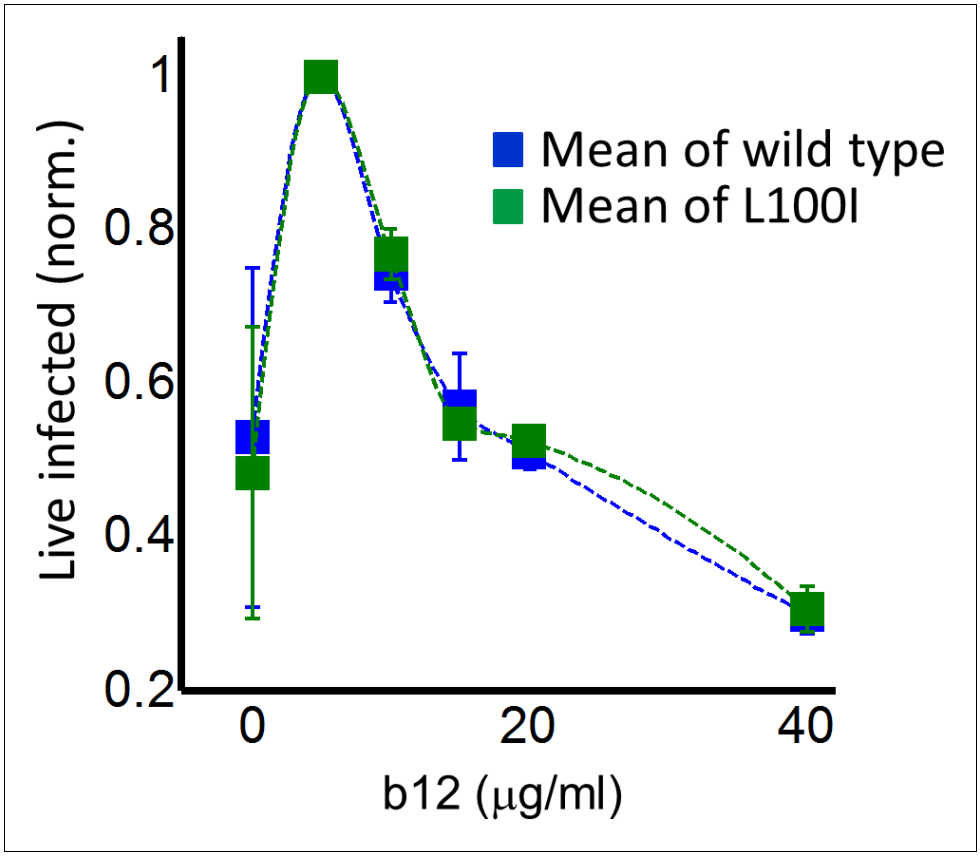

Figure 4. Partial inhibition of coculture infection with neutralizing antibody results in higher numbers of live infected cells. Shown are the numbers of live infected cells normalized by the maximum number of live infected cells in coculture infection as a function of b12 antibody concentration. Infection was by either EFV-sensitive HIV (blue) or the L100I EFV-resistant mutant (green). Dashed lines are a guide to the eye. Shown are means and standard errors for three independent experiments.

DOI: https://doi.org/10.7554/eLife.30134.014

The following figure supplement is available for figure 4:

Figure supplement 1. The number of live infected cells with cell-free infection in the face of neutralizing antibody b12.

DOI: https://doi.org/10.7554/eLife.30134.015

live infected cells by the exclusion of dead cells with the fixable death detection dye eFluor660 followed by single cell staining for HIV Gag using anti-p24 antibody (***Figure 5A***).

In each of the lymph nodes tested, we observed a peak in live infected cells at intermediate EFV concentrations. Lymph node cells from participant 205 showed a peak of live infected cells at 100 nM EFV (***Figure 5A***, first row). The infection optimum in the lymph node cells of study participant 257 was visible as a plateau between 50 and 200 nM EFV. In the presence of EFV, there was a decrease in the fraction of dead cells that was offset by a similar increase in the fraction of live infected cells for lymph nodes from all participants. There were more overall detectable cells with EFV, resulting in differences in the absolute concentrations of live infected cells being larger than the differences in the fractions of live infected cells between EFV and non-drug-treated cells (right two columns in ***Figure 5A***, with absolute number of live infected cells shown in parentheses in the flow cytometry plots). This is most likely due to cells which died early becoming fragments and so being excluded from the total population in the absence of EFV. Peaks in the number of live infected cells in the face of drug may be specific to lymph node derived cells. Cell-to-cell infection of peripheral blood mononuclear cells (PBMC) with wild-type HIV showed a slight peak at a very low EFV concentration in cells from one blood donor, which was not repeated in cells from two other donors (***Figure 5—figure supplement 1***).

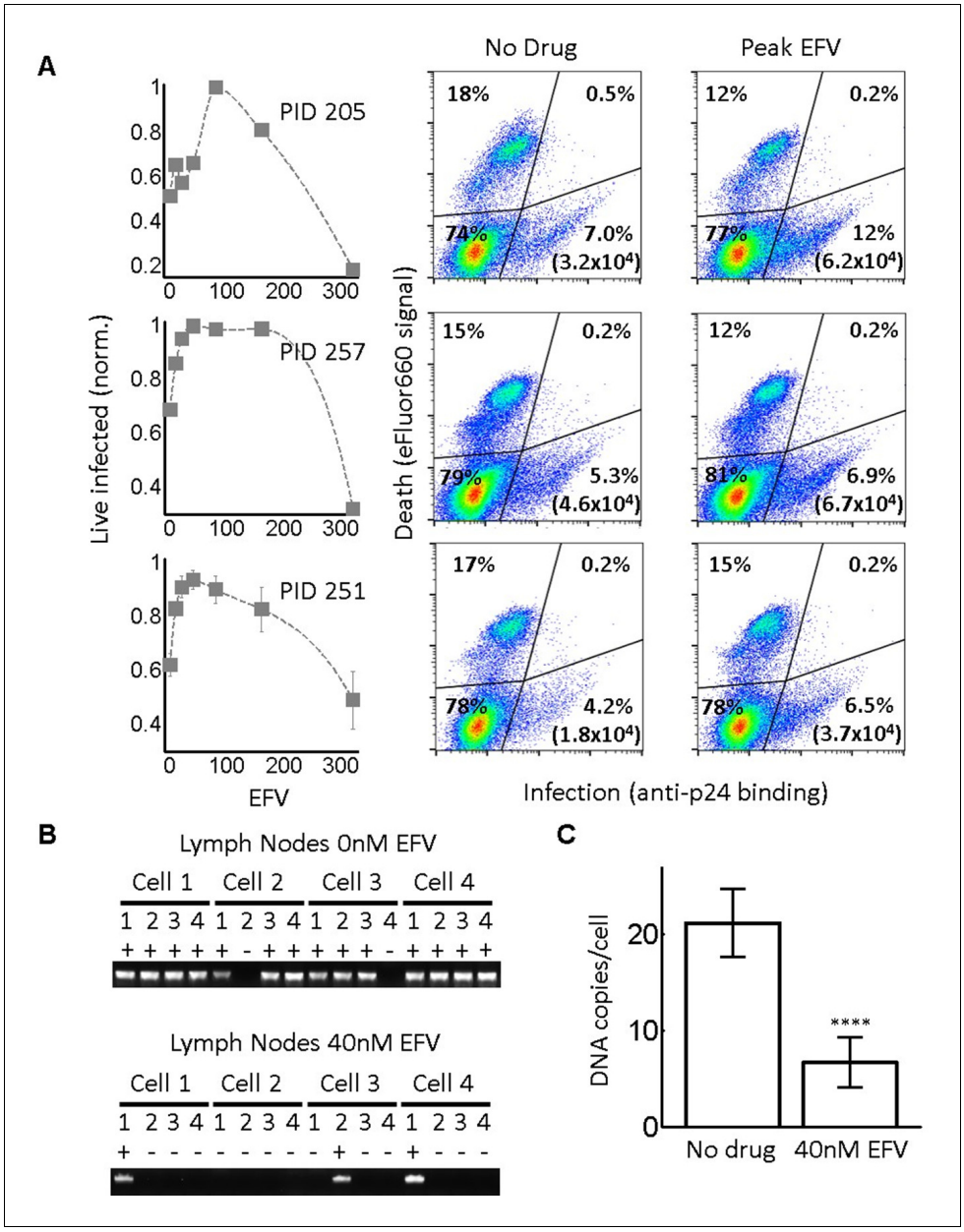

Figure 5. Infection optimum with EFV in lymph node cells. (**A**) Number of live infected cells as a function of EFV. Each row shows in vitro infected lymph node cells from one participant. Left column is the number of live infected cells normalized by maximum number of live infected cells in coculture infection. Middle and right columns are flow cytometry dot plots of infection without drug and at the infection optimum, with HIV p24 on x-axis and death detection by eFluor660 on y-axis. Infected live cells are bottom right. Number in brackets represents live infected cell density per ml. PID, participant identification number. For PID205 and 257, cells were sufficient for one experiment. For PID251, means and standard errors for three independent experiments are shown. Dashed lines are a guide to the eye. (**B**) HIV DNA copy number per cell was quantified by sorting fixed p24-positive cells from PID251 into individual wells. Cells were lysed and de-crosslinking performed. Each lysate was divided into four wells and PCR performed to detect HIV DNA. First row is representative of cells with no drug, second row is representative of 40 nM EFV. (**C**) Mean and standard error of the number of HIV DNA copies without drug and with 40 nM EFV after assay sensitivity correction. N = 56 cells from three independent experiments for each condition. ****$p=4\times10^{-9}$, two tailed t-test.

DOI: https://doi.org/10.7554/eLife.30134.016

The following figure supplements are available for figure 5:

Figure 5 continued on next page

Figure 5 continued

Figure supplement 1. Cell-to-cell infection of peripheral blood mononuclear cells in the presence of EFV does not lead to a discernable peak in live infected cells.

DOI: https://doi.org/10.7554/eLife.30134.017

Figure supplement 2. Raw HIV DNA copy numbers per lymph node cell.

DOI: https://doi.org/10.7554/eLife.30134.018

We used a lymph node from study participant 251, where we obtained more cells, to examine the number of HIV DNA copies per cell. Cells from this lymph node showed an infection optimum at 50 nM EFV (***Figure 5A***, third row). To detect the effect of EFV on integrations per cell, we sorted single cells based on p24-positive signal, de-crosslinked to remove the fixative (Materials and methods), then divided each cell lysate into four wells. Using fewer wells saved reagents without changing sensitivity, as demonstrated in the ACH-2 cell line (***Figure 2—figure supplement 1C***). We detected HIV DNA copies by PCR 2 days post-infection. We observed multiple DNA copies in EFV-untreated lymph node cells. The number of copies decreased with EFV (***Figure 5B***). We corrected for sensitivity of detection as quantified in ACH-2 cells (Materials and methods). The corrected numbers were 21 HIV DNA copies with no drug, and five copies in the presence of EFV at the infection optimum (***Figure 5C***, see ***Figure 5—figure supplement 2*** for histograms of raw HIV DNA copy numbers per cell). Hence, the decrease in the number of copies still results in sufficient copies to infect the cell.

Since L100I does not often occur in the absence of other drug resistance mutations according to the Stanford HIV Drug Resistance Database (***Rhee et al., 2003***), we repeated the experiment with the K103N mutant, a frequently observed mutation in virologic failure with a higher level of resistance to EFV relative to the L100I mutant. We used cell-free infection to obtain drug inhibition per virion at each level of EFV, which we denote d_{103} (***Figure 6A***, see ***Figure 6—figure supplement 1*** for logarithmic y-axis plot). The fits showed a monotonic decrease with IC_{50} = 26.0 nM and Hill coefficient of 1.5 (***Figure 6A***, black line). We then proceeded to use the K103N mutant in coculture infection, using cells from two different lymph nodes in different experiments (see ***Figure 6—figure supplement 2*** for results of individual experiments). We observed an infection optimum with EFV in lymph node cells. The peak in the number of live infected cells in the presence of drug was between 80 and 160 nM EFV (***Figure 6B***). We fit the experimental data with ***Equation (3)*** using d_{103} values and the number of DNA copies in the absence of drug measured for L100I infection. We did not calculate the predicted number of infected cells for $P_{\lambda/d}$ values since the lymph node is a complex environment containing different cell subsets (***Sallusto et al., 1999***) and the number of infectable target cells at the start of infection is difficult to determine. Hence, we normalized both the experimental number of live infected cells and the $P_{\lambda/d}$ values from ***Equation (3)*** to the maximum value in each case. The fits recapitulated the experimental results when r = 0.91 and q = 0.15, with a fitted peak at 90 nM EFV (***Figure 6B***, black line). The q value matched the measured result in the cell line, while the r value was much higher. However, the fitted r value in this case is not expected to be accurate since we were unable to constrain it with the number of infected cells relative to the starting number of target cells.

To examine if the observed peak in live cells may be due to EFV alone, we measured cell viability in lymph node cells from one of the study participants used in the above experiment as a function of EFV without infection. No clear dependence on EFV in the absence of infection was detected (***Figure 6—figure supplement 3***).

Discussion

The optimal virulence concept in ecology proposes that virulence needs to be balanced against host survival for optimal pathogen spread (***Bonhoeffer et al., 1996***; ***Bonhoeffer and Nowak, 1994***; ***Gandon et al., 2001***; ***Jensen et al., 2006***). At the cellular level, this implies that the number of successfully infected cells may increase when infection virulence is reduced. The current study is, to our knowledge, the first to address this question experimentally at the level of individual cells infected with HIV.

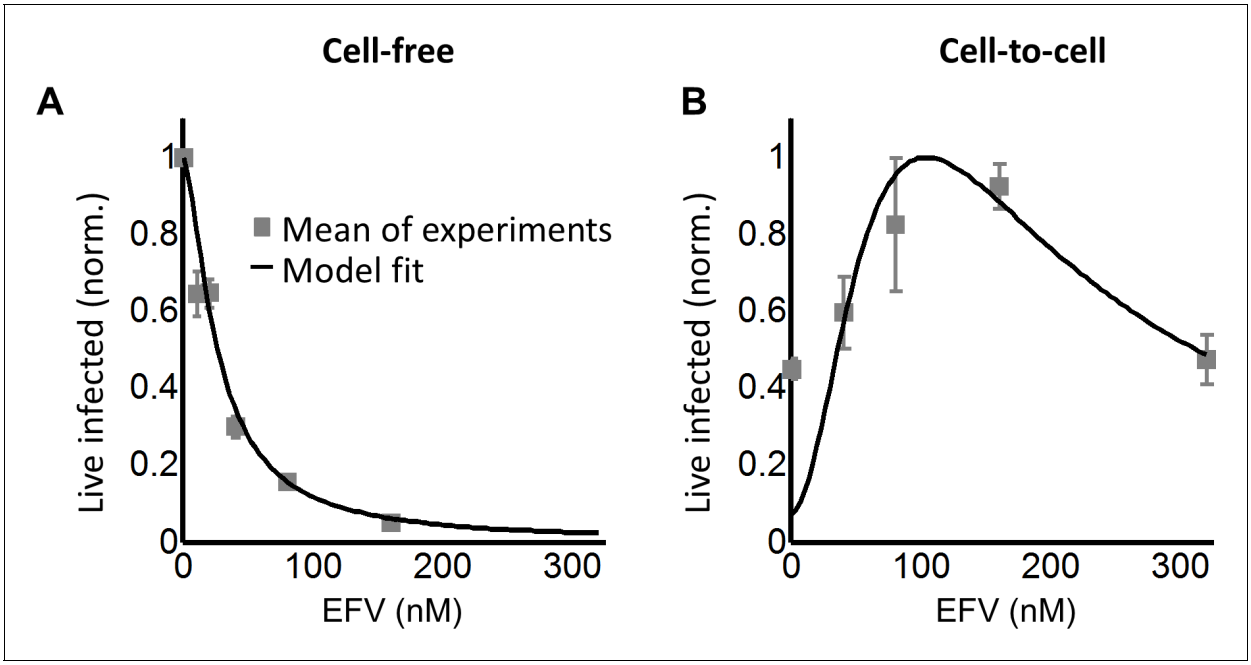

Figure 6. Infection with the K103N mutant shows an infection optimum at clinically observed lymph node EFV concentrations. (**A**) The number of live infected cells normalized by the maximum number of live infected cells in cell-free infection as a function of EFV for the K103N mutant. Black line is best-fit for EFV suppression of cell-free infection (IC_{50} = 26 nM, h = 1.5). Shown are means and standard errors for two independent experiments using cells from PID251. (**B**) The number of live infected cells normalized by the maximum number of live infected cells in coculture infection as a function of EFV for the K103N mutant. Black line represents best-fit model for the effect of EFV on coculture infection according to ***Equation (3)***, with *d* values calculated based on the cell-free infection data for the K103N mutant, and the mean number of HIV DNA copies in the absence of drug determined for L100I. The fits recapitulated the experimental results when $r = 0.91$ and $q = 0.15$. Shown are means and standard errors for three independent experiments. There were sufficient lymph node cells from PID251 for two of the three experiments, and the third experiment was performed with lymph node cells from PID274.

DOI: https://doi.org/10.7554/eLife.30134.019

The following figure supplements are available for figure 6:

Figure supplement 1. The number of live infected cells in cell-free infection with the K103N mutant.

DOI: https://doi.org/10.7554/eLife.30134.020

Figure supplement 2. Response of K103N coculture infection to EFV in individual experiments.

DOI: https://doi.org/10.7554/eLife.30134.021

Figure supplement 3. Effect of EFV on viability of uninfected lymph node cells from PID274.

DOI: https://doi.org/10.7554/eLife.30134.022

Using a model where cells are infected and die in a probabilistic way, we found that there were two possible outcomes of partially inhibiting infection. In the case where cells were infected by single infection attempts, inhibition always led to a decline in the number of live infected cells, since inhibition reduced the number of infections per cell from one to zero. In contrast, in the case of multiple infection attempts per cell, the possibility existed that inhibition reduced the number of integrating HIV DNA copies, without extinguishing infection of the cell completely. If each HIV DNA copy increases the probability of cell death, reducing the number of HIV DNA copies without eliminating infection should lead to an increased probability of infected cell survival. This would consequently lead to an increase in the number of live infected cells.

We investigated the outcome of partial inhibition of infection in both a cell line and primary lymph node cells. In both systems, we observed that there was a peak in live infected cell number at intermediate inhibitor concentrations. This correlated to a decreased number of viral DNA copies per cell. Further increasing inhibitor concentration led to a decline in live infected cell numbers, and infecting with EFV resistant mutants shifted the peak in live infected number to higher EFV concentrations. Our model as described by ***Equation (3)*** reproduced the essential behaviour of the experimental results. Construction of the model assumed independence of productive infection and cell

death. However, as shown in the Appendix 1, an equivalent model can be constructed assuming a dependence of cell death on infection. Neither model accurately captures infection dynamics at high-drug concentrations, away from the infection optimum. In this range, where the number of infection attempts per cell is much lower than 1, infection declined more slowly with drug than predicted. The model can be further refined using a distribution for the number of DNA copies per cell. Moreover, the probability of death per HIV DNA copy we denote q may be dependent on how many infection attempts preceded the current infection attempt, and the model can be improved by measuring this dependence.

Physiologically, an infection optimum in the face of an antiretroviral drug may be important in HIV infection of lymph node cells and may be less pronounced in cells from peripheral blood. We used EFV in our study since it is a common component of first line antiretroviral therapy, with frequent drug resistance mutations. However, the infection optimum we describe should occur with other classes of antiretroviral drugs, since all drugs should decrease the multiplicity of infection between cells. In terms of modeling, a future therapy component such as the integrase inhibitor dolutegravir would exert its effect on r and not λ in our model. However, the effect is symmetrical since $e^{-(\lambda/d)^r} = e^{-\lambda(r/d)}$. The more complex outcome of partial inhibition of infection should also be considered in other infections where multiple pathogens infect one cell and host cell death is a possible outcome (***Mahamed et al., 2017***).

These observations reinforce previous results showing that successful completion of reverse transcription leads to cellular cytotoxicity. In addition to HIV cytotoxicity caused by viral integrations through the mechanism of double strand breaks (***Cooper et al., 2013***), other mechanisms of HIV-induced death are also present, including IFI16-dependent innate immune system sensing of abortive reverse transcripts following non-productive infection of resting T cells (***Doitsh et al., 2014***; ***Monroe et al., 2014***). The experiments presented here reflect the effect of partial inhibition on productive infection of HIV target cells, which mostly consist of activated T-cell subsets, not resting T cells. More complex models would be needed to decipher the effect of partial inhibition of HIV infection on resting T-cell numbers and the outcome of this in terms of available T-cell targets in future infection cycles.

This study may have implications for the establishment of viral reservoirs in the context of poorly controlled infections, infections with some degree of drug resistance, or infections where some replication may take place in the face of ART, since infected cell survival is a pre-requisite for long-term persistence. The clinical implications of an infection optimum in the presence of EFV with EFV-sensitive HIV strains are likely to be negligible, since the drug concentrations at which the infection optimum occurs are extremely low. However, for EFV-resistant HIV, the infection optimum shifts to the range of EFV concentrations observed in lymph nodes (~100 nM) (***Fletcher et al., 2014b***), and can be expected to shift to even higher EFV concentrations with more resistant mutants. As EFV has a longer half-life than the other antiretroviral drugs co-formulated with it, it may be the only agent present in partially adherent individuals for substantial periods of time (***Taylor et al., 2007***). Therefore, partial inhibition of HIV infection with EFV may provide a surprising advantage to EFV resistant mutants, and may allow individuals failing therapy to better transmit drug resistant strains.

Materials and methods

Ethical statement

Lymph nodes were obtained from the field of surgery of participants undergoing surgery for diagnostic purposes and/or complications of inflammatory lung disease. Informed consent was obtained from each participant, and the study protocol approved by the University of KwaZulu-Natal Institutional Review Board (approval BE024/09). Blood for PBMC was obtained from healthy blood donors under the same study protocol.

Inhibitors, viruses and cell lines

The following reagents were obtained through the AIDS Research and Reference Reagent Program, National Institute of Allergy and Infectious Diseases, National Institutes of Health: the antiretroviral EFV; RevCEM cells from Y. Wu and J. Marsh; HIV molecular clone pNL4-3 from M. Martin; ACH-2 cells from T. Folks. Cell-free viruses were produced by transfection of HEK293 cells with pNL4-3

using TransIT-LT1 (Mirus, Madison, WI) or Fugene HD (Roche, Risch-Rotkreuz, Switzerland) transfection reagents. Virus containing supernatant was harvested after 2 days of incubation and filtered through a 0.45 µm filter (Corning, New York, NY). b12 antibody was produced from transfecting HEK293 cells with a b12 expression plasmid (expressed under a CMV promoter on a pHAGE6 lentiviral plasmid backbone, gift from A. Balazs), followed by harvesting of cell supernatant and purification at the California Institute of Technology protein expression core. The number of virus genomes in viral stocks was determined using the RealTime HIV-1 viral load test (Abbott Diagnostics, Santa Clara, CA). For r and q measurement, 0.45 µm filtered cell-free supernatants from infected RevCEM cells were used, to include any secreted factors which may modulate cell-death. The L100I and K103N mutants were evolved by serial passages of wild-type NL4-3 in RevCEM cells in the presence of 20 nM EFV. After 16 days of selection, the reverse transcriptase gene was cloned from the proviral DNA and the mutant reverse transcriptase gene was inserted into the NL4-3 molecular clone. RevCEM clones E7 and G2 used in this study were generated as previously described (***Boullé et al., 2016***). Briefly, the E7 clone was generated by subcloning RevCEM cells at single-cell density. Surviving clones were subdivided into replicate plates. One of the plates was screened for the fraction of GFP expressing cells upon HIV infection using microscopy, and the clone with the highest fraction of GFP-positive cells was selected. To generate the G2 clone, E7 cells were stably infected with the mCherry gene under the EF-1α promoter on a pHAGE2-based lentiviral vector (gift from A. Balazs), subcloned, and screened for >99% mCherry-positive cells. All cell lines not authenticated, and mycoplasma negative. Cell culture and experiments were performed in complete RPMI 1640 medium supplemented with L-Glutamine, sodium pyruvate, HEPES, non-essential amino acids (Lonza, Basel, Switzerland), and 10% heat-inactivated FBS (GE Healthcare Bio-Sciences, Pittsburgh, PA).

Primary cells

Lymph node cells were obtained by mechanical separation of lymph nodes and frozen at 5×10^6 cells/ml in a solution of 90% FBS and 10% DMSO with 2.5 µg/ml Amphotericin B (Lonza). Cells were stored in liquid nitrogen until use, then thawed and resuspended at 10^6 cells/ml in complete RPMI 1640 medium supplemented with L-Glutamine, sodium pyruvate, HEPES, non-essential amino acids (Lonza), 10% heat-inactivated FBS (Hyclone), and IL-2 at 5 ng/ml (PeproTech). Phytohemagglutinin at 10 µg/ml (Sigma-Aldrich, St Louis, MO) was added to activate cells. PBMCs were isolated by density gradient centrifugation using Histopaque 1077 (Sigma-Aldrich) and cultured at 10^6 cells/ml in complete RPMI 1640 medium supplemented with L-Glutamine, sodium pyruvate, HEPES, non-essential amino acids (Lonza), 10% heat-inactivated FBS (GE Healthcare Bio-Sciences, Pittsburgh, PA), and IL-2 at 5 ng/ml (PeproTech, Rocky Hill, NJ). Phytohemagglutinin at 10 µg/ml (Sigma-Aldrich) was added to activate cells. For both primary cell types, donor cells for coculture infection were cultured for one day then infected by cell-free virus, while target cells were cultured for three days and infected with either cell-free HIV or infected donor cells.

Subcloning of ACH-2 cells

Cells from the parental ACH-2 cell line were diluted to 10 cells/ml in conditioned medium, with conditioned medium generated by culturing ACH-2 cells to 10^6 cells/ml, then filtering through a 0.22 µm filter (Corning). 25 µl of the diluted cell suspension was then distributed to each well of a Greiner µClear 384-well plate (mean of 0.5 cells per well). Clones were cultured for 3 weeks, where each week an additional 25 µl of conditioned medium was added to each well. Clones were detected in 5% of wells and two clones, designated D6 and C3, were randomly chosen and further expanded.

Infection

For a cell-free infection of RevCEM clones, PBMC and lymph node cells, 10^6 cells/ml were infected with 2×10^8 NL4-3 viral copies/ml (~20ng p24 equivalent) for 2 days. For coculture infection, infected cells from the cell-free infection were used as the donors and cocultured with 10^6 cells/ml target cells. For RevCEM clones, 2% infected donor cells were added to uninfected targets and cocultured for 2 days in tissue culture experiments, and 20% infected donor cells were added to uninfected targets and cocultured for 2 days for time-lapse experiments. For lymph node cells and

PBMCs, a ratio of 1:4 donor to targets cells was used. Infection was over 2 days in PBMC infection and for 4 days for infection of lymph node cells.

Staining and flow cytometry

To determine the number of live infected cells in reporter cell line experiments, E7 RevCEM reporter cells were infected as above used as donor cells. Prior to co-incubation with target cells, donor cells were stained with CellTrace Far Red (CTFR, Thermo Fisher Scientific, Waltham, MA) at 1 µM and washed according to manufacturer's instructions. The G2 mCherry-positive reporter cells were used as infection targets, and cocultured with 2% infected donor cells for 2 days. The coculture infection was pulsed with 100 ng/ml DAPI (Sigma-Aldrich) immediately before flow cytometry and the number of live infected targets cells was determined by the number of DAPI negative, CTFR negative and mCherry and GFP double positive cells on a FACSAria Fusion machine (BD Biosciences, Sparks, MD) using the 355, 488 and 633 nm laser lines. For cell-free infections where fewer fluorescence channels were used, a pulse of 300 nM of the far-red live cell impermeable dye DRAQ7 (Biolegend, San Diego, CA) immediately before flow cytometry was substituted for DAPI, and live infected cells detected as the number of DRAQ7-negative, GFP-positive cells on a FACSCaliber machine using 488 and 633 nm laser lines. Lymph node cells were resuspended in 1 ml of phosphate buffered saline (PBS) and stained at a 1:1000 dilution of the eFlour660 dye (Thermo Fisher Scientific) according to the manufacturer's instructions. Cells were then fixed and permeabilized using the BD Cytofix/Cytoperm Fixation/Permeabilization kit (BD Biosciences) according to the manufacturer's instructions. Cells were then stained with anti-p24 FITC conjugated antibody (KC57, Beckman Coulter, Brea, CA). Live infected lymph node cells were detected as the number of eFluor660-negative, p24-positive cells. Cells were acquired with a FACSAriaIII or FACSCaliber machine (BD Biosciences) using 488 and 633 nm laser lines. Results were analysed with FlowJo 10.0.8 software. For single-cell sorting to detect the number of HIV DNA copies per cell, cells were single-cell sorted using 85 micron nozzle in a FACSAriaIII machine. GFP-positive, DRAQ7-negative RevCEM clones were sorted 1 day post-infection into 96 well plates (Biorad, Hercules, CA) containing 30 µl lysis buffer (2.5 µl 0.1M Dithiothreitol, 5 µl 5% NP40 and 22.5 µl molecular biology grade water [***Kurimoto et al., 2007***]). For experiments to determine the number of HIV DNA copies to measure r and q, the DRAQ7-negative subset was sorted. Fixed, p24-positive, eFluor660-negative lymph node cells were single-cell sorted two days post-infection into 96-well plates containing 5 µl of PKD buffer (Qiagen, Hilden, Germany) with 1:16 proteinase K solution (Qiagen) (***Thomsen et al., 2016***). Sorted plates were snap frozen and kept at −80˚C until ready for PCR. For analysis by flow cytometry, a minimum of 50,000 cells were collected per data point.

Time-lapse microscopy and image analysis

For imaging infection by time-lapse microscopy, cell density was reduced to 5×10^4 cells/ml and cells were attached to ploy-l-lysine (Sigma-Aldrich) coated optical six-well plates (MatTek, **Ashland, MA**). Infections with and without EFV were imaged in tandem using a Metamorph-controlled Nikon TiE motorized microscope with a Yokogawa spinning disk with a 20x, 0.75 NA phase objective in a biosafety level three facility. Excitation sources were 488 (GFP) and 561 (mCherry) laser lines and emission was detected through a Semrock Brightline quad band 440–40/521–21/607-34/700-45 nm filter. Images were captured using an 888 EMCCD camera (Andor, Belfast, UK). Temperature (37˚C), humidity and CO_2 (5%) were controlled using an environmental chamber (OKO Labs, Naples, Italy). Fields of view were captured every 20 min. To facilitate automated image analysis of time-lapse experiment data, mCherry expressing G2 clone cells were used as targets and E7 clone cells used as infected donors. The number of live cells was measured as the number of cells expressing mCherry since intracellular mCherry protein is soluble and hence lost upon cell death when cellular membrane integrity is compromised. The number of live infected cells was measured as the number of cells expressing both mCherry and GFP. Three independent experiments were performed. Movies were analyzed using custom code developed with the Matlab R2014a Image Analysis Toolbox. Images in the mCherry channel were thresholded and the imfindcircle function used to detect round objects within the cell radius range. Cell centers were found. GFP signal underwent the same binary thresholding. The number of mCherry-positive 16 pixel^2 squares around the cell centers was used as the as

the number of total target cells at each time-point, and the number of squares double positive for fluorescence in the GFP channel was used as the number of infected target cells.

Determination of HIV DNA copy number in individual cells

96-well plates of cells previously sorted at 1 cell per well were thawed at room temperature and spun down. Fixed cells were de-crosslinked by incubating in a thermocycler at 56˚C for 1 hr. The lysate from each well was split equally over 10 wells (2.5 µl each well after correction for evaporation) for E7 RevCEM or four wells (6.8 µl each well after correction for evaporation) for lymph nodes, containing 50 µl of Phusion hot start II DNA polymerase (New England Biolabs, Ipswich, MA) PCR reaction mix (10 µl 5X Phusion HF buffer, 1 µl dNTPs, 2.5 µl of the forward primer, 2.5 µl of the reverse primer, 0.5 µl Phusion hot start II DNA polymerase, 2.5 µl of DMSO and molecular biology grade water to 50 µl reaction volume). Two rounds of PCR were performed. The first round reaction amplified a 700 bp region of the reverse transcriptase gene using the forward primer 5' CCTACACCTG TCAACATAATTGGAAG 3' and reverse primer 5' GAATGGAGGTTCTTTCTGATG 3'. Cycling program was 98˚C for 30 s, then 34 cycles of 98˚C for 10 s, 63˚C for 30 s and 72˚C for 15 s with a final extension of 72˚C for 5 min. 1 µl of the first round product was then transferred into a PCR mix as above, with nested second round primers (forward 5' TAAAAGCATTAGTAGAAATTTGTACAGA 3', reverse 5' GGTAAATCCCCACCTCAACAGATG 3'). The second round PCR amplified a 550 bp product which was then visualized on a 1% agarose gel. PCR reactions were found to work best if sorted plates were thawed no more than once, and plates which underwent repeated freeze-thaw cycles showed poor amplification.

Correction of raw number of detected DNA copies for detection sensitivity

A stochastic simulation in Matlab was used to generate a distribution for the number of positive wells per cell for each mean number of DNA copies per cell λ. The probability for a DNA copy to be present within a given well and be detected was set as σ/w, where σ was the detection sensitivity calculated as the number of ACH-2 with detectable integrations divided by the total number of ACH-2 cells assayed (38/166, σ = 0.23), and w was the number of wells. A random number m representing DNA copies per cell from a Poisson distribution with a mean λ was drawn, and a vector R of m random numbers from a uniform distribution was generated. If there existed an element R_i of the vector with a value between 0 and σ/w, the first well was occupied. If an element existed with a value between $\sigma/w+\gamma$ and $2(\sigma/w)$, where γ <<1, the second well was occupied, and if between $(\sigma/w+\gamma)(n-1)$ and $n(\sigma/w)$, the *nth* well was occupied. The sum of wells occupied at least once was determined, and the process repeated j times for each λ, where j was the number of cells in the experimental data. A least squares fit was performed to select λ which best fit the experimental results across well frequencies, and mean and standard deviation for λ was derived by repeating the simulation 10 times.

Fit of the EFV response for single infections using IC_{50} and Hill coefficient

To obtain d, we normalized ***Equation (2)*** by the fraction of infected cells in the absence of drug (***Sigal et al., 2011***) to obtain Tx = (infected targets with EFV)/ (infected targets no EFV)= $((1-(1\ r)^{\lambda/d})(1-q)^{\lambda/d})/((1-(1\ r)^{\lambda})(1-q)^{\lambda})$. We approximate the result at small r, q to $Tx = (1-e^{-r\lambda/d})\,e^{-q\lambda/d}/(1-e^{-r\lambda})\,e^{-q\lambda} = eq^{q\lambda(1-1/d)}\,((1-e^{-r\lambda/d})/(1-e^{-r\lambda}))$. Expanding the exponentials we obtain $Tx = (1+q\lambda(1-1/d))\,((-r\lambda/d)/-r\lambda) = (1+q\lambda(1-1/d))(1/d)$. We note that at λ <1, $q\lambda(1-1/d)$<<1, and hence $Tx \cong 1/d$. Tx was measured from the experiments to obtain d values at the EFV concentrations used for cell-free infection, where $\lambda < 1$. To obtain a fit of d as a function of the concentration of drug that gives half-maximal inhibition (IC_{50}) and Hill coefficient (h) for EFV, we used the relation for the fraction cells remaining infected in the face of drug (***Canini and Perelson, 2014***), whose definition is equivalent to Tx at $\lambda < 1$:

$$\frac{1}{d} = 1 - = 1 - \frac{[EFV]^h}{[EFV]^h + IC_{50}^h}. \quad (4)$$

Measurement of *r*

Cell-free supernatant used in infection was derived as follows: 10^6 cells/ml were infected with 2×10^8 NL4-3 viral copies/ml (~20ng p24 equivalent) for 2 days. Thereafter 0.2% of the infected cells from the cell-free infection were added to 10^6 cells/ml target cells. The infected supernatant from the coculture 2 days post-infection was filtered using a 0.45 µm filter (Corning) and added to cells at a 1:8 dilution, where the dilution was calibrated to result in non-saturating infection in terms of GFP expression. A fraction of the cells were sorted into lysis buffer at one cell per well 1 day post infection, split over four wells, and PCR performed as described above to determine HIV copy number per cell. The remaining cells from the same infection were used to determine frequency of DRAQ-7-negative, GFP-positive cells 2 days post-infection using flow cytometry.

Measurement of *q*

Cell-free supernatant used in infection was derived as for *r*, except that 1 day before harvesting of the viral supernatant from infected cells, infected cells were washed twice with PBS and serum-free growth medium added. At the same time, the target cells for the infection were washed twice with PBS and serum-free growth medium added. Cells were split into two wells, and EFV to a final concentration of 40 nM was added to one of the wells. Supernatant was harvested and filtered as described for *r*, and added to cells at a 1:2 dilution. A fraction of the cells were sorted into lysis buffer at one cell per well 1 day post-infection, split over four wells, and PCR performed as described above to determine HIV copy number per cell. The remaining cells from the same infection were used to determine the frequency of live and dead cells two days post-infection. The concentration of live cells was measured using the TC20™ automated cell counter (Bio-Rad) with trypan blue staining (Lonza).

Acknowledgements

This work was supported by National Institutes of Health Grant R21MH104220. AS was supported by a Human Frontiers Science Program Career Development Award CDA 00050/2013. RAN is supported by the European Research Council through grant Stg. 260686. LJ and JH are supported by a fellowship from the South African National Research Foundation. IMF is supported through a Sub-Saharan African Network for TB/HIV Research Excellence (SANTHE, a DELTAS Africa Initiative (grant #DEL-15–006)) fellowship, and a Poliomyelitis Research Foundation fellowship 17/59. Open access publication of this article has been made possible through support from the Victor Daitz Information Gateway, an initiative of the Victor Daitz Foundation and the University of KwaZulu-Natal.

Additional information

Competing interests

Richard A Neher: Reviewing editor, *eLife*. The other authors declare that no competing interests exist.

Funding

Funder	Grant reference number	Author
Human Frontier Science Program	CDA 00050/2013	Alex Sigal
European Research Council	Stg. 260686	Richard A Neher
DELTAS Africa Initiative	Graduate Fellowship (DEL-15–006)	Isabella Markham Ferreira
National Research Foundation	Graduate Fellowship	Laurelle Jackson Jessica Hunter
National Institutes of Health	R21MH104220	Alex Sigal
Poliomyelitis Research Foundation	Graduate Fellowship	Isabella Markham Ferreira

The funders had no role in study design, data collection and interpretation, or the decision to submit the work for publication.

Author contributions

Laurelle Jackson, Conceptualization, Data curation, Validation, Investigation, Visualization, Methodology, Writing—original draft, Project administration, Writing—review and editing; Jessica Hunter, Data curation, Validation, Investigation, Visualization, Methodology, Writing—original draft; Sandile Cele, Isabella Markham Ferreira, Andrew C Young, Yashica Ganga, Mikael Boulle, Investigation, Methodology; Farina Karim, Rajhmun Madansein, Resources, Project administration; Kaylesh J Dullabh, Resources, Data curation, Validation, Investigation; Chih-Yuan Chen, Resources, Investigation; Noel J Buckels, Khadija Khan, Resources; Gila Lustig, Resources, Investigation, Methodology, Project administration; Richard A Neher, Conceptualization, Methodology; Alex Sigal, Conceptualization, Resources, Data curation, Software, Formal analysis, Supervision, Funding acquisition, Validation, Investigation, Visualization, Writing—original draft, Project administration, Writing—review and editing

Author ORCIDs

Andrew C Young http://orcid.org/0000-0003-3616-7956
Richard A Neher http://orcid.org/0000-0003-2525-1407
Alex Sigal http://orcid.org/0000-0001-8571-2004

Ethics

Human subjects: Lymph nodes were obtained from the field of surgery of participants undergoing surgery for diagnostic purposes and/or complications of inflammatory lung disease. Informed consent was obtained from each participant, and the study protocol approved by the University of KwaZulu-Natal Institutional Review Board (approval BE024/09).

Decision letter and Author response

Decision letter https://doi.org/10.7554/eLife.30134.039
Author response https://doi.org/10.7554/eLife.30134.040

Additional files

Supplementary files

- Supplementary file 1. S Table 1: Parameters and definitions.
DOI: https://doi.org/10.7554/eLife.30134.023
- Supplementary file 2. S Table 2: Measurement of *r* and *q*
DOI: https://doi.org/10.7554/eLife.30134.024
- Supplementary file 3. S Table 3: Participant information.
DOI: https://doi.org/10.7554/eLife.30134.025
- Source code 1. script1r2.m: Matlab source code for ***Figure 1***.
DOI: https://doi.org/10.7554/eLife.30134.026
- Source code 2. script2r2: Matlab source code for copy number correction for RevCEM clones based on HIV copy detection efficiency in ACH-2 cells.
DOI: https://doi.org/10.7554/eLife.30134.027
- Source code 3. script3r2.m: Matlab source code for cell-free and coculture infection model fits for RevCEM cells infected with wild-type HIV in ***Figure 2***.
DOI: https://doi.org/10.7554/eLife.30134.028
- Source code 4. Script4.m: Matlab source code for histograms of raw HIV copy numbers for cell-free and coculture infection and fits of different distributions to coculture copy number frequencies.
DOI: https://doi.org/10.7554/eLife.30134.029
- Source code 5. Script5.m: Matlab source code for image analysis of time-lapse data for ***Figure 2—figure supplement 5***.

DOI: https://doi.org/10.7554/eLife.30134.030

• Source code 6. script6r2.m: Matlab source code for cell-free and coculture infection model fits for RevCEM cells infected with L100I mutant HIV in ***Figure 3***.

DOI: https://doi.org/10.7554/eLife.30134.031

• Source code 7. Script7.m: Matlab source code for copy number correction for lymph node cells based on HIV copy detection efficiency is ACH-2 cells.

DOI: https://doi.org/10.7554/eLife.30134.032

• Source code 8. script8r2.m: Matlab source code for cell-free and coculture infection model fits for lymph node cells infected with K103N mutant HIV in ***Figure 6***.

DOI: https://doi.org/10.7554/eLife.30134.033

• Transparent reporting form

DOI: https://doi.org/10.7554/eLife.30134.034

References

Ariën KK, Troyer RM, Gali Y, Colebunders RL, Arts EJ, Vanham G. 2005. Replicative fitness of historical and recent HIV-1 isolates suggests HIV-1 attenuation over time. *AIDS* **19**:1555–1564. DOI: https://doi.org/10.1097/01.aids.0000185989.16477.91, PMID: 16184024

Banda NK, Bernier J, Kurahara DK, Kurrle R, Haigwood N, Sekaly RP, Finkel TH. 1992. Crosslinking CD4 by human immunodeficiency virus gp120 primes T cells for activation-induced apoptosis. *Journal of Experimental Medicine* **176**:1099–1106. DOI: https://doi.org/10.1084/jem.176.4.1099, PMID: 1402655

Baxter AE, Russell RA, Duncan CJ, Moore MD, Willberg CB, Pablos JL, Finzi A, Kaufmann DE, Ochsenbauer C, Kappes JC, Groot F, Sattentau QJ. 2014. Macrophage infection via selective capture of HIV-1-infected CD4+ T cells. *Cell Host & Microbe* **16**:711–721. DOI: https://doi.org/10.1016/j.chom.2014.10.010, PMID: 25467409

Bonhoeffer S, Lenski RE, Ebert D. 1996. The curse of the pharaoh: the evolution of virulence in pathogens with long living propagules. *Proceedings of the Royal Society B: Biological Sciences* **263**:715–721. DOI: https://doi.org/10.1098/rspb.1996.0107, PMID: 8763793

Bonhoeffer S, May RM, Shaw GM, Nowak MA. 1997. Virus dynamics and drug therapy. *PNAS* **94**:6971–6976. DOI: https://doi.org/10.1073/pnas.94.13.6971, PMID: 9192676

Bonhoeffer S, Nowak MA. 1994. Mutation and the evolution of virulence. *Proceedings of the Royal Society B: Biological Sciences* **258**:133–140. DOI: https://doi.org/10.1098/rspb.1994.0153

Boullé M, Müller TG, Dähling S, Ganga Y, Jackson L, Mahamed D, Oom L, Lustig G, Neher RA, Sigal A. 2016. HIV Cell-to-Cell Spread Results in Earlier Onset of Viral Gene Expression by Multiple Infections per Cell. *PLoS Pathogens* **12**:e1005964. DOI: https://doi.org/10.1371/journal.ppat.1005964, PMID: 27812216

Brenchley JM, Schacker TW, Ruff LE, Price DA, Taylor JH, Beilman GJ, Nguyen PL, Khoruts A, Larson M, Haase AT, Douek DC. 2004. CD4+ T cell depletion during all stages of HIV disease occurs predominantly in the gastrointestinal tract. *The Journal of Experimental Medicine* **200**:749–759. DOI: https://doi.org/10.1084/jem.20040874, PMID: 15365096

Canini L, Perelson AS. 2014. Viral kinetic modeling: state of the art. *Journal of Pharmacokinetics and Pharmacodynamics* **41**:431–443. DOI: https://doi.org/10.1007/s10928-014-9363-3, PMID: 24961742

Chun TW, Carruth L, Finzi D, Shen X, DiGiuseppe JA, Taylor H, Hermankova M, Chadwick K, Margolick J, Quinn TC, Kuo YH, Brookmeyer R, Zeiger MA, Barditch-Crovo P, Siliciano RF. 1997. Quantification of latent tissue reservoirs and total body viral load in HIV-1 infection. *Nature* **387**:183–188. DOI: https://doi.org/10.1038/387183a0, PMID: 9144289

Cooper A, García M, Petrovas C, Yamamoto T, Koup RA, Nabel GJ. 2013. HIV-1 causes CD4 cell death through DNA-dependent protein kinase during viral integration. *Nature* **498**:376–379. DOI: https://doi.org/10.1038/nature12274, PMID: 23739328

Dale BM, McNerney GP, Thompson DL, Hubner W, de Los Reyes K, Chuang FY, Huser T, Chen BK. 2011. Cell-to-cell transfer of HIV-1 via virological synapses leads to endosomal virion maturation that activates viral membrane fusion. *Cell Host & Microbe* **10**:551–562. DOI: https://doi.org/10.1016/j.chom.2011.10.015, PMID: 22177560

Dang Q, Chen J, Unutmaz D, Coffin JM, Pathak VK, Powell D, KewalRamani VN, Maldarelli F, Hu WS, Ws H. 2004. Nonrandom HIV-1 infection and double infection via direct and cell-mediated pathways. *PNAS* **101**:632–637. DOI: https://doi.org/10.1073/pnas.0307636100, PMID: 14707263

Del Portillo A, Tripodi J, Najfeld V, Wodarz D, Levy DN, Chen BK. 2011. Multiploid inheritance of HIV-1 during cell-to-cell infection. *Journal of Virology* **85**:7169–7176. DOI: https://doi.org/10.1128/JVI.00231-11, PMID: 21543479

Deleage C, Wietgrefe SW, Del Prete G, Morcock DR, Hao XP, Piatak M, Bess J, Anderson JL, Perkey KE, Reilly C, McCune JM, Haase AT, Lifson JD, Schacker TW, Estes JD. 2016. Defining HIV and SIV reservoirs in lymphoid tissues. *Pathogens and Immunity* **1**:68. DOI: https://doi.org/10.20411/pai.v1i1.100, PMID: 27430032

Descours B, Petitjean G, López-Zaragoza JL, Bruel T, Raffel R, Psomas C, Reynes J, Lacabaratz C, Levy Y, Schwartz O, Lelievre JD, Benkirane M. 2017. CD32a is a marker of a CD4 T-cell HIV reservoir harbouring

replication-competent proviruses. *Nature* **543**:564–567. DOI: https://doi.org/10.1038/nature21710, PMID: 28297712

Dixit NM, Perelson AS. 2004. Multiplicity of human immunodeficiency virus infections in lymphoid tissue. *Journal of Virology* **78**:8942–8945. DOI: https://doi.org/10.1128/JVI.78.16.8942-8945.2004, PMID: 15280505

Doitsh G, Cavrois M, Lassen KG, Zepeda O, Yang Z, Santiago ML, Hebbeler AM, Greene WC. 2010. Abortive HIV infection mediates CD4 T cell depletion and inflammation in human lymphoid tissue. *Cell* **143**:789–801. DOI: https://doi.org/10.1016/j.cell.2010.11.001, PMID: 21111238

Doitsh G, Galloway NL, Geng X, Yang Z, Monroe KM, Zepeda O, Hunt PW, Hatano H, Sowinski S, Muñoz-Arias I, Greene WC. 2014. Cell death by pyroptosis drives CD4 T-cell depletion in HIV-1 infection. *Nature* **505**:509–514. DOI: https://doi.org/10.1038/nature12940, PMID: 24356306

Duncan CJ, Russell RA, Sattentau QJ. 2013. High multiplicity HIV-1 cell-to-cell transmission from macrophages to CD4+ T cells limits antiretroviral efficacy. *AIDS* **27**:2201–2206. DOI: https://doi.org/10.1097/QAD.0b013e3283632ec4, PMID: 24005480

Embretson J, Zupancic M, Ribas JL, Burke A, Racz P, Tenner-Racz K, Haase AT. 1993. Massive covert infection of helper T lymphocytes and macrophages by HIV during the incubation period of AIDS. *Nature* **362**:359–362. DOI: https://doi.org/10.1038/362359a0, PMID: 8096068

Finkel TH, Tudor-Williams G, Banda NK, Cotton MF, Curiel T, Monks C, Baba TW, Ruprecht RM, Kupfer A. 1995. Apoptosis occurs predominantly in bystander cells and not in productively infected cells of HIV- and SIV-infected lymph nodes. *Nature Medicine* **1**:129–134. DOI: https://doi.org/10.1038/nm0295-129, PMID: 7585008

Fletcher CV, Staskus K, Wietgrefe SW, Rothenberger M, Reilly C, Chipman JG, Beilman GJ, Khoruts A, Thorkelson A, Schmidt TE, Anderson J, Perkey K, Stevenson M, Perelson AS, Douek DC, Haase AT, Schacker TW. 2014a. Persistent HIV-1 replication is associated with lower antiretroviral drug concentrations in lymphatic tissues. *PNAS* **111**:2307–2312. DOI: https://doi.org/10.1073/pnas.1318249111

Fletcher CV, Staskus K, Wietgrefe SW, Rothenberger M, Reilly C, Chipman JG, Beilman GJ, Khoruts A, Thorkelson A, Schmidt TE, Anderson J, Perkey K, Stevenson M, Perelson AS, Douek DC, Haase AT, Schacker TW. 2014b. Persistent HIV-1 replication is associated with lower antiretroviral drug concentrations in lymphatic tissues. *PNAS* **111**:2307–2312. DOI: https://doi.org/10.1073/pnas.1318249111, PMID: 24469825

Galloway NL, Doitsh G, Monroe KM, Yang Z, Muñoz-Arias I, Levy DN, Greene WC. 2015. Cell-to-cell transmission of hiv-1 is required to trigger pyroptotic death of lymphoid-tissue-derived CD4 T Cells. *Cell Reports* **12**:1555–1563. DOI: https://doi.org/10.1016/j.celrep.2015.08.011, PMID: 26321639

Gandon S, Mackinnon MJ, Nee S, Read AF. 2001. Imperfect vaccines and the evolution of pathogen virulence. *Nature* **414**:751–756. DOI: https://doi.org/10.1038/414751a, PMID: 11742400

Gratton S, Cheynier R, Dumaurier MJ, Oksenhendler E, Wain-Hobson S. 2000. Highly restricted spread of HIV-1 and multiply infected cells within splenic germinal centers. *PNAS* **97**:14566–14571. DOI: https://doi.org/10.1073/pnas.97.26.14566, PMID: 11121058

Groot F, Welsch S, Sattentau QJ. 2008. Efficient HIV-1 transmission from macrophages to T cells across transient virological synapses. *Blood* **111**:4660–4663. DOI: https://doi.org/10.1182/blood-2007-12-130070, PMID: 18296630

Groppelli E, Starling S, Jolly C. 2015. Contact-induced mitochondrial polarization supports HIV-1 virological synapse formation. *Journal of Virology* **89**:14–24. DOI: https://doi.org/10.1128/JVI.02425-14, PMID: 25320323

Gummuluru S, KewalRamani VN, Emerman M. 2002. Dendritic cell-mediated viral transfer to T cells is required for human immunodeficiency virus type 1 persistence in the face of rapid cell turnover. *Journal of Virology* **76**:10692–10701. DOI: https://doi.org/10.1128/JVI.76.21.10692-10701.2002, PMID: 12368311

Hollingsworth TD, Anderson RM, Fraser C. 2008. HIV-1 transmission, by stage of infection. *The Journal of Infectious Diseases* **198**:687–693. DOI: https://doi.org/10.1086/590501, PMID: 18662132

Hübner W, McNerney GP, Chen P, Dale BM, Gordon RE, Chuang FY, Li XD, Asmuth DM, Huser T, Chen BK. 2009. Quantitative 3D video microscopy of HIV transfer across T cell virological synapses. *Science* **323**:1743–1747. DOI: https://doi.org/10.1126/science.1167525, PMID: 19325119

Jensen KH, Little TJ, Little T, Skorping A, Ebert D. 2006. Empirical support for optimal virulence in a castrating parasite. *PLoS Biology* **4**:e197. DOI: https://doi.org/10.1371/journal.pbio.0040197, PMID: 16719563

Jolly C, Kashefi K, Hollinshead M, Sattentau QJ. 2004. HIV-1 cell to cell transfer across an Env-induced, actin-dependent synapse. *The Journal of Experimental Medicine* **199**:283–293. DOI: https://doi.org/10.1084/jem.20030648, PMID: 14734528

Jolly C, Welsch S, Michor S, Sattentau QJ. 2011. The regulated secretory pathway in CD4(+) T cells contributes to human immunodeficiency virus type-1 cell-to-cell spread at the virological synapse. *PLoS Pathogens* **7**:e1002226. DOI: https://doi.org/10.1371/journal.ppat.1002226, PMID: 21909273

Josefsson L, King MS, Makitalo B, Brännström J, Shao W, Maldarelli F, Kearney MF, Hu WS, Chen J, Gaines H, Mellors JW, Albert J, Coffin JM, Palmer SE. 2011. Majority of CD4+ T cells from peripheral blood of HIV-1-infected individuals contain only one HIV DNA molecule. *PNAS* **108**:11199–11204. DOI: https://doi.org/10.1073/pnas.1107729108, PMID: 21690402

Josefsson L, Palmer S, Faria NR, Lemey P, Casazza J, Ambrozak D, Kearney M, Shao W, Kottilil S, Sneller M, Mellors J, Coffin JM, Maldarelli F. 2013. Single cell analysis of lymph node tissue from HIV-1 infected patients reveals that the majority of CD4+ T-cells contain one HIV-1 DNA molecule. *PLoS Pathogens* **9**:e1003432. DOI: https://doi.org/10.1371/journal.ppat.1003432, PMID: 23818847

Jung A, Maier R, Vartanian JP, Bocharov G, Jung V, Fischer U, Meese E, Wain-Hobson S, Meyerhans A. 2002. Recombination: Multiply infected spleen cells in HIV patients. *Nature* **418**:144. DOI: https://doi.org/10.1038/418144a, PMID: 12110879

Kurimoto K, Yabuta Y, Ohinata Y, Saitou M. 2007. Global single-cell cDNA amplification to provide a template for representative high-density oligonucleotide microarray analysis. *Nature Protocols* **2**:739–752. DOI: https://doi.org/10.1038/nprot.2007.79, PMID: 17406636

Law KM, Komarova NL, Yewdall AW, Lee RK, Herrera OL, Wodarz D, Chen BK. 2016. In Vivo HIV-1 Cell-to-Cell transmission promotes multicopy micro-compartmentalized infection. *Cell Reports* **15**:2771–2783. DOI: https://doi.org/10.1016/j.celrep.2016.05.059, PMID: 27292632

Mahamed D, Boulle M, Ganga Y, Mc Arthur C, Skroch S, Oom L, Catinas O, Pillay K, Naicker M, Rampersad S, Mathonsi C, Hunter J, Wong EB, Suleman M, Sreejit G, Pym AS, Lustig G, Sigal A. 2017. Intracellular growth of*Mycobacterium tuberculosis*after macrophage cell death leads to serial killing of host cells. *eLife* **6**:e22028. DOI: https://doi.org/10.7554/eLife.22028, PMID: 28130921

Mattapallil JJ, Douek DC, Hill B, Nishimura Y, Martin M, Roederer M. 2005. Massive infection and loss of memory CD4+ T cells in multiple tissues during acute SIV infection. *Nature* **434**:1093–1097. DOI: https://doi.org/10.1038/nature03501, PMID: 15793563

Monroe KM, Yang Z, Johnson JR, Geng X, Doitsh G, Krogan NJ, Greene WC. 2014. IFI16 DNA sensor is required for death of lymphoid CD4 T cells abortively infected with HIV. *Science* **343**:428–432. DOI: https://doi.org/10.1126/science.1243640, PMID: 24356113

Münch J, Rücker E, Ständker L, Adermann K, Goffinet C, Schindler M, Wildum S, Chinnadurai R, Rajan D, Specht A, Giménez-Gallego G, Sánchez PC, Fowler DM, Koulov A, Kelly JW, Mothes W, Grivel JC, Margolis L, Keppler OT, Forssmann WG, et al. 2007. Semen-derived amyloid fibrils drastically enhance HIV infection. *Cell* **131**:1059–1071. DOI: https://doi.org/10.1016/j.cell.2007.10.014, PMID: 18083097

Nowak M, May RM. 2000. *Virus dynamics: mathematical principles of immunology and virology: mathematical principles of immunology and virology*. UK: Oxford University Press.

O'Doherty U, Swiggard WJ, Jeyakumar D, McGain D, Malim MH. 2002. A sensitive, quantitative assay for human immunodeficiency virus type 1 integration. *Journal of Virology* **76**:10942–10950. DOI: https://doi.org/10.1128/JVI.76.21.10942-10950.2002, PMID: 12368337

Payne R, Muenchhoff M, Mann J, Roberts HE, Matthews P, Adland E, Hempenstall A, Huang KH, Brockman M, Brumme Z, Sinclair M, Miura T, Frater J, Essex M, Shapiro R, Walker BD, Ndung'u T, McLean AR, Carlson JM, Goulder PJ. 2014. Impact of HLA-driven HIV adaptation on virulence in populations of high HIV seroprevalence. *PNAS* **111**:E5393–E5400. DOI: https://doi.org/10.1073/pnas.1413339111, PMID: 25453107

Perelson AS. 2002. Modelling viral and immune system dynamics. *Nature Reviews Immunology* **2**:28–36. DOI: https://doi.org/10.1038/nri700, PMID: 11905835

Phillips AN. 1996. Reduction of HIV concentration during acute infection: independence from a specific immune response. *Science* **271**:497–499. DOI: https://doi.org/10.1126/science.271.5248.497, PMID: 8560262

Quiñones-Mateu ME, Arts EJ. 2006. Virus fitness: concept, quantification, and application to HIV population dynamics. *Current Topics in Microbiology and Immunology* **299**:83–140. PMID: 16568897

Reh L, Magnus C, Schanz M, Weber J, Uhr T, Rusert P, Trkola A. 2015. Capacity of Broadly Neutralizing Antibodies to Inhibit HIV-1 Cell-Cell Transmission Is Strain- and Epitope-Dependent. *PLoS Pathogens* **11**:e1004966. DOI: https://doi.org/10.1371/journal.ppat.1004966, PMID: 26158270

Rhee SY, Gonzales MJ, Kantor R, Betts BJ, Ravela J, Shafer RW. 2003. Human immunodeficiency virus reverse transcriptase and protease sequence database. *Nucleic Acids Research* **31**:298–303. DOI: https://doi.org/10.1093/nar/gkg100, PMID: 12520007

Ribeiro RM, Qin L, Chavez LL, Li D, Self SG, Perelson AS. 2010. Estimation of the initial viral growth rate and basic reproductive number during acute HIV-1 infection. *Journal of Virology* **84**:6096–6102. DOI: https://doi.org/10.1128/JVI.00127-10, PMID: 20357090

Russell RA, Martin N, Mitar I, Jones E, Sattentau QJ. 2013. Multiple proviral integration events after virological synapse-mediated HIV-1 spread. *Virology* **443**:143–149. DOI: https://doi.org/10.1016/j.virol.2013.05.005, PMID: 23722103

Sallusto F, Lenig D, Förster R, Lipp M, Lanzavecchia A. 1999. Two subsets of memory T lymphocytes with distinct homing potentials and effector functions. *Nature* **401**:708–712. DOI: https://doi.org/10.1038/44385, PMID: 10537110

Sanchez JL, Hunt PW, Reilly CS, Hatano H, Beilman GJ, Khoruts A, Jasurda JS, Somsouk M, Thorkelson A, Russ S, Anderson J, Deeks SG, Schacker TW. 2015. Lymphoid fibrosis occurs in long-term nonprogressors and persists with antiretroviral therapy but may be reversible with curative interventions. *Journal of Infectious Diseases* **211**:1068–1075. DOI: https://doi.org/10.1093/infdis/jiu586, PMID: 25344521

Shen L, Peterson S, Sedaghat AR, McMahon MA, Callender M, Zhang H, Zhou Y, Pitt E, Anderson KS, Acosta EP, Siliciano RF. 2008. Dose-response curve slope sets class-specific limits on inhibitory potential of anti-HIV drugs. *Nature Medicine* **14**:762–766. DOI: https://doi.org/10.1038/nm1777, PMID: 18552857

Sherer NM, Lehmann MJ, Jimenez-Soto LF, Horensavitz C, Pypaert M, Mothes W. 2007. Retroviruses can establish filopodial bridges for efficient cell-to-cell transmission. *Nature Cell Biology* **9**:310–315. DOI: https://doi.org/10.1038/ncb1544, PMID: 17293854

Sigal A, Kim JT, Balazs AB, Dekel E, Mayo A, Milo R, Baltimore D. 2011. Cell-to-cell spread of HIV permits ongoing replication despite antiretroviral therapy. *Nature* **477**:95–98. DOI: https://doi.org/10.1038/nature10347, PMID: 21849975

Sourisseau M, Sol-Foulon N, Porrot F, Blanchet F, Schwartz O. 2007. Inefficient human immunodeficiency virus replication in mobile lymphocytes. *Journal of Virology* **81**:1000–1012. DOI: https://doi.org/10.1128/JVI.01629-06, PMID: 17079292

Sowinski S, Jolly C, Berninghausen O, Purbhoo MA, Chauveau A, Köhler K, Oddos S, Eissmann P, Brodsky FM, Hopkins C, Onfelt B, Sattentau Q, Davis DM. 2008. Membrane nanotubes physically connect T cells over long distances presenting a novel route for HIV-1 transmission. *Nature Cell Biology* **10**:211–219. DOI: https://doi.org/10.1038/ncb1682, PMID: 18193035

Taylor S, Boffito M, Khoo S, Smit E, Back D. 2007. Stopping antiretroviral therapy. *AIDS* **21**:1673–1682. DOI: https://doi.org/10.1097/QAD.0b013e3281c61394, PMID: 17690564

Tenner-Racz K, Stellbrink HJ, van Lunzen J, Schneider C, Jacobs JP, Raschdorff B, Grosschupff G, Steinman RM, Racz P. 1998. The unenlarged lymph nodes of HIV-1-infected, asymptomatic patients with high CD4 T cell counts are sites for virus replication and CD4 T cell proliferation. The impact of highly active antiretroviral therapy. *The Journal of Experimental Medicine* **187**:949–959. DOI: https://doi.org/10.1084/jem.187.6.949, PMID: 9500797

Thomsen ER, Mich JK, Yao Z, Hodge RD, Doyle AM, Jang S, Shehata SI, Nelson AM, Shapovalova NV, Levi BP, Ramanathan S. 2016. Fixed single-cell transcriptomic characterization of human radial glial diversity. *Nature Methods* **13**:87–93. DOI: https://doi.org/10.1038/nmeth.3629, PMID: 26524239

Wawer MJ, Gray RH, Sewankambo NK, Serwadda D, Li X, Laeyendecker O, Kiwanuka N, Kigozi G, Kiddugavu M, Lutalo T, Nalugoda F, Wabwire-Mangen F, Meehan MP, Quinn TC. 2005. Rates of HIV-1 transmission per coital act, by stage of HIV-1 infection, in Rakai, Uganda. *The Journal of Infectious Diseases* **191**:1403–1409. DOI: https://doi.org/10.1086/429411, PMID: 15809897

Westendorp MO, Frank R, Ochsenbauer C, Stricker K, Dhein J, Walczak H, Debatin KM, Krammer PH. 1995a. Sensitization of T cells to CD95-mediated apoptosis by HIV-1 Tat and gp120. *Nature* **375**:497–500. DOI: https://doi.org/10.1038/375497a0, PMID: 7539892

Westendorp MO, Shatrov VA, Schulze-Osthoff K, Frank R, Kraft M, Los M, Krammer PH, Dröge W, Lehmann V. 1995. HIV-1 Tat potentiates TNF-induced NF-kappa B activation and cytotoxicity by altering the cellular redox state. *The EMBO Journal* **14**:546–554. PMID: 7859743

Wodarz D, Levy DN. 2007. Human immunodeficiency virus evolution towards reduced replicative fitness in vivo and the development of AIDS. *Proceedings of the Royal Society B: Biological Sciences* **274**:2481–2491. DOI: https://doi.org/10.1098/rspb.2007.0413, PMID: 17666377

Wu Y, Beddall MH, Marsh JW. 2007. Rev-dependent indicator T cell line. *Current HIV Research* **5**:394–402 . DOI: https://doi.org/10.2174/157016207781024018, PMID: 17627502

Zeng M, Haase AT, Schacker TW. 2012. Lymphoid tissue structure and HIV-1 infection: life or death for T cells. *Trends in Immunology* **33**:306–314. DOI: https://doi.org/10.1016/j.it.2012.04.002, PMID: 22613276

Zhong P, Agosto LM, Ilinskaya A, Dorjbal B, Truong R, Derse D, Uchil PD, Heidecker G, Mothes W. 2013. Cell-to-cell transmission can overcome multiple donor and target cell barriers imposed on cell-free HIV. *PLoS One* **8**: e53138. DOI: https://doi.org/10.1371/journal.pone.0053138, PMID: 23308151

Appendix 1

DOI: https://doi.org/10.7554/eLife.30134.035

Supplementary Mathematical Analysis for Jackson *et al.*

I Derivation of infection model assuming independence of infection and cell death

We consider a model of infection where is the probability of one HIV DNA copy to successfully infect the cell and is the probability of the cell to die as a result of the infection attempt. The probability of being infected when virions enter the cell is:

$$P_n = (1-(1-r)^n)(1-q)^n. \tag{AE1}$$

If the number of infection attempts, n, is Poisson distributed with mean λ, the fraction of cells that are productively infected is:

$$\begin{aligned} P_\lambda &= e^{-\lambda}\sum_n \tfrac{\lambda^n}{n!}P_n = e^{-\lambda}\sum_n \tfrac{\lambda^n}{n!}(1-(1-r)^n)(1-q)^n \\ &= e^{-\lambda}\sum_n \tfrac{(\lambda(1-q))^n}{n!} - \tfrac{(\lambda(1-r)(1-q))^n}{n!} \\ &= e^{-\lambda q}(1-e^{-\lambda r(1-q)}). \end{aligned} \tag{AE2}$$

We introduce a drug strength value d, where $d=1$ in the absence of drug and $d>1$ in the presence of drug. In the presence of drug, λ is decreased to λ/d. The drug therefore tunes λ. The probability of a cell to be infected and live given drug strength d is therefore:

$$P_{\lambda/d} = e^{-\lambda q/d}(1-e^{-\lambda r(1-q)/d}). \tag{AE3}$$

Experimentally, we measure P_λ, the number of infected cells, and L_λ, the number of live cells remaining two days post-infection for the cell line.

Assuming a Poisson distribution of the number of infection attempts, the probability of being productively infected is

$$P_\lambda = 1-e^{-\lambda r} \quad \Rightarrow \quad r = -\frac{\log(1-P_\lambda)}{\lambda}. \tag{AE4}$$

Similarly, the probability of a cell to live is

$$L_\lambda = e^{-\lambda q} \quad \Rightarrow \quad q = -\frac{\log(L_\lambda)}{\lambda}. \tag{AE5}$$

II Derivation of infection model assuming dependence of infection and cell death

Cellular infection and death may be the result of independent processes. For example, cell death may be a programmed response to DNA damage induced by the infection attempt and therefore may occur regardless of whether or not the cell is successfully infected. Infection and death may also be dependent. One example of dependence is the cytotoxicity mediated by expressed viral proteins after integration into the host genome.

In this case, the probability of productive infection and survival of the cell given n attempts is

$$P_n = \sum_{m=1}^{n}\binom{n}{m}(r'(1-q'))^m(1-r')^{n-m} \tag{AE6}$$

Here, r' and q' are the probabilities for infection and death respectively. Their relationship to the experimentally measured r and q are discussed in the next section. $[r'(1-q')]^m$ is the probability that m infection attempts are successful and none of the attempts triggers cell

death, while $(1-r')^{n-m}$ accounts for $n-m$ unsuccessful infections. To obtain the total probability of productive infection without cell death given n attempts, we sum over all cases with $m' \geq 1$ sucessful infections.

Realizing that:

$$\begin{aligned}\sum_{m=1}^{n}\binom{n}{m}(r'(1-q'))^m(1-r')^{n-m} &= \sum_{m=0}^{n}\binom{n}{m}(r(1-q))^m(1-r')^{n-m}-(1-r')^n \\ &= (r'(1-q')+(1-r'))^n-(1-r')^n,\end{aligned} \tag{AE7}$$

we can simplify the above to:

$$P_n = (r'(1-q')+(1-r'))^n-(1-r')^n = (1-r'q')^n-(1-r')^n. \tag{AE8}$$

Averaging this over a Poisson distribution with meanλ, we find:

$$e^{-\lambda}\sum_n \frac{\lambda^n}{n!}P_n = e^{-\lambda}\sum_n \frac{\lambda^n}{n!}((1-r'q')^n-(1-r')^n) = e^{-\lambda r'q'}-e^{-\lambda r'}. \tag{AE9}$$

III Equivalence of the two models

The two models predict same dependence on λ (the difference of two exponentials) but the parameters r, q and r', q' play slightly different roles. The models are the same if:

$$r'q' = q \quad \text{and} \quad r' = r(1-q)+q. \tag{AE10}$$

Hence the two models are a re-parametrization of the same process. The experimental measurement of r and q, as described in the main manuscript, consists of estimating r as the fraction of infected cells when the fraction of dead cells is low due to a low number of measured DNA copies per cell. The death rate q is derived by measuring the number of live cells remaining when the number of HIV DNA copies per cell is known. If the probability of death is dependent on infection, then death is only of infected cells and is a product of the probability to be infected and die ($r'q'$). Likewise, the underlying probability of infection r' will account for the fraction dead cells (q) and any cells which are infected but not dead ($r(1-q)$).

HIV complementation creates a quasispecies of wildtype and mutant virus in the face of selection

Laurelle Jackson[1,2], **Jessica Hunter**[1,2], **Sandile Cele**[1], **Isabella Markham Ferreira**[3], **Andrew C. Young**[1], **Mikael Boulle**[1,2], **Fabio Zanini**[4], **Gila Lustig**[1], **Tulio de Oliveira**[3], **Richard A. Neher**[4], **Alex Sigal**[1,2,5*]

***For correspondence:** Alex.Sigal@ahri.org (AS)

[1]Africa Health Research Institute, Durban, South Africa; [2]School of Laboratory Medicine and Medical Sciences, University of KwaZulu-Natal, Durban, South Africa; [3]KwaZulu-Natal Research Innovation and Sequencing Platform, Durban, South Africa; [4]Biozentrum and SIB Swiss Institute of Bioinformatics, University of Basel, Basel, Switzerland; [5]Max Planck Institute for Infection Biology, Berlin, Germany

Abstract HIV exists as multiple genotypes in a single infected individual, referred to as a quasispecies. How such sequence heterogeneity can be maintained in the same environment remains unclear. Here we reproduced a quasispecies *in vitro* by using the antiretroviral drug efavirenz (EFV) as the selective pressure. We observed that while the frequency of EFV resistant mutant virus increased with time, it never completely supplanted the wildtype genotype. Instead, the wildtype stabilized at 20 percent of the virus population. Single-cell sequencing of viral genotypes showed that the fraction of drug resistant virus in the population increased when the majority of cells were infected with wild type virus only, but plateaued when cells were co-infected with wildtype and mutant. This suggests that in co-infected cells, wildtype virus may package mutant reverse transcriptase (RT) and vice versa otherwise known as complementation. To test for complementation, we singly transfected CFP labelled wildtype and YFP labelled EFV resistant mutant molecular viral clones, or co-transfected both. When virus made by transfected cells was tested, YFP and CFP expressing virus was similarly resistant to EFV in the co-transfection, but followed the expected resistance pattern in single transfections. These results indicate that complementation is one mechanism which drives quasispecies formation.

Introduction

The HIV quasispecies consist of multiple viral genomes sampled from an environment such as the blood. One consequence of a quasispecies is diversity in the HIV Env gene. This allows HIV to escape neutralizing antibodies (***Frost et al.*** (***2005***); ***Rong et al.*** (***2009***)). In the face of antiretroviral therapy, a quasispecies is formed which results in a mixture of HIV genomes that are resistant to different degrees to antiretroviral drugs (ARVs) (***Brenner et al.*** (***2002***); ***Allers et al.*** (***2007***)). A quasispecies may also allow HIV to maintain sufficient heterogeneity to escape effective T cell suppression (***Phillips et al.*** (***1991***); ***Goulder et al.*** (***2001***)).

Due to the errors in reverse transcription, HIV replication generates a quasispecies where variants are at low frequencies around the main viral sequence (***Brenner et al.*** (***2002***); ***Coffin*** (***1992***); ***Katz and Skalka*** (***1990***). However, how a stable quasispecies with variants at high frequencies is maintained is unclear. One possibility is that different anatomical environments apply different

selective pressures, therefore leading to a diverse viral pool (***Paranjpe et al.*** (***2002***); ***Schnell et al.*** (***2010***)). One mechanism to create a quasispecies that does not rely on the assumption of different environments is complementation or phenotypic mixing (***Domingo et al.*** (***2012***); ***Hill et al.*** (***2012***)). In this mechanism, co-infection and viral protein expression from two different viral genotypes in the same cell results in sharing of viral components. This mechanism is distinct from recombination, where two viral genomes co-packaged in the same cell recombine to form a new genome (***Levy et al.*** (***2004***)). In complementation, a virus of genotype 1 may contain proteins from virus of genotype 2 and vice versa. If one of the genotypes has a fitness cost relative to the other, the difference in fitness will be masked (***Andino and Domingo*** (***2015***)). This process has been shown to operate in viruses (***Froissart et al.*** (***2004***); ***Vignuzzi et al.*** (***2006***)) including HIV (***Mo et al.*** (***2004***); ***Gelderblom et al.*** (***2008***)). There is no known mechanism which prevents one HIV strain packaging components such as RT from another HIV strain if both strains are in the same cell since RT molecules mix in the cell cytoplasm (***Freed*** (***2001***)).

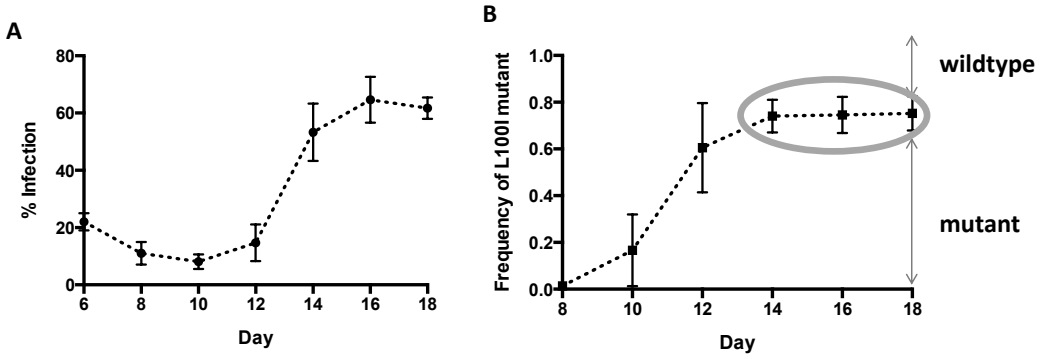

Figure 1. Frequency of EFV resistant mutant plateaus in the face of EFV selection. (A) The fraction of infected cells as a function of time in the presence of 20 nM EFV. Mean and standard deviation of 3 independent experiments. (B) Frequency of EFV resistant mutants as a function of time derived from population illumina sequencing of the cell population for cell populations from (A). Mean and standard deviation of 3 independent experiments.

Here we used *in vitro* HIV evolution in the presence of RT inhibitor EFV to ask whether a quasispecies can be formed by complementation. We observed that drug resistant mutant reproducibly evolved during infection in the face of EFV. Initially, mutant infection rapidly expanded. However, once the fraction of mutant infected cells reached 0.8, the frequency of mutant stabilized. This correlated with co-infection of wild-type and mutant genomes, and such co-infection led to virions with wild type or mutant genotypes displaying a similar level of EFV resistance. This shows that complementation should have an important role in the formation of the quasispecies during HIV drug resistant evolution.

Results

To test whether a quasispecies can be reproduced *in vitro*, we infected the RevCEM E7 clone (***Boullé et al.*** (***2016***); ***Jackson et al.*** (***2018***)) with HIV in the face of inhibition by EFV. This clone of the RevCEM cell line expresses GFP in the presence of the HIV Rev protein (***Wu et al.*** (***2007***)), with the maximum frequency of GFP positive cells being over 80 percent (***Jackson et al.*** (***2018***)). Infection was maintained at 2 percent of the total cell population by diluting infected cells every 2 days. The number of infected cells at the end of each two day cycle, before dilution, was 10 percent, resulting in a replication ratio (R) of approximately 5. It then increased moderately on day 10 and sharply on day 12, indicating that the evolution of drug resistance has taken place (Fig 1A). Illumina sequencing of the HIV DNA population at each day showed that starting day 10, the L100I mutation in the HIV RT gene, which confers resistance to EFV, was detected at a frequency of 10 percent of the total

viral genomes (Fig 1A). This reached about 60 percent on day 12 and 80 percent on day 14. The L100I frequency stabilized at 80 percent on day 16 and day 18. Other EFV resistant mutants, such as K103N, accounted for less than 1 percent of genotypes in total up to and including day 18. Wild type HIV accounted for most of the remaining 20 percent (Fig 1B).

To examine whether the plateau in the frequency of mutant HIV was correlated with co-infection of the same cell with wild-type and mutant HIV, we single-cell sequenced HIV DNA by sorting GFP positive infected cells into wells of a multi-well plate at 1 cell per well, then lysing and amplifying the RT region followed by illumina sequencing. 60 cells were sequenced and analyzed for each time point, except for day 4 and day 12, where 30 cells were analyzed. At day 4, before selective pressure was applied, all infected cells showed wildtype HIV genomes (Fig 2). At day 10, there were 21 cells (35 percent) with EFV resistance mutations, consisting of 16 L100I mutations, 1 K103N mutation and 4 G190A mutations. Interestingly, all mutations were co-expressed with wild type (Fig 2). The rest of the HIV DNA genomes were wild type only. In contrast, on day 18, where the mutant frequency stabilized at 80 percent, cells were infected by EFV resistant and wildtype HIV as follows: L100I (90 percent), K103N (28 percent), and G190A (62 percent) and wildtype (5 percent) (Fig 2).

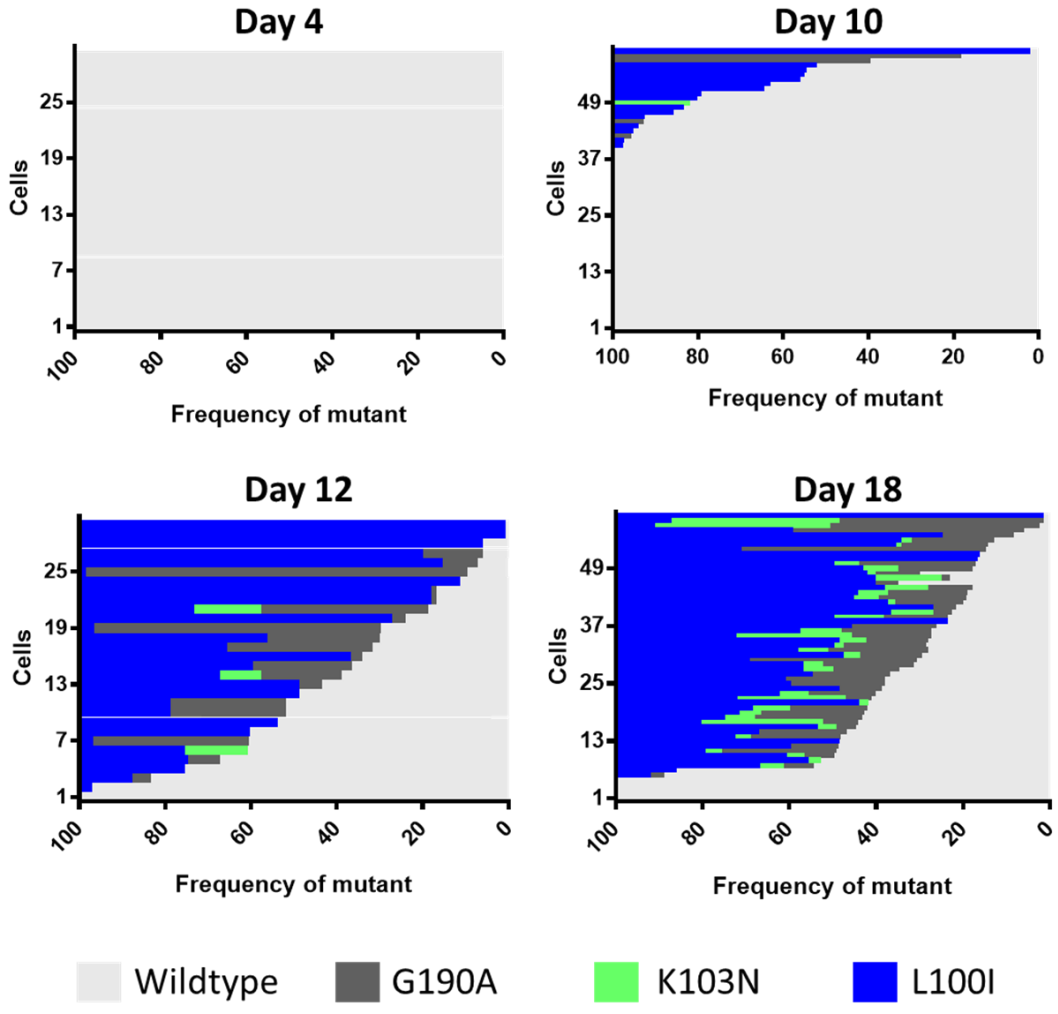

Figure 2. Sequencing of viral genomes in single cells shows increasing frequency of co-infected cells with time. The relative frequencies of wild type and mutant HIV genomes per cell for the day 4, day 10, day 12 and day 18. Frequency is on the x-axis, cell number on y-axis. Cells were ranked by lowest to highest wild type frequency. Light grey is wild type virus, blue is the L100I mutant, green is K103N mutant and dark grey is G190A mutant.

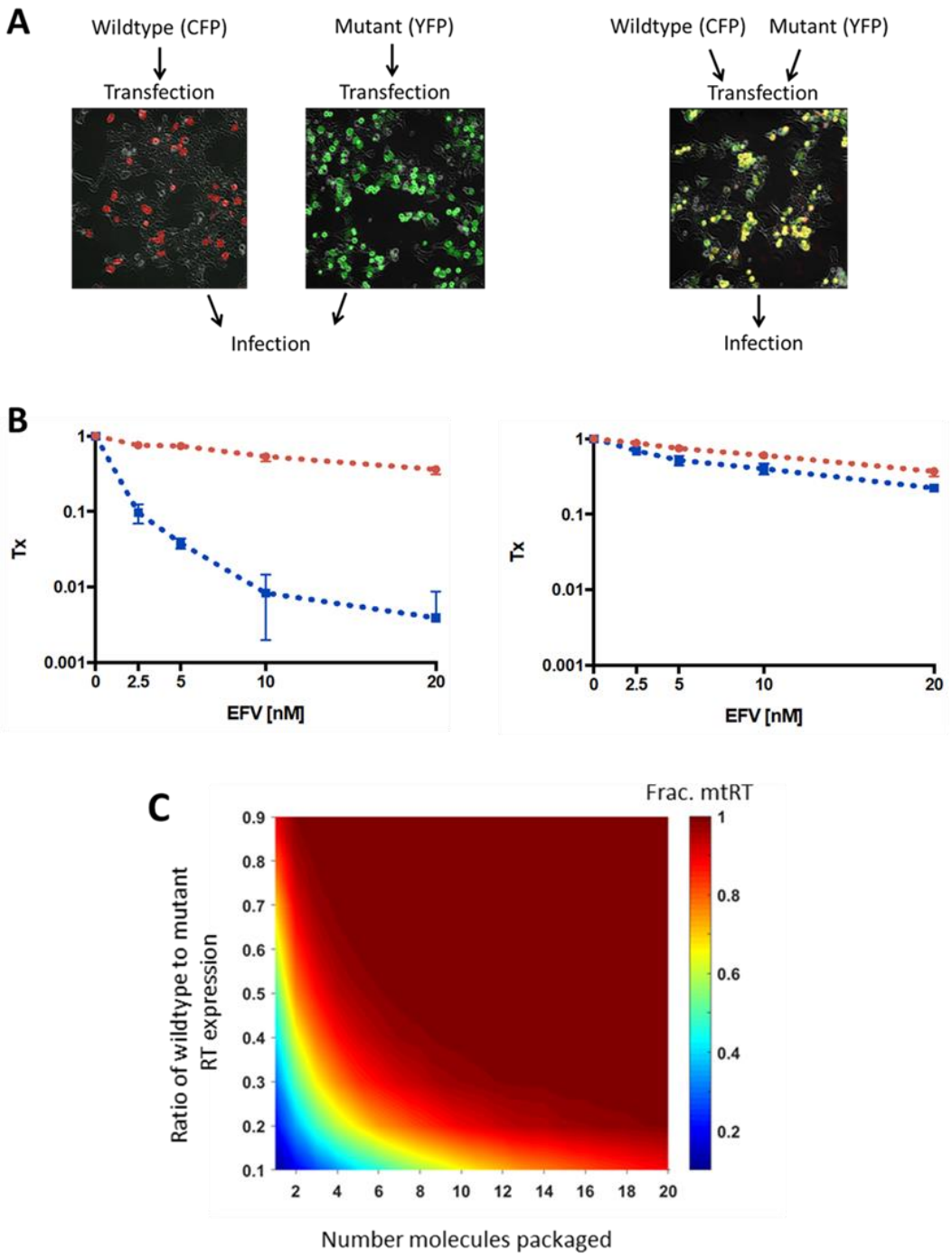

Figure 3. Co-transfection of wild type and mutant molecular clones yields resistant virus independent of genotype. (A) CFP expressing wild type and YFP expressing L100I EFV resistant mutant molecular clones were either transfected separately (left) or co-transfected (right) into a virus producer cell line. Shown are images after producer line transfection, with CFP pseudo-coloured as red and YFP pseudo-coloured as green. Co-transfected cells which express both fluorescent proteins are yellow. (B) Sensitivity of cell-free virus collected from the transfections to EFV. Sensitivity was measured as the transmission index (Tx), the ratio of the number of infected cells in the presence of EFV divided by the number of infected cells in the absence of EFV. Left panel shows virus from separate transfections, while right panel shows virus from the co-transfection, with red and blue points mutant and wild type genotypes respectively. Error bars represent SD from two independent experiments. For the left panel, the Tx values at 20nM EFV were significantly different for mutant and wildtype ($p=0.05$, two tailed t-test). The Tx values at 20nM EFV for mutant and wildtype in the right panel were not significantly different. (C) Predicted fraction of virions containing at least one mutant RT molecule as a function of the ratio of genomic copies of drug sensitive versus resistant virus and the number of RT molecules packaged.

To directly test whether EFV resistant mutant HIV can complement wild type virus, we used transfection of molecular viral clones consisting of plasmids expressing a mutant and wild type virus in conjunction with a fluorescent protein. Upon transfection, molecular clones produce fully functional replicating virus which can be tested for resistance to EFV (Fig 3A). We transfected a molecular clone expressing CFP (***Levy et al.*** (***2004***)) with a wild type genome into a virus producer cell line. The producer cells showed only CFP fluorescence (3A, left image). We next replaced the RT region of a YFP expressing HIV (***Levy et al.*** (***2004***)) with the L100I mutant to create a molecular clone of the mutant. When we transfected this molecular clone into cells, the producer cell line showed YFP expression only (Fig 3A, middle image). We then co-transfected the molecular clones, which resulted in dual CFP and YFP expression from most fluorescent cells, indicating both viral strains being expressed from the same cell (Fig 3A, right image). We collected virus from each of the three conditions and used it to infect MT4 cells (see Fig S1 for gating strategy). Cells infected with virus made by single transfected cells were either sensitive (CFP expressing) or resistant (YFP expressing) to EFV (Fig 3B, left panel). In contrast, virus from the co-transfection showed resistance both for the wildtype CFP expressing genotype and YFP expressing mutant genotype (Fig 3B, right panel). For wildtype, resistance gained was comparable but slightly less relative to the YFP resistant mutant. However, the slight difference may be explained by incomplete co-transfection with both molecular clones (Fig 3A, right graph). This indicates that the wild type virus was able to complement with the mutant virus.

To examine the expected effects of complementation of mutant and wild type HIV on the replication of each genotype, we constructed a computational model which considers the number of RT molecules packaged per virion and the ratio of wild type to mutant viral genomes (Fig 3C). The benefit to the wild type drug sensitive virus in complementation decreases at low numbers of RT molecules and higher number of wild type genomes, since in this case wild type virus does not package mutant RT. At the reported numbers of RT molecules per virion (roughly 50) (***Panet and Kra-Oz*** (***1978***); ***Bauer and Temin*** (***1980***)) and ratios of wild type to mutant genomes of close to 1, complementation of the wild type can be complete.

Discussion

We have observed that a quasispecies is formed in the face of EFV selective pressure, where wildtype HIV persists despite a fitness disadvantage. The fraction of drug sensitive HIV stabilized upon co-infection with EFV resistant virus in the same cell. Co-transfection of mutant and wildtype molecular clone in the same cell enabled the wild type to gain EFV phenotypic resistance. The necessary condition for complementation to occur *in vivo* is expression of multiple viral genotypes in the same cell. Multiple infections can occur by cell-to-cell spread, a directed mode of HIV transmission efficiently delivering HIV from the donor to target cell (***Jolly et al.*** (***2004***); ***Sattentau*** (***2008***); ***Kinoshita et al.*** (***1998***); ***Sigal et al.*** (***2011***)). The frequency of HIV multiple infection per cell has been controversial, with some studies showing multiple infection per cell higher than expected by the Poisson distribution, hence supporting a directed process for viral transmission (***Jung et al.*** (***2002***); ***Law et al.*** (***2016***)). Other studies did not show multiple infections at a frequency greater than that predicted by the Poisson distribution (***Josefsson et al.*** (***2011***, 2013)). Clearly, the frequency of multiple infections per cell with different genotypes needs to be established before the effect of complementation *in vivo* can be quantified.

Complementation interferes with selection and hence reduces fitness of the viral population by preventing the selection of more fit genotypes (***Froissart et al.*** (***2004***)). There is evidence that the quasispecies stabilized by complementation is beneficial for the fitness of the population, since this allows deleterious variants to share components and result in a more functional virion, or keep a heterogeneous pool of virus which can react to rapid changes in the infection environment (***Vignuzzi et al.*** (***2006***); ***Domingo et al.*** (***2012***); ***Lauring et al.*** (***2013***); ***Andino and Domingo*** (***2015***)). Interestingly, the majority mutant HIV in this study was coinfected with wildtype, despite non-saturating infection of the cell population. In contrast, most of wildtype infected cells had only the wildtype genotype.

This may indicate that wildtype infection may make the cells permissive for the L100I mutant; a benefit conferred by the quasispecies.

The data here suggests that complementation could be important as a counter-force to drug resistant evolution. Inhibiting co-infection by interfering with mechanisms which cause co-infection, such as cell-to-cell spread, may therefore not only reduce infection in the face of ART and other forms of inhibition (***Deeks et al.*** (***2012***); ***Hill et al.*** (***2014***)), but also limit viral diversity and hence the ability of HIV to evolve resistance.

Methods and Materials

Inhibitors, viruses and cell lines

The antiretroviral EFV was obtained through the AIDS Research and Reference Reagent Program, National Institute of Allergy and Infectious Diseases, National Institutes of Health. RevCEM cells from Y. Wu and J. Marsh; MT-4 cells from D. Richman and HIV molecular clone pNL4-3 from M. Martin. The NL4-3YFP and NL4-3CFP molecular clones were gifts from D. Levy. Cell-free viruses were produced by transfection of HEK293 cells with pNL4-3 using TransIT-LT1 (Mirus) or Fugene HD (Roche) transfection reagents. Virus containing supernatant was harvested after two days of incubation and filtered through a 0.45µm filter (Corning). The number of virus genomes in viral stocks was determined using the RealTime HIV-1 viral load test (Abbott Diagnostics). The L100I mutant was evolved by serial passages of wild type NL4-3 in RevCEM cells in the presence of 20nM EFV. After 18 days of selection, the RT gene was cloned from the proviral DNA and the mutant RT gene was inserted into the NL4-3 molecular clone. RevCEM clone E7 used in this study were generated as previously described (Boullé, Müller et al. 2016). Briefly, the E7 clone was generated by subcloning RevCEM cells at single cell density. Surviving clones were subdivided into replicate plates. One of the plates was screened for the fraction of GFP expressing cells upon HIV infection using microscopy, and the clone with the highest fraction of GFP positive cells was selected. All cell lines not authenticated, and mycoplasma negative. Cell culture and experiments were performed in complete RPMI 1640 medium supplemented with L-Glutamine, sodium pyruvate, HEPES, non-essential amino acids (Lonza), and 10 percent heat-inactivated FBS (Hyclone).

Infection

For a cell-free infection of RevCEM clones, 10^6 cells/ml were infected with $2X10^8$ NL4-3 viral copies/ml (roughly 20ng p24 equivalent) for 2 days (day 0). For coculture infection, infected cells from the cell-free infection were used as the donors and cocultured with 10^6 cells/ml target cells (day 2). After two days of infection, two percent of the infected cells were added to uninfected targets and cocultured for a 2-day cycle (day 4). Thereafter, 2 percent of resuspended infected cells were added to uninfected targets in the presence of EFV and co-cultured for a 2-day cycle. This infection process was repeated every 2 days until day 18.

Complementation infection

To produce mixed CFP:YFP virus, NL4-3YFP and NL4-3CFP were added in equal concentrations (0.5 ug/ul) to the Fugene HD (Roche) mixture for co-transfection into HEK293 cells. YFP and CFP virus was also produced separately, and added to a Fugene HD (Roche) at a concentration of 1ug/ul. For a cell-free infection of MT4 cells, 106 cells/ml were infected with 1x108 viral copies/ml with the following viral mixes: (1) co-transfected CFP:YFP virus; (2) a mix of CFP and YFP virus; (3) CFP virus; (4) YFP virus.

Staining and flow cytometry

The frequency of RevCEM E7 infected cells was detected by the amount of GFP positive cells on the FACSCaliber (BD Biosciences) machine using the 488 laser lines. The number of CFP and YFP positive cells in the MT4 infection was determined by the amount of CFP or YFP positive cells on the

FACAriaIII (BD Biosciences) using the 488nm laser line. Results were analysed with FlowJo 10.0.8 software. For single cell sorting to detect the number of HIV DNA copies per cell, cells were single cell sorted using 85 micron nozzle in a FACSAriaIII machine. GFP positive RevCEM clones were sorted into 96 well plates (Biorad) containing 30μl lysis buffer (2.5μl 0.1M Dithiothreitol, 5μl 5 percent NP40 and 22.5μl molecular biology grade water (Kurimoto, Yabuta et al. 2007)).

Microscopy

For imaging infection by microscopy, cell density was reduced to 5X10^4 cells/ml and cells were attached to ploy-l-lysine (Sigma-Aldrich) coated optical six well plates (MatTek). Infections were imaged using a Metamorph-controlled Nikon TiE motorized microscope with a Yokogawa spinning disk with a 20x, 0.75 NA phase objective in a biosafety level 3 facility. Excitation sources were 488 (GFP) and 445 (CFP) laser lines and emission was detected through a Semrock Brightline quad band 440-40 /521-21/607-34/700-45 nm filter. Images were captured using an 888 EMCCD camera (Andor). Images were analyzed using custom code developed with the Matlab Image Analysis Toolbox.

Deep sequencing for detection of drug resistant mutants

For single cells, the cells were lysed and DNA was kept suspended in the lysis buffer. For populations of cells, genomic DNA was extracted using the QIAamp DNA mini kit (Qiagen). Phusion hot start II DNA polymerase (New England Biolabs) PCR reaction mix (10μl 5X Phusion HF buffer, 1μl dNTPs, 2.5μl of the forward primer, 2.5μl of the reverse primer, 0.5μl Phusion hot start II DNA polymerase, 2.5μl of DMSO and molecular biology grade water to 50μl reaction volume) was added to the lysed single cells or extracted genomic DNA of cell populations. Two rounds of PCR were performed. The first-round reaction amplified a region of the RT gene in the proviral DNA using the forward primer 5' tcgtcggcagcgtcagatgtgtataagagacagTTAATAAGAGAACTCAAGATTTC 3' and reverse primer 5' gtctcgtgggctcggagatgtgtataagagacagCCCCACCTCAACAGATGTTGTC 3'. The bold and italicised portion of the primers represents the Nextera® XT Index Kit adaptor. Cycling program was 98C for 30 seconds, then 35 cycles of 98C for 10 seconds, 50C for 30 seconds and 72C for 15 seconds with a final extension of 72C for 5 minutes. 1μl of the first round product was then transferred into a PCR mix as above, with second round Nextera XT Index Kit adaptor primers (forward 5' tcgtcggcagcgtca-gatgtgtataagagacag 3', reverse 5' gtctcgtgggctcggagatgtgtataagagacag 3'). The second round PCR amplified a 400bp product which was then visualized on a 1 percent agarose gel. The PCR amplicon was gel extracted using the QIAquick gel extraction kit (Qiagen). Illumina indices were attached to the amplicon with the Nextera XT Index Kit and deep sequenced using the Illumina Miseq. Fast-q files were analysed in Geneious. Both 5' and 3' ends were trimmed with an error probability limit of 0.1. Drug resistant mutations were found based on a minimum variant frequency of 0.01 for populations of cells and 0.5 for single cells. The maximum variant P-value was 10^{-6}.

Model

A stochastic simulation was performed to find the probability of a virus packaging at least one mutant RT molecule as a function of the total number of RT molecules packaged by one virus and the fraction of RT molecules in the cell produced by the mutant RT gene. A vector of random numbers with number of entries equal to the number of total RT molecules packaged was chosen using Matlab from a uniform distribution between 0 and 1. If at least one of the numbers was less than 1-Fwt, where Fwt is the wildtype frequency, the iteration was scored as containing at least one mutant RT. 10^4 iterations were performed for each combination of total RT molecules and Fwt, and the frequency of iterations with at least one mutant RT graphed.

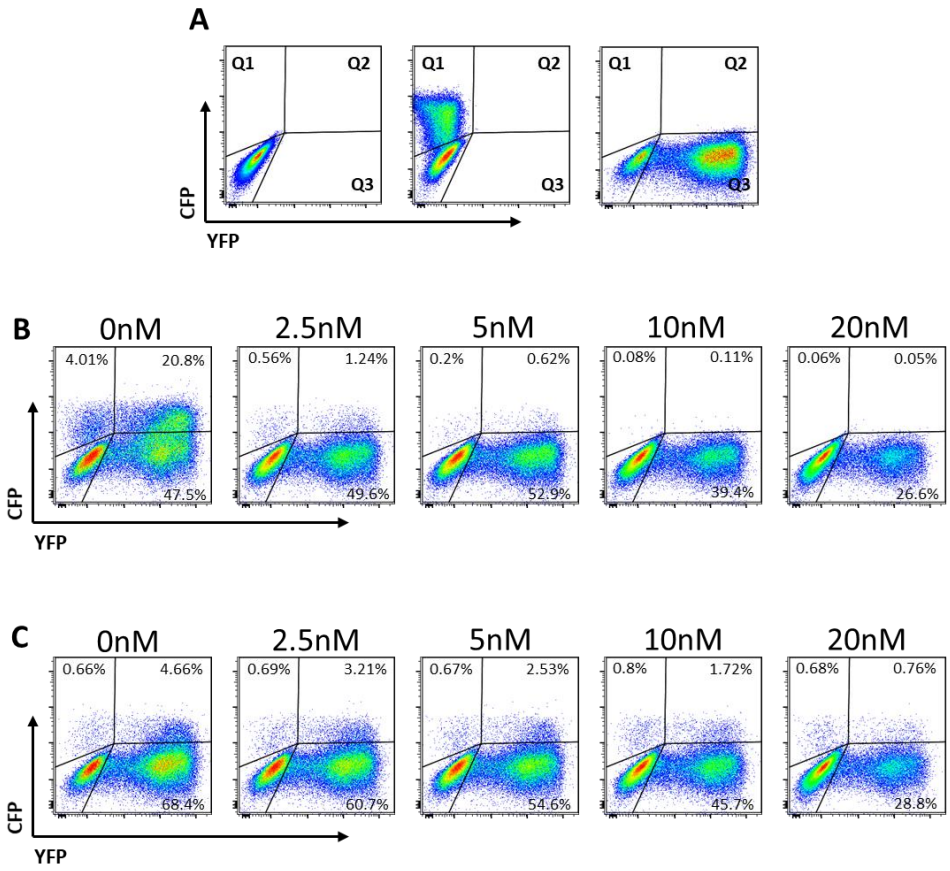

Figure S1. Gating strategy to detect EFV sensitivity virus from singly infected and co-infected molecular clones. Virus was collected from producer cells singly transfected with wild type HIV expressing CFP or L100I mutant HIV expressing YFP, or co-transfected with both molecular clones. MT4 cells were then infected with the virus derived from the co-transfection, or with the virus derived from the single transfections, where CFP and YFP expressing virus was mixed 1:1 before the infection. The numbers of infected cells in quadrant Q1 and Q2 was measured as the total number of cells infected with the CFP expressing virus, and Q2 and Q3 as the total number of cells infected with YFP expressing virus. (A) Uninfected (left panel), CFP virus only (middle panel) or YFP virus only (right panel) controls. (B) Infection with virus from single transfections mixed 1:1. (C) Infection from virus from the co-transfection. Efavirenz was added to each infection condition. The concentration of Efavirenz added is indicated above each FACs plot.

Acknowledgments

This work was supported by National Institutes of Health Grant R21MH104220. AS was supported by a Human Frontiers Science Program Career Development Award CDA 00050/2013. RAN is supported by the European Research Council through grant Stg. 260686. LJ and JH are supported by a fellowship from the South African National Research Foundation. IMF is supported through a Sub- Saharan African Network for TB/HIV Research Excellence (SANTHE, a DELTAS Africa Initiative (grant DEL-15–006)) fellowship, and a Poliomyelitis Research Foundation fellowship 17/59.

References

Allers K, Knoepfel SA, Rauch P, Walter H, Opravil M, Fischer M, Günthard HF, Metzner KJ. Persistence of lamivudine-sensitive HIV-1 quasispecies in the presence of lamivudine in vitro and in vivo. JAIDS Journal of Acquired Immune Deficiency Syndromes. 2007; 44(4):377–385.

Andino R, Domingo E. Viral quasispecies. Virology. 2015; 479-480:46–51. https://www.ncbi.nlm.nih.gov/pubmed/25824477, doi: 10.1016/j.virol.2015.03.022.

Bauer G, Temin HM. Specific antigenic relationships between the RNA-dependent DNA polymerases of avian reticuloendotheliosis viruses and mammalian type C retroviruses. J Virol. 1980; 34(1):168–77. https://www.ncbi.nlm.nih.gov/pubmed/6154804.

Boullé M, Müller TG, Dähling S, Ganga Y, Jackson L, Mahamed D, Oom L, Lustig G, Neher RA, Sigal A. HIV cell-to-cell spread results in earlier onset of viral gene expression by multiple infections per cell. PLoS pathogens. 2016; 12(11):e1005964.

Brenner BG, Routy JP, Petrella M, Moisi D, Oliveira M, Detorio M, Spira B, Essabag V, Conway B, Lalonde R. Persistence and fitness of multidrug-resistant human immunodeficiency virus type 1 acquired in primary infection. Journal of virology. 2002; 76(4):1753–1761.

Coffin JM. Genetic diversity and evolution of retroviruses. Curr Top Microbiol Immunol. 1992; 176:143–64. https://www.ncbi.nlm.nih.gov/pubmed/1600751.

Deeks SG, Autran B, Berkhout B, Benkirane M, Cairns S, Chomont N, Chun TW, Churchill M, Di Mascio M, Katlama C. Towards an HIV cure: a global scientific strategy. Nature reviews Immunology. 2012; 12(8):607.

Domingo E, Sheldon J, Perales C. Viral quasispecies evolution. Microbiology and Molecular Biology Reviews. 2012; 76(2):159–216.

Freed EO. HIV-1 replication. Somatic cell and molecular genetics. 2001; 26(1-6):13–33.

Froissart R, Wilke CO, Montville R, Remold SK, Chao L, Turner PE. Co-infection weakens selection against epistatic mutations in RNA viruses. Genetics. 2004; 168(1):9–19. https://www.ncbi.nlm.nih.gov/pubmed/15454523, doi: 10.1534/genetics.104.030205.

Frost SD, Wrin T, Smith DM, Pond SLK, Liu Y, Paxinos E, Chappey C, Galovich J, Beauchaine J, Petropoulos CJ. Neutralizing antibody responses drive the evolution of human immunodeficiency virus type 1 envelope during recent HIV infection. Proceedings of the National Academy of Sciences. 2005; 102(51):18514–18519.

Gelderblom HC, Vatakis DN, Burke SA, Lawrie SD, Bristol GC, Levy DN. Viral complementation allows HIV-1 replication without integration. Retrovirology. 2008; 5:60. https://www.ncbi.nlm.nih.gov/pubmed/18613957, doi: 10.1186/1742-4690-5-60.

Goulder PJ, Brander C, Tang Y, Tremblay C, Colbert RA, Addo MM, Rosenberg ES, Nguyen T, Allen R, Trocha A. Evolution and transmission of stable CTL escape mutations in HIV infection. Nature. 2001; 412(6844):334.

Hill AL, Rosenbloom DI, Fu F, Nowak MA, Siliciano RF. Predicting the outcomes of treatment to eradicate the latent reservoir for HIV-1. Proceedings of the National Academy of Sciences. 2014; 111(37):13475–13480.

Hill AL, Rosenbloom DI, Nowak MA. Evolutionary dynamics of HIV at multiple spatial and temporal scales. Journal of molecular medicine. 2012; 90(5):543–561.

Jackson L, Hunter J, Cele S, Ferreira IM, Young AC, Karim F, Madansein R, Dullabh KJ, Chen CY, Buckels NJ, Ganga Y, Khan K, Boulle M, Lustig G, Neher RA, Sigal A. Incomplete inhibition of HIV infection results in more HIV infected lymph node cells by reducing cell death. eLife. 2018; 7:e30134.

Jolly C, Kashefi K, Hollinshead M, Sattentau QJ. HIV-1 cell to cell transfer across an Env-induced, actin-dependent synapse. J Exp Med. 2004; 199(2):283–93. http://www.ncbi.nlm.nih.gov/pubmed/14734528.

Josefsson L, King MS, Makitalo B, Brännström J, Shao W, Maldarelli F, Kearney MF, Hu WS, Chen J, Gaines H. Majority of CD4+ T cells from peripheral blood of HIV-1–infected individuals contain only one HIV DNA molecule. Proceedings of the National Academy of Sciences. 2011; 108(27):11199–11204.

Josefsson L, Palmer S, Faria NR, Lemey P, Casazza J, Ambrozak D, Kearney M, Shao W, Kottilil S, Sneller M. Single cell analysis of lymph node tissue from HIV-1 infected patients reveals that the majority of CD4+ T-cells contain one HIV-1 DNA molecule. PLoS pathogens. 2013; 9(6):e1003432.

Jung A, Maier R, Vartanian JP, Bocharov G, Jung V, Fischer U, Meese E, Wain-Hobson S, Meyerhans A. Recombination: Multiply infected spleen cells in HIV patients. Nature. 2002; 418(6894):144.

Katz RA, Skalka AM. Generation of diversity in retroviruses. Annu Rev Genet. 1990; 24:409–45. https://www.ncbi.nlm.nih.gov/pubmed/1708222, doi: 10.1146/annurev.ge.24.120190.002205.

Kinoshita S, Chen BK, Kaneshima H, Nolan GP. Host control of HIV-1 parasitism in T cells by the nuclear factor of activated T cells. Cell. 1998; 95(5):595–604.

289 **Lauring AS**, Frydman J, Andino R. The role of mutational robustness in RNA virus evolution. Nat Rev Microbiol.
290 2013; 11(5):327–36. https://www.ncbi.nlm.nih.gov/pubmed/23524517, doi: 10.1038/nrmicro3003.

291 **Law KM**, Komarova NL, Yewdall AW, Lee RK, Herrera OL, Wodarz D, Chen BK. In vivo HIV-1 cell-to-cell transmission
292 promotes multicopy micro-compartmentalized infection. Cell reports. 2016; 15(12):2771–2783.

293 **Levy DN**, Aldrovandi GM, Kutsch O, Shaw GM. Dynamics of HIV-1 recombination in its natural target cells.
294 Proceedings of the National Academy of Sciences. 2004; 101(12):4204–4209.

295 **Mo H**, Lu L, Pithawalla R, Kempf DJ, Molla A. Complementation in cells cotransfected with a mixture of wild-
296 type and mutant human immunodeficiency virus (HIV) influences the replication capacities and phenotypes
297 of mutant variants in a single-cycle HIV resistance assay. J Clin Microbiol. 2004; 42(9):4169–74. https:
298 //www.ncbi.nlm.nih.gov/pubmed/15365007, doi: 10.1128/JCM.42.9.4169-4174.2004.

299 **Panet A**, Kra-Oz Z. A competition immunoassay for characterizing the reverse transcriptase of mammalian RNA
300 tumor viruses. Virology. 1978; 89(1):95–101. https://www.ncbi.nlm.nih.gov/pubmed/80059.

301 **Paranjpe S**, Craigo J, Patterson B, Ding M, Barroso P, Harrison L, Montelaro R, Gupta P. Subcompartmentalization
302 of HIV-1 quasispecies between seminal cells and seminal plasma indicates their origin in distinct genital
303 tissues. AIDS research and human retroviruses. 2002; 18(17):1271–1280.

304 **Phillips RE**, Rowland-Jones S, Nixon DF, Gotch FM, Edwards JP, Ogunlesi AO, Elvin JG, Rothbard JA, Bangham
305 CR, Rizza CR. Human immunodeficiency virus genetic variation that can escape cytotoxic T cell recognition.
306 Nature. 1991; 354(6353):453.

307 **Rong R**, Li B, Lynch RM, Haaland RE, Murphy MK, Mulenga J, Allen SA, Pinter A, Shaw GM, Hunter E. Escape from
308 autologous neutralizing antibodies in acute/early subtype C HIV-1 infection requires multiple pathways. PLoS
309 pathogens. 2009; 5(9):e1000594.

310 **Sattentau Q**. Avoiding the void: cell-to-cell spread of human viruses. Nat Rev Microbiol. 2008; 6(11):815–26.
311 https://www.ncbi.nlm.nih.gov/pubmed/18923409, doi: 10.1038/nrmicro1972.

312 **Schnell G**, Price RW, Swanstrom R, Spudich S. Compartmentalization and clonal amplification of HIV-1 variants
313 in the cerebrospinal fluid during primary infection. Journal of virology. 2010; 84(5):2395–2407.

314 **Sigal A**, Kim JT, Balazs AB, Dekel E, Mayo A, Milo R, Baltimore D. Cell-to-cell spread of HIV permits ongoing
315 replication despite antiretroviral therapy. Nature. 2011; 477(7362):95.

316 **Vignuzzi M**, Stone JK, Arnold JJ, Cameron CE, Andino R. Quasispecies diversity determines pathogenesis through
317 cooperative interactions in a viral population. Nature. 2006; 439(7074):344–8. https://www.ncbi.nlm.nih.gov/
318 pubmed/16327776, doi: 10.1038/nature04388.

319 **Wu Y**, Beddall MH, Marsh JW. Rev-dependent indicator T cell line. Current HIV research. 2007; 5(4):394–402.

Determination of the number of HIV infections per cell in lymph nodes from HIV infected individuals

Laurelle Jackson[1,2] **and Alex Sigal**[1,2,3*]

***For correspondence:**
Alex.Sigal@ahri.org (AS)

[1]Africa Health Research Institute, Durban, South Africa; [2]School of Laboratory Medicine and Medical Sciences, University of KwaZulu-Natal, Durban, South Africa; [3]Max Planck Institute for Infection Biology, Berlin, Germany

Abstract Measurement of the number of expressed viral genomes in *in vivo* infected individual cells requires new approaches involving high throughput detection of HIV transcript number and sequence per cell. Here we have tested the potential of several approaches for detecting and sequencing the transcriptional profiles of HIV infected cells.

Introduction

Multiple infections per cell impact: 1) degree of sensitivity of infection to drug (***Sigal et al.*** (***2011***)); 2) survival of infected cells (***Jackson et al.*** (***2018***)); 3) Timing of infection (***Boullé et al.*** (***2016***); 4) Evolution of drug resistance and maintenance of a quasispecies (***Jackson et al.*** (***2018***)). The clinical relevance of multiple infections per cell will depend on their frequency in *in vivo* infection. There is controversy over the frequency of cells which are multiply infected *in vivo*. One critical compartment where multiple infection could occur is lymph nodes/lymphoid tissue. Lymph nodes (LNs) may represent critical HIV reservoirs due to the high concentration of lymphocytes and the density of cellular interactions, which may make LN conducive to cell-to-cell spread (***Jolly et al.*** (***2004***); ***Sigal et al.*** (***2011***); ***Sigal and Baltimore*** (***2012***)); and because limited drug penetration may make ongoing replication possible even in the presence of antiretroviral therapy (***Fletcher et al.*** (***2014***); ***Lorenzo-Redondo et al.*** (***2016***)). Specific T cell subsets present in the LN have been reported to be central to the reservoir. These include CD3+CD4+PD1+CXCR5+ T follicular helper cells (***Fukazawa et al.*** (***2015***); ***Banga et al.*** (***2016***)) and CD45RA-CCR7+CD27+ central memory T cells (***Sallusto et al.*** (***1999***); ***Chomont et al.*** (***2009***)). However, the number of HIV infections per cell, and the viral sequences expressed by them, has not been characterized with high throughput approaches.

Detection of expressed viral sequences in infected single cells requires detection of HIV transcripts. A novel approach to define the HIV cellular reservoir and associated sequences at the level of the single infected cell with high throughput is the emerging technology of single cell RNA-Seq. This enables analysis of single-cell transcriptomes to discover cell type/state (***Paltiel et al.*** (***2009***)), and can potentially be used to detect HIV transcripts in individual cells. One such approach is Seq-Well (***Gierahn et al.*** (***2017***)), a microwell-based platform containing roughly 86,000 subnanoliter wells pre-loaded with barcoded mRNA capture beads. In this approach, each cell is captured with a single bead in a single well using gravity. The wells are then sealed using a semi-permeable membrane, cells are lysed within the array, and cellular mRNAs are captured on barcoded beads. Reverse transcription, library preparation and paired-end sequencing are then carried out. Seq-Well enables transcriptomic profiling of thousands of cells in parallel, with each cell profiled individually

by applying unfixed cells in suspension to the microwell chip (***Macosko et al.*** (***2015***)). It has been successfully applied to human tissue isolates including human lymph node biopsies, tumors, gut pinch biopsies, cerebrospinal fluid and other cellular sources (***Gaublomme et al.*** (***2015***); ***Kimmerling et al.*** (***2016***); ***Tirosh et al.*** (***2016***)).

In addition to Seq-Well, other single cell RNA-Seq approaches can be used to specifically detect and analyze the transcriptomes of HIV infected cells. These techniques sequence cells in a 96-well format and therefore would rely on enrichment strategies for HIV infected cells. One such approach is using Fixed and Recovered Intact Single-cell RNA (FRISCR) (***Thomsen et al.*** (***2016***)). In this approach, HIV infected cells can be enriched using intracellular anti-HIV Gag (p24) single cell staining using a fluorescently labelled antibody. With FRISCR, the RNA content of the fixed, antibody labelled cells would be accessed by reversing the fixation. Fixed HIV infected cells would be single cell sorted, lysed, then de-crosslinked by heating. FRISCR has been successfully applied to radial glia cells of the human neocortex, yielding expression data similar to that of unfixed cells (***Thomsen et al.*** (***2016***)). Another approach may be detection of HIV infected cells based on HIV envelope protein (Env) detection on the cell surface (***Cohn et al.*** (***2018***)). This technique does not require fixation since ENV is not the cell surface, but is predicted to have a low signal to noise ratio based on the paucity of expressed Env (***Zhu et al.*** (***2006***)) . If direct detection of HIV is not possible, an alternative is single cell RNA-Seq of cell types enriched for HIV infection. Here, cells are sorted based of cell-surface markers rather than fixing and using intracellular staining. These cell types are single cell sorted directly into a lysis buffer. As mentioned above, specific T cell subsets present in the LN, such as CD3+CD4+PD1+CXCR5+ T follicular helper cells, and CD45RA-CCR7+CD27+ central memory T cells have been reported to be central to the reservoir and these cell types may be frequently infected.

To test feasibility of single cell RNA-Seq to detect HIV transcripts and sequences, we performed single cell RNA-Seq for the determination of infection frequency and the number of expressed HIV sequences per infected cell. This was applied to an *in vitro* infection. We also assessed the application of this approach to a cohort of LN from HIV infected study participants that we assembled.

Single cell RNA-Seq detects multiple HIV sequences in *in vitro* infection

We used an HIV *in vitro* infection of a cell line to test the feasibility of single cell RNA-Seq for detecting of multiple HIV sequences per cell. RevCEM cells (***Wu et al.*** (***2007***)) are engineered to express GFP upon HIV Rev protein expression. Three different infections were setup with RevCEMs. We infected cells with: (1) HIV expressing wildtype reverse transcriptase (RT); (2) HIV harboring a single nucleotide RT mutant; (3) a co-infection of cells with wild type and mutant HIV. After two days of infection, we cell sorted at one cell per well based on GFP expression and used plate-based single cell RNA-Seq (***Shalek et al.*** (***2013***); ***Patel et al.*** (***2014***)) to examine individual cells for viral transcripts (Figure 1). In these cells, we detected wild type HIV RT by single cell RNA-Seq when infection was with wild type virus, and mutant HIV RT when infection was with mutant virus. Importantly, we were able to detect both wild type and mutant transcripts in the same cell in co-infected cells (Figure 1A). The approach allowed us to detect not only the sequences, but also the abundance of HIV transcripts per cell (Figure 1B). Therefore, our approach would enable us to rank the different HIV infected cell subsets by their quantitative contribution to the reservoir based on the number of HIV transcripts each cell produces.

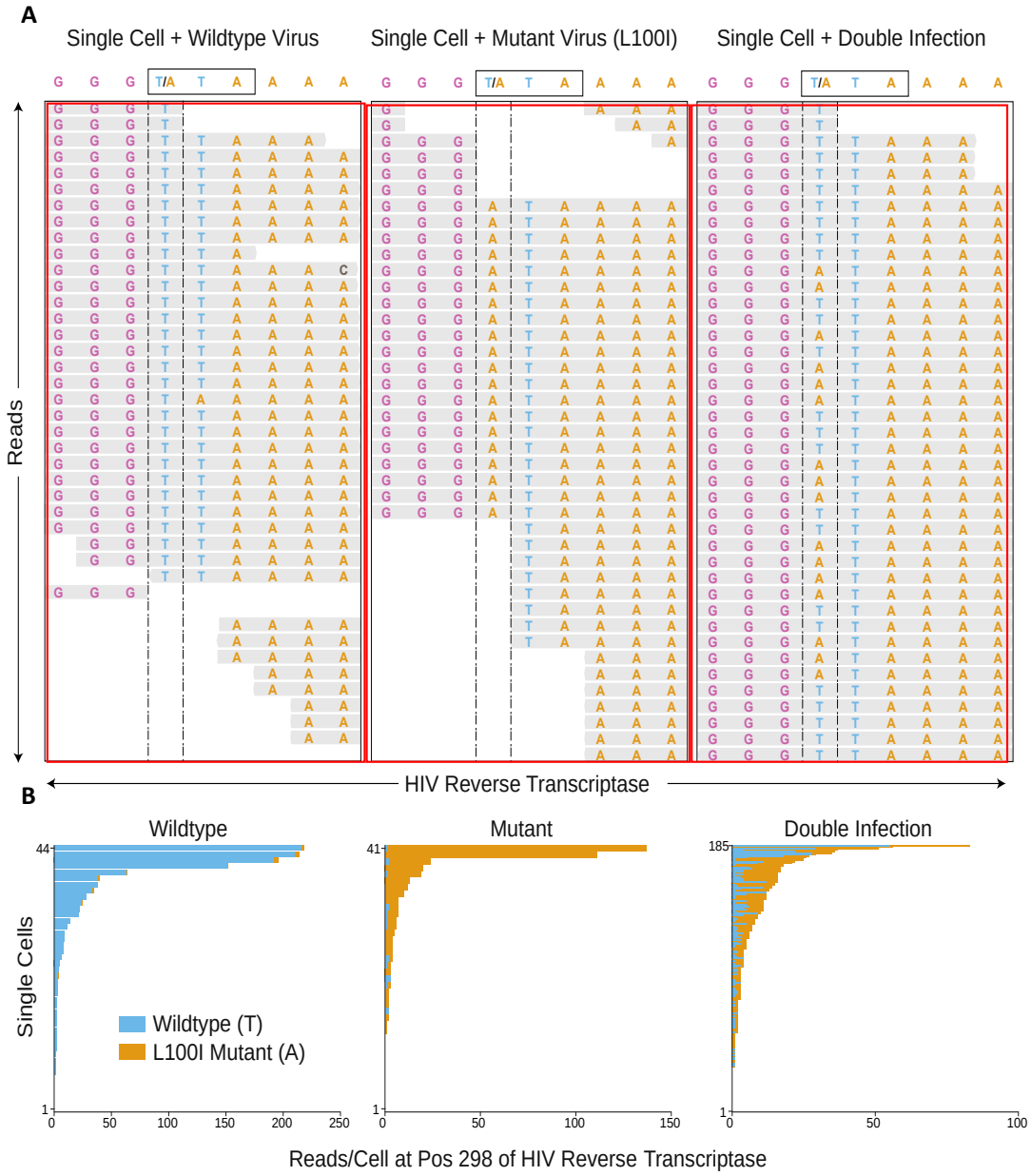

Figure 1. Single-cell RNA-Seq strategy to identify HIV variants and number of transcripts per cell. (A) Reads from three representative cells infected with wild type HIV (left panel), the L100I mutant of the reverse transcriptase (RT) which confers EFV resistance (middle panel), or co-infected with wild type and mutant viruses (right panel). Each red rectangle represents HIV transcripts sequenced by single cell RNA-Seq from one cell. First nucleotide in boxed codon at the top is the mutation site. The wild type RT was detected in the wild type HIV infected cells, the mutant RT in the mutant infected cells, and both were detected in the cell co-infected with both variants. (B) Multiple individual cells were analysed from each infection condition for HIV transcript number. Each cell is represented by a horizontal bar, with bar length corresponding to the number of HIV transcripts expressed by the cell at position 298 of the reverse Transcriptase (Pos 298). Bar colour represents the number of sequences which were wildtype (blue) or mutant (yellow). Note that wild type transcripts were more common than mutant transcripts in co-infected cells.

Single cell RNA-Seq applied to cells from LN

We next tested whether Seq-Well is feasible for both transcriptional profiling cell types as well as the detection of HIV transcripts from lung LN cells. We applied the Seq-Well technique to a sorted

live population of lung LN cells of a participant from a cohort of resected lymph nodes from HIV infected individuals (Table 1 and 2). The main populations of cells from the LN we identified as T cells, B cells and antigen presenting cells (APCs, Figure 2A). In addition, we identified 30 cells expressing HIV transcripts in the T cell and APC populations (Figure 2B). The contribution of the cell subset to the reservoir may be determined by the number of viral transcripts produced by the cell. Important to note is that clinical parameters can skew the transcriptional profile of cells (***Riou et al.*** (***2016***)). In the case of the LNs from the clinical cohort (described below), both history of multidrug resistant (MDR) or extremely drug resistant (XDR) TB may be confounding factors in the transcriptional profiles.

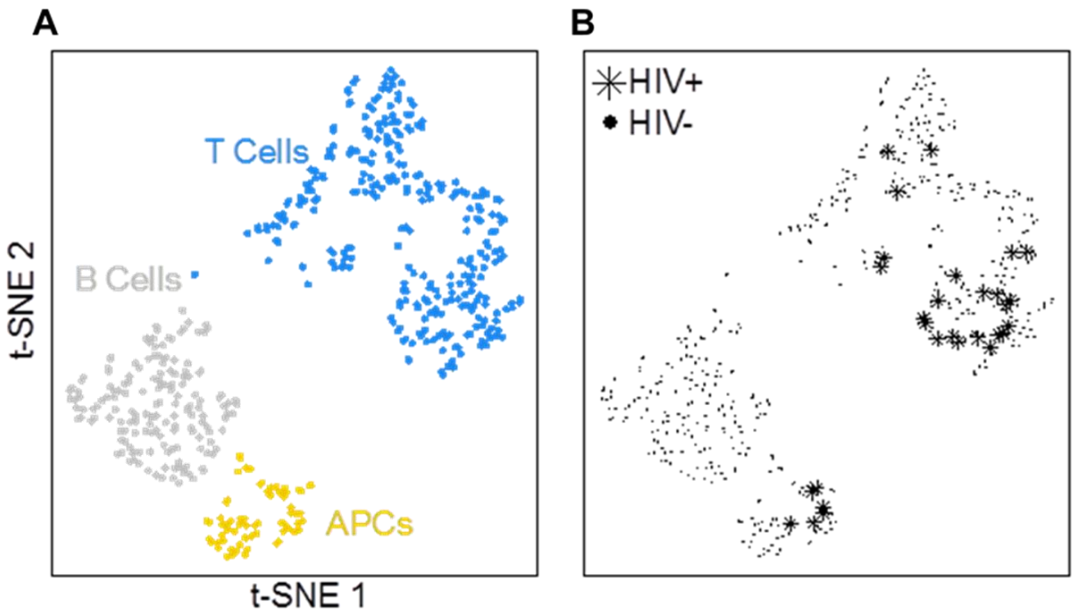

Figure 2. Determining infected cell types in LNs from HIV positive patients by single cell RNA-Seq. (A) Complete preparation of single cells from a LN from an antiretroviral therapy (ART) treated individual (participant 024-09-0198) was processed using Seq-Well. Single cell libraries were sequenced, and cells were clustered according to their transcriptomes to obtain B cell, T cell and APC subsets. (B) HIV transcripts were detected in cell subsets from (A).

Enrichment strategies

With Seq-Well, only roughly 35 percent of the cells are recovered from loading the chip and only roughly 10 percent of the cells give readable depth and coverage of sequencing for analysis. Both the low frequency of HIV infected cells in the total population and the subsequent low yield in HIV transcriptomic data results in very few HIV infected cells being analyzed. There are two ways to increase the yield of HIV infected cells for analysis. Firstly, adapt the mRNA capture beads used in Seq-Well to prime from specific regions of HIV, secondly, to enrich on HIV infected cells. Enrichment can be done by: (1) Sorting directly on HIV positive cells using identification by either intracellular HIV Gag or surface HIV Env; (2) sorting on cell populations that have a higher frequency of HIV infection than other cell types.

We first tested whether we could enrich for HIV based on cell type selection. To confirm whether cells were enriched for HIV infection or not, we used staining for intracellular HIV Gag. We found that the frequency of infected cells in the CD3+CD8-CD4+ subset from an HIV *in vitro* infection of Peripheral blood mononuclear cells (PBMCs) was 11.3 percent (Figure 3A). When compared to the frequency of infected cells in the total live population (Figure 3B), the CD3+CD8-CD4+ subset yielded a 3-fold enrichment for infected cells. This approach can be further refined by testing additional cell surface markers to obtain cell subsets with higher enrichment for HIV infection.

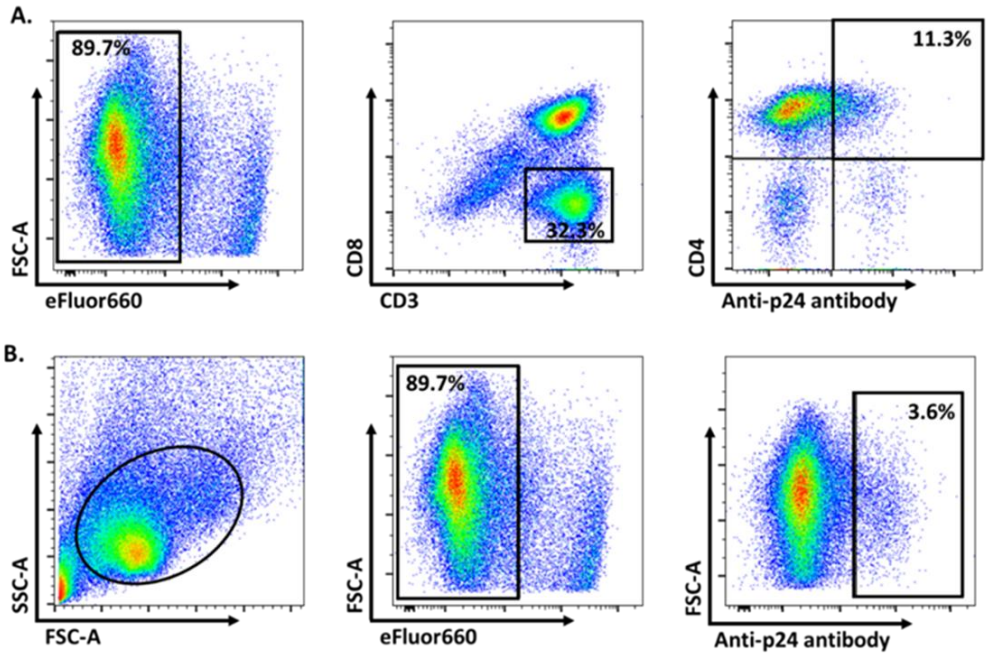

Figure 3. Enrichment of HIV infected cells by staining for cell subsets. p24 staining of PBMCs from an in vitro infection with NL43-AD8. Infection was detected at the level of individual cells by staining with anti-HIV Gag (p24) antibody in the FITC channel. (A) Gating strategy for selecting live, CD3+CD8-CD4+p24+ cells. Live cells were selected by exclusion of the death detection dye eFluor660. (B) The same infected PBMCs that as were gated in (A) without selection of the D3+CD8-CD4+ subset.

Assembly of a cohort of lymph nodes from HIV infected participants and detection of infected cells

We assembled a cohort of LN from the field of surgery from individuals on suppressive ART undergoing indicated lung lobe resection in collaboration with clinicians at the Department of Cardiothoracic Surgery at Inkosi Albert Luthuli Central Hospital in Durban, South Africa. This cohort was assembled over a two-year period (2016-2018). Written informed consent was obtained in the home language for each participant (English or IsiZulu). The study protocol has been approved by the University of KwaZulu-Natal Institutional Review Board (approval BE024/09) and by the Institutional Biosafety Committee. In addition to LN, matched blood was obtained from each participant.

Clinical parameters collected for each study participant included clinically diagnosed TB status (active TB highlighted in red in Table 1), gender, age, nadir CD4+ count, HIV diagnosis date, duration of infection before treatment, ART start date, and duration of ART before LN resection (Table 1). Out of the 24 study participants, 8 (33 percent) were clinically diagnosed with active TB. There were 13 female participants (54 percent). Most active TB cases were in males (5/8, 62 percent). Time before ART initiation was variable and ranged from less than 1 year to 6 years. Time on ART ranged from less than 1 year to 13 years. The active TB group was enriched with individuals with a history of MDR or XDR TB, with 4 out of 6 MDR/XDR cases.

Table 1. Clinical parameters of LN cohort

PID	Active TB	Gender	Age	Nadir CD4	Diagnosis date	Years untreated	ART start date	Years on ART	MDR/XDR episode	LN location
024-09-0181	No	Female	73	268	2016	N/A	N/A	N/A		N/A
024-09-0198	Yes	Male	52	N/A	N/A	N/A	N/A	N/A	XDR	N/A
024-09-0201	Yes	Male	41	138	2010	3	2013	3		N/A
024-09-0207	No	Female	53	N/A	N/A	N/A	2014	2		Lateral bronchus
024-09-0227	No	Male	40	227	2011	5	2016	<1		Left anterior medial basal
024-09-0240	No	Female	28	129	2016	<1	2016	<1		Bronchial
024-09-0244	Yes	Male	26	477	2012	2	2014	2	MDR	Bronchial
024-09-0255	No	Female	39	N/A	2013	<1	2013	4		Bronchopulmonary
024-09-0258	No	Female	42	301	2016	<1	2016	1		Parabronchial
024-09-0264	No	Male	47	49	2011	5	2016	1		Parabronchial
024-09-0276	No	Male	32	563	2016	<1	2016	1		Mediastinal
024-09-0286	No	Male	46	N/A	N/A	N/A	N/A	N/A		Mediastinal
024-06-0304	Yes	Female	42	492	2006	N/A	N/A	N/A	MDR	Right lateral
024-09-0308	Yes	Male	27	N/A	N/A	N/A	2017	<1	MDR	Hilar
024-06-0310	No	Female	58	N/A	2011	3	2014	4	MDR	Hilar
024-09-0310	No	Female	58	1536	2014	<1	2014	4		Bronchial
024-06-0312	No	Female	47	N/A	2003	2	2005	13		Peribronchial
024-06-0313	No	Male	32	48	2011	<1	2011	7		Hilar
024-06-0314	No	Male	42	N/A	2015	<1	2015	3		Bet. pulmonary artery & vein
024-09-0314	Yes	Female	41	324	2016	<1	2016	2		Hilar
024-06-0316	No	Female	64	N/A	2002	6	2008	10		Perihilar
024-06-0319	Yes	Male	40	N/A	2012	N/A	N/A	N/A		Mediastinal
024-06-0320	No	Female	33	85	N/A	N/A	N/A	N/A	MDR	Peri-bronchus intermedius
024-06-0330	Yes	Female	42	320	2018	<1	2018	<1		Hilar

Entries in red indicate participants with clinical diagnosis of active TB. PID, participant identification.

To determine ART status, antiretroviral drug (ARV) levels of efavirenz (EFV), emtricitabine (FTC), tenofovir (TDF), ritonavir (RTV), lopinavir (LPV), and abacavir (ABC) were measured in-house by liquid chromatography coupled with tandem mass spectrometry (LC/MS/MS). Viral load was measured using the Abbott RealTime HIV-1 Viral Load Assay, with a limit of detection of 40 copies/ml (Table 2). Interestingly, in the active TB group, 4/8 (50 percent) of participants showed low level viremia (LLV), compared to 2/16 (12 percent) in the TB cured group This difference was significant (p=0.02 by bootstrap).

Table 2: Measured parameters of LN cohort

PID	Viral load	TDF	FTC	EFV	LPV	RTV	ABC	3TC	Regimen by LC/MS/MS
024-09-0181	<40	72.3	259	3410	BLQ	BLQ	BLQ	BLQ	EFV/TDF/FTC
024-09-0198	<40	51.8	380	1340	BLQ	BLQ	BLQ	BLQ	EFV/TDF/FTC
024-09-0201	224	N/A	N/A	N/A	N/A	N/A	N/A	N/A	N/A
024-09-0207	<40	76.9	301	1860	BLQ	BLQ	BLQ	BLQ	EFV/TDF/FTC
024-09-0227	<40	50.8	327	1470	BLQ	BLQ	BLQ	BLQ	EFV/TDF/FTC
024-09-0240	285	51.3	222	1630	BLQ	BLQ	BLQ	BLQ	EFV/TDF/FTC
024-09-0244	<40	N/A	N/A	N/A	N/A	N/A	N/A	N/A	N/A
024-09-0255	<40	BLQ	BLQ	BLQ	5990	395	BLQ	949	LPV/r/3TC
024-09-0258	<40	57.1	283	1890	BLQ	BLQ	BLQ	BLQ	EFV/TDF/FTC
024-09-0264	34613	BLQ	BLQ	BLQ	BLQ	BLQ	1760	1030	ABC/3TC
024-09-0276	<40	66.8	255	1310	BLQ	BLQ	BLQ	BLQ	EFV/TDF/FTC
024-09-0286	78603	BLQ	BLQ	BLQ	BLQ	BLQ	BLQ	BLQ	Naïve
024-06-0304	<40	47.5	150	6450	BLQ	BLQ	N/A	BLQ	EFV/TDF/FTC
024-09-0308	180	47	254	2070	BLQ	BLQ	N/A	BLQ	EFV/TDF/FTC
024-06-0310	68	126	352	2090	BLQ	BLQ	N/A	BLQ	EFV/TDF/FTC
024-09-0310	<40	N/A	N/A	N/A	N/A	N/A	N/A	N/A	N/A
024-06-0312	<40	BLQ	44	1970	BLQ	BLQ	N/A	BLQ	EFV/FTC
024-06-0313	<40	BLQ	BLQ	BLQ	25200	1630	BLQ	1980	LPV/r/3TC
024-06-0314	<40	BLQ	BLQ	1640	BLQ	BLQ	N/A	51.4	EFV/3TC
024-09-0314	2464	BLQ	BLQ	401	814	51	N/A	371	EFV/LPV/RTV/3TC
024-06-0316	<40	177	1850	BLQ	BLQ	BLQ	BLQ	BLQ	EFV/TDF/FTC
024-06-0319	<40	33.2	449	3910	BLQ	BLQ	BLQ	BLQ	EFV/TDF/FTC
024-06-0320	<40	BLQ	BLQ	BLQ	247	7	BLQ	14	LPV/r/3TC
024-06-0330	55	Pend	Pend	Pend	Pend	Pend	Pend	Pend	Pend

All ARV in ng/ml in plasma. Entries in red indicate participants with a clinical diagnosis of active TB. Entries in blue indicate participants with no viral suppression. PID, participant identification number. BLQ, below level of quantitation. N/A, Not available. Pend, pending.

In order to use single cell RNA-Seq approaches with the LNs described above, we first needed to test whether the LN cells harbored HIV. We tested LNs for HIV DNA copies, a measure of the HIV reservoir (***Chun et al.*** (***1997***); ***Eriksson et al.*** (***2013***); ***Laird et al.*** (***2013***)). We stained LN cells from HIV positive participants for host surface markers and sorted non-activated CD3+CD4+ T cells from LN (Figure 4A) into 96-well plates at 10 cells per well and determined the frequency of infection. We performed PCR to a conserved region of the HIV-1 reverse transcriptase gene (Figure 4B). We detected a DNA copy frequency of 0.8 percent, within range for HIV DNA frequency observed for CD4+ T cells of rectal origin in ART suppressed individuals (***Eriksson et al.*** (***2013***)).

To examine HIV protein expression in LN, we used anti-p24 single-cell staining to detect HIV Gag after 12 hour activation with phytohemagglutinin (PHA) and IL-2. The short activation time should reflect *in vivo* infection without additional cycles *in vitro* (***Boullé et al.*** (***2016***)). Four LN were analyzed from three ART suppressed participants. LN cells from an HIV negative individual infected or uninfected *in vitro* were used as positive and negative controls, respectively (Figure 4C). p24-positive cell frequency in ART suppressed participants ranged from 0.01 percent to 0.07 percent, with different LNs from the same individual showing a similar percentage of infected cells. Frequencies were an order of magnitude lower than reported for HIV DNA positive CD4+ cells from rectal biopsy samples (***Eriksson et al.*** (***2013***)) and our measurement of HIV DNA frequency. This may indicate that only a subset of cells with HIV DNA produce HIV proteins .

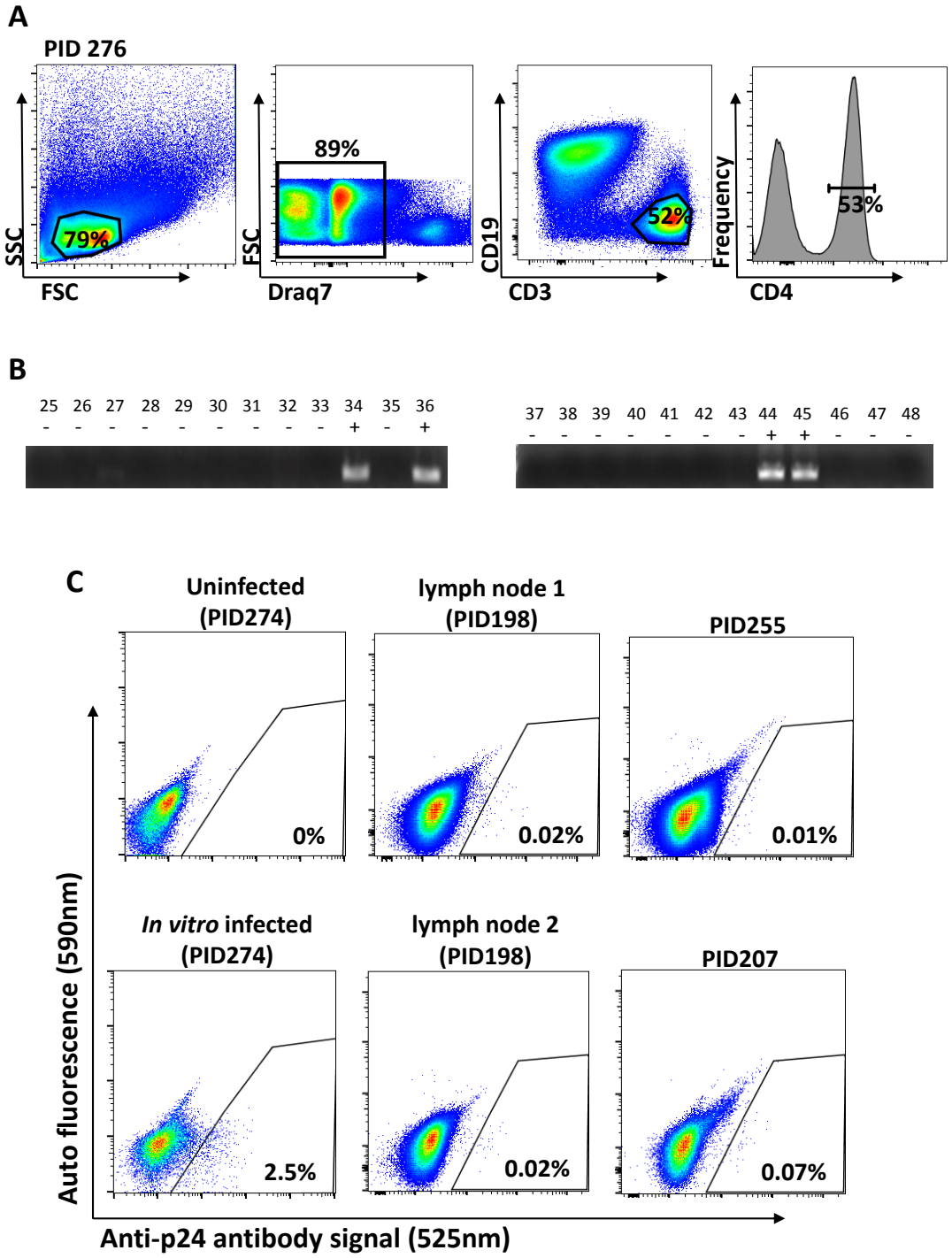

Figure 4. Measures of the HIV reservoir in lung LN in the face of ART. (A) Gating strategy is shown for LN cells of study participant 024-09-0276. Live cells were selected by exclusion of the death detection dye Draq7. CD19-CD3+CD4+ were sorted for further analysis. Percentages correspond to the fraction of the population within the gate marked. PID: Patient ID. (B) Frequency of HIV-1 DNA in the T cell subset from (A). 10 cells were sorted into lysis buffer per well of a 96-well plate and nested PCR with primers to the HIV reverse transcriptase performed. Representative bands on a DNA gel. (C) Number of HIV Gag expressing cells in LN after 12 hours of activation with PHA. Single-cell infection was detected by staining with anti-HIV Gag (p24) antibody in the FITC channel. X-axis shows p24 signal, y-axis is auto-fluorescence, and infected cells are in the gate outlined in black. The two plots in the left column show LN cells from an uninfected individual (PID 024-09-0274) which either remain uninfected (top plot) or are *in vitro* infected with the NL4-3 strain of HIV (bottom plot). The two plots in the middle column show two different LN from an HIV infected, ART suppressed individual (PID 024-09-0198). The two plots in the right column show LN from two HIV infected, ART suppressed individuals (PID 024-09-0255 and 024-09-0207).

Discussion

Here, we have shown that single cell RNA-seq is a technique that can be used to determine the frequency of infection, the number of HIV infections per cell, as well as cell types in *in vivo* infected lymph nodes. Additionally, our ability to elucidate the viral sequence can be used to identify resistance mutations which may result in ongoing replication by ARV resistant HIV. This could also allow us to sequence and clone out the ENV protein and test tropism in relation to the cell subset the virus was detected in.

Further improvement to determining the frequency of infection would require calibration of optimal protocols for enrichment of infected cells based on detection of HIV infection, or enrichment for infected cell types. This would enable us to quantitatively detect with high throughput HIV expression in individual cells, and importantly, determine the frequency of cells which express more than one HIV sequence. Furthermore, standard mRNA priming from polyA may not result in sufficient HIV genome coverage, leading to gaps in the coverage of all viral variants in the cells. To circumvent this problem, in future work we will engineer the Seq-Well capture beads to bind HIV specific mRNA at different locations on the HIV genome (***Macosko et al.*** (***2015***)). This should yield greater coverage of the HIV genome and thus allow us to better quantify the number of different HIV sequences that occur per infected cell.

Acknowledgments

This work was supported by National Institutes of Health Grant R21MH104220. AS was supported by a Human Frontiers Science Program Career Development Award CDA 00050/2013. LJ is supported by a fellowship from the South African National Research Foundation.

References

Banga R, Procopio FA, Noto A, Pollakis G, Cavassini M, Ohmiti K, Corpataux JM, de Leval L, Pantaleo G, Perreau M. PD-1(+) and follicular helper T cells are responsible for persistent HIV-1 transcription in treated aviremic individuals. Nat Med. 2016; 22(7):754–61. https://www.ncbi.nlm.nih.gov/pubmed/27239760, doi: 10.1038/nm.4113.

Boullé M, Müller TG, Dähling S, Ganga Y, Jackson L, Mahamed D, Oom L, Lustig G, Neher RA, Sigal A. HIV cell-to-cell spread results in earlier onset of viral gene expression by multiple infections per cell. PLoS pathogens. 2016; 12(11):e1005964.

Chomont N, El-Far M, Ancuta P, Trautmann L, Procopio FA, Yassine-Diab B, Boucher G, Boulassel MR, Ghattas G, Brenchley JM, Schacker TW, Hill BJ, Douek DC, Routy JP, Haddad EK, Sekaly RP. HIV reservoir size and persistence are driven by T cell survival and homeostatic proliferation. Nat Med. 2009; 15(8):893–900. http://www.ncbi.nlm.nih.gov/pubmed/19543283.

Chun TW, Carruth L, Finzi D, Shen X, DiGiuseppe JA, Taylor H, Hermankova M, Chadwick K, Margolick J, Quinn TC, Kuo YH, Brookmeyer R, Zeiger MA, Barditch-Crovo P, Siliciano RF. Quantification of latent tissue reservoirs and total body viral load in HIV-1 infection. Nature. 1997; 387(6629):183–188.

Cohn LB, da Silva IT, Valieris R, Huang AS, Lorenzi JCC, Cohen YZ, Pai JA, Butler AL, Caskey M, Jankovic M, Nussenzweig MC. Clonal CD4(+) T cells in the HIV-1 latent reservoir display a distinct gene profile upon reactivation. Nat Med. 2018; 24(5):604–609. https://www.ncbi.nlm.nih.gov/pubmed/29686423, doi: 10.1038/s41591-018-0017-7.

Eriksson S, Graf EH, Dahl V, Strain MC, Yukl SA, Lysenko ES, Bosch RJ, Lai J, Chioma S, Emad F, Abdel-Mohsen M, Hoh R, Hecht F, Hunt P, Somsouk M, Wong J, Johnston R, Siliciano RF, Richman DD, O'Doherty U, et al. Comparative analysis of measures of viral reservoirs in HIV-1 eradication studies. PLoS pathogens. 2013; 9(2):e1003174.

Fletcher CV, Staskus K, Wietgrefe SW, Rothenberger M, Reilly C, Chipman JG, Beilman GJ, Khoruts A, Thorkelson A, Schmidt TE, Anderson J, Perkey K, Stevenson M, Perelson AS, Douek DC, Haase AT, Schacker TW. Persistent HIV-1 replication is associated with lower antiretroviral drug concentrations in lymphatic tissues. Proc Natl Acad Sci U S A. 2014; 111(6):2307–12. https://www.ncbi.nlm.nih.gov/pubmed/24469825, doi: 10.1073/pnas.1318249111.

Fukazawa Y, Lum R, Okoye AA, Park H, Matsuda K, Bae JY, Hagen SI, Shoemaker R, Deleage C, Lucero C, Morcock D, Swanson T, Legasse AW, Axthelm MK, Hesselgesser J, Geleziunas R, Hirsch VM, Edlefsen PT, Piatak J M, Estes JD, et al. B cell follicle sanctuary permits persistent productive simian immunodeficiency virus infection in elite controllers. Nat Med. 2015; 21(2):132–9. http://www.ncbi.nlm.nih.gov/pubmed/25599132.

Gaublomme JT, Yosef N, Lee Y, Gertner RS, Yang LV, Wu C, Pandolfi PP, Mak T, Satija R, Shalek AK, Kuchroo VK, Park H, Regev A. Single-Cell Genomics Unveils Critical Regulators of Th17 Cell Pathogenicity. Cell. 2015; 163(6):1400–12. http://www.ncbi.nlm.nih.gov/pubmed/26607794.

Gierahn TM, Wadsworth II MH, Hughes TK, Bryson BD, Butler A, Satija R, Fortune S, Love JC, Shalek AK. Seq-Well: portable, low-cost RNA sequencing of single cells at high throughput. Nature Methods. 2017; 14(4):395–398.

Jackson L, Hunter J, Cele S, Ferreira IM, Young AC, Karim F, Madansein R, Dullabh KJ, Chen CY, Buckels NJ, Ganga Y, Khan K, Boulle M, Lustig G, Neher RA, Sigal A. Incomplete inhibition of HIV infection results in more HIV infected lymph node cells by reducing cell death. eLife. 2018; 7:e30134.

Jolly C, Kashefi K, Hollinshead M, Sattentau QJ. HIV-1 cell to cell transfer across an Env-induced, actin-dependent synapse. J Exp Med. 2004; 199(2):283–93. http://www.ncbi.nlm.nih.gov/pubmed/14734528.

Kimmerling RJ, Lee Szeto G, Li JW, Genshaft AS, Kazer SW, Payer KR, de Riba Borrajo J, Blainey PC, Irvine DJ, Shalek AK, Manalis SR. A microfluidic platform enabling single-cell RNA-seq of multigenerational lineages. Nat Commun. 2016; 7:10220. http://www.ncbi.nlm.nih.gov/pubmed/26732280.

Laird GM, Eisele EE, Rabi SA, Lai J, Chioma S, Blankson JN, Siliciano JD, Siliciano RF. Rapid quantification of the latent reservoir for HIV-1 using a viral outgrowth assay. PLoS Pathog. 2013; 9(5):e1003398.

Lorenzo-Redondo R, Fryer HR, Bedford T, Kim EY, Archer J, Kosakovsky Pond SL, Chung YS, Penugonda S, Chipman JG, Fletcher CV, Schacker TW, Malim MH, Rambaut A, Haase AT, McLean AR, Wolinsky SM. Persistent HIV-1 replication maintains the tissue reservoir during therapy. Nature. 2016; 530(7588):51–6. http://www.ncbi.nlm.nih.gov/pubmed/26814962.

Macosko EZ, Basu A, Satija R, Nemesh J, Shekhar K, Goldman M, Tirosh I, Bialas AR, Kamitaki N, Martersteck EM, Trombetta JJ, Weitz DA, Sanes JR, Shalek AK, Regev A, McCarroll SA. Highly Parallel Genome-wide Expression Profiling of Individual Cells Using Nanoliter Droplets. Cell. 2015; 161(5):1202–14. http://www.ncbi.nlm.nih.gov/pubmed/26000488.

Paltiel AD, Freedberg KA, Scott CA, Schackman BR, Losina E, Wang B, Seage GR, Sloan CE, Sax PE, Walensky RP. HIV preexposure prophylaxis in the United States: impact on lifetime infection risk, clinical outcomes, and cost-effectiveness. Clinical Infectious Diseases. 2009; 48(6):806–815.

Patel AP, Tirosh I, Trombetta JJ, Shalek AK, Gillespie SM, Wakimoto H, Cahill DP, Nahed BV, Curry WT, Martuza RL. Single-cell RNA-seq highlights intratumoral heterogeneity in primary glioblastoma. Science. 2014; 344(6190):1396–1401.

Riou C, Bunjun R, Muller TL, Kiravu A, Ginbot Z, Oni T, Goliath R, Wilkinson RJ, Burgers WA. Selective reduction of IFN-gamma single positive mycobacteria-specific CD4+ T cells in HIV-1 infected individuals with latent tuberculosis infection. Tuberculosis (Edinb). 2016; 101:25–30. https://www.ncbi.nlm.nih.gov/pubmed/27865393, doi: 10.1016/j.tube.2016.07.018.

Sallusto F, Lenig D, Forster R, Lipp M, Lanzavecchia A. Two subsets of memory T lymphocytes with distinct homing potentials and effector functions. Nature. 1999; 401(6754):708–12. http://www.ncbi.nlm.nih.gov/pubmed/10537110, doi: 10.1038/44385.

Shalek AK, Satija R, Adiconis X, Gertner RS, Gaublomme JT, Raychowdhury R, Schwartz S, Yosef N, Malboeuf C, Lu D. Single-cell transcriptomics reveals bimodality in expression and splicing in immune cells. Nature. 2013; 498(7453):236.

Sigal A, Baltimore D. As good as it gets? The problem of HIV persistence despite antiretroviral drugs. Cell host & microbe. 2012; 12(2):132–138.

Sigal A, Kim JT, Balazs AB, Dekel E, Mayo A, Milo R, Baltimore D. Cell-to-cell spread of HIV permits ongoing replication despite antiretroviral therapy. Nature. 2011; 477(7362):95.

Thomsen ER, Mich JK, Yao Z, Hodge RD, Doyle AM, Jang S, Shehata SI, Nelson AM, Shapovalova NV, Levi BP, Ramanathan S. Fixed single-cell transcriptomic characterization of human radial glial diversity. Nat Methods. 2016; 13(1):87–93. http://www.ncbi.nlm.nih.gov/pubmed/26524239, doi: 10.1038/nmeth.3629.

254 **Tirosh I**, Izar B, Prakadan SM, Wadsworth n M H, Treacy D, Trombetta JJ, Rotem A, Rodman C, Lian C, Murphy G,
255 Fallahi-Sichani M, Dutton-Regester K, Lin JR, Cohen O, Shah P, Lu D, Genshaft AS, Hughes TK, Ziegler CG, Kazer
256 SW, et al. Dissecting the multicellular ecosystem of metastatic melanoma by single-cell RNA-seq. Science.
257 2016; 352(6282):189–96. http://www.ncbi.nlm.nih.gov/pubmed/27124452.

258 **Wu Y**, Beddall MH, Marsh JW. Rev-dependent indicator T cell line. Current HIV research. 2007; 5(4):394–402.

259 **Zhu P**, Liu J, Bess J J, Chertova E, Lifson JD, Grise H, Ofek GA, Taylor KA, Roux KH. Distribution and three-
260 dimensional structure of AIDS virus envelope spikes. Nature. 2006; 441(7095):847–52. https://www.ncbi.nlm.
261 nih.gov/pubmed/16728975, doi: 10.1038/nature04817.

GENERAL DISCUSSION

Host cell survival and adaptability of HIV during therapy are pre-requisites to long-term persistence. This in turn means that HIV needs to: (1) strike a delicate balance between virulence and survival in its host to be optimally infectious; (2) evolve and maintain genetic diversity in order to adapt to selective pressures. In this thesis I show that when cells become multiply infected with HIV, through a mode of infection such as cell-to-cell spread, partially reducing infection with inhibitors results in: (1) increased number of live infected cells (2) the evolution of a quasispecies which is maintained through complementation. Furthermore, I show that single cell RNA-Seq methods are feasible to quantify multiple infections per cell from *in vivo* HIV infected lymph node cells.

In Chapter 2, I demonstrated that when cells are infected and die in a probabilistic way, there are two possible outcomes of partially inhibiting infection. In the case where cells are infected by single infection attempts, inhibition always leads to a decline in the number of live infected cells, since inhibition reduces the number of infections per cell from one to zero. In contrast, in the case of multiple infection attempts per cell, the possibility exists that inhibition reduces the number of integrating HIV DNA copies without extinguishing infection of the cell completely. If each HIV DNA copy increases the probability of cell death, reducing the number of HIV DNA copies without eliminating infection would lead to an increased probability of infected cell survival. In turn, this would lead to an increase in the number of live infected cells. In both a cell line and lymph node cells, I observed an increase in the number of live infected cells. This correlated to fewer viral DNA copies per cell. Further increasing inhibitor concentration led to a decline in live infected cell numbers, and infecting with EFV resistant mutants shifted the peak in live infected number to higher EFV concentrations. The work here reinforces previous findings that successful completion of reverse transcription and infection leads to cellular cytotoxicity and in addition measures for the first time the probability of infection and cell death per copy of HIV DNA. This work supports recent findings that ARVs promote persistent infection by increasing the half-life of latently infected cells in HIV reservoirs, since a live cell is the prerequisite of a latently infected one [1].

In Chapter 3, I showed that during evolution in the face of drug, drug sensitive HIV can be maintained in the quasispecies despite a fitness disadvantage. I demonstrated that the fraction of drug sensitive HIV stabilized upon co-infection with an EFV resistant HIV mutant. Co-transfection of a mutant and wildtype molecular clone proved this in a controlled experiment. Complementation

may interfere with selection and hence reduce fitness of the viral population by preventing the selection of more fit genotypes [2]. However, there is evidence that the quasispecies allows the infection to keep a heterogeneous pool of virus which is more able to react to rapid changes in the infection environment, hence greatly enhancing the ability of infection to rapidly adapt to selective pressure [3-6].

The necessary condition for both a peak in the number of live cells in the face of partial inhibition and complementation to occur *in vivo* is expression of multiple viral copies in the same cell. The presence of multiple infections of the same cell has been controversial, with some studies showing multiple infections per cell [7,8] whilst other studies did not show multiple infections at a frequency greater than that predicted by the Poisson distribution [9,10]. In Chapter 4, I showed that single cell RNA-Seq methods can be used to determine whether lymph node cells are multiply infected. Enrichment strategies are necessity for some of the single cell RNA-Seq techniques given the current limitations on depth of coverage in the sequencing. Given that certain cell types such as CD3+CD4+PD1+CXCR5+ T follicular helper cells [11,12] and CD45RA-CCR7+CD27+ central memory T cells [13,14] have been reported to be central to the reservoir in lymph nodes , it should be possible to enrich for these groups as the next step.

In both Chapter 2 and 3, the main antiretroviral used was EFV, a common component of first line therapy which is vulnerable to drug resistant mutations. An infection optimum should occur with other classes of antiretrovirals, since all drugs should decrease the multiplicity of infection between cells. Complementation may be possible with other antiretrovirals such as integrase or protease inhibitors. Like reverse transcriptase, there is no known mechanism which prevents one HIV strain packaging integrase or protease from another HIV strain if both strains are in the same cell. The number of these molecules packaged into one virion and how many molecules are needed to perform their function are other factors which would determine whether phenotypic mixing or complementation of integrase or protease is enough to maintain the quasispecies.

Taken together, the results in this thesis show that under sub-optimal inhibition, HIV can become optimally infectious and generate a quasispecies. These features are necessary for HIV to survive and as described in this thesis, are possible when cells become multiply infected. Furthermore, I demonstrated that single cell RNA-Seq methods are feasible for validating whether cells from *in vivo* infected lymph nodes are multiply infected. Results from Chapter 2 and 3 may have important implications in the establishment of reservoirs in the context of poorly controlled infections,

infections with some degree of drug resistance or infections where some replication takes place in the face of ARVs. Currently, proposed approaches to eliminate non-replicating reservoirs - where cells are latently infected with HIV - is to purge these cells by activating HIV production with HDAC inhibitors [15-18]. This strategy may not successfully eliminate HIV because latently infected cells may contain few functional HIV proviral copies, and therefore these cells would not die when reactivated – as the probability of infection with a single virion is low. The results in this thesis may also suggest that inhibiting cell-to-cell spread, may not only reduce infection in the face of ARVs and other forms of inhibitors, but limit viral diversity and the ability of HIV to evolve resistance.

References

1 Joseph, S. B. *et al.* in *XXII International AIDS Conference, 2018* (Amsterdam, Netherlands, 2018).

2 Froissart, R. *et al.* Co-infection weakens selection against epistatic mutations in RNA viruses. *Genetics* **168**, 9-19 (2004).

3 Andino, R. & Domingo, E. Viral quasispecies. *Virology* **479-480**, 46-51 (2015).

4 Lauring, A. S., Frydman, J. & Andino, R. The role of mutational robustness in RNA virus evolution. *Nat Rev Microbiol* **11**, 327-336, doi:10.1038/nrmicro3003 (2013).

5 Vignuzzi, M., Stone, J. K., Arnold, J. J., Cameron, C. E. & Andino, R. Quasispecies diversity determines pathogenesis through cooperative interactions in a viral population. *Nature* **439**, 344-348 (2006).

6 Domingo, E., Sheldon, J. & Perales, C. Viral quasispecies evolution. *Microbiology and Molecular Biology Reviews* **76**, 159-216 (2012).

7 Jung, A. *et al.* Recombination: Multiply infected spleen cells in HIV patients. *Nature* **418**, 144 (2002).

8 Law, K. M. *et al.* In Vivo HIV-1 Cell-to-Cell Transmission Promotes Multicopy Micro-compartmentalized Infection. *Cell Rep* **15**, 2771-2783 (2016).

9 Josefsson, L. *et al.* Majority of CD4+ T cells from peripheral blood of HIV-1–infected individuals contain only one HIV DNA molecule. *Proceedings of the National Academy of Sciences* **108**, 11199-11204 (2011).

10 Josefsson, L. *et al.* Single cell analysis of lymph node tissue from HIV-1 infected patients reveals that the majority of CD4+ T-cells contain one HIV-1 DNA molecule. *PLoS pathogens* **9**, e1003432 (2013).

11 Banga, R. *et al.* PD-1(+) and follicular helper T cells are responsible for persistent HIV-1 transcription in treated aviremic individuals. *Nat Med* **22**, 754-761, doi:10.1038/nm.4113 (2016).

12 Fukazawa, Y. *et al.* B cell follicle sanctuary permits persistent productive simian immunodeficiency virus infection in elite controllers. *Nat Med* **21**, 132-139 (2015).

13 Chomont, N. *et al.* HIV reservoir size and persistence are driven by T cell survival and homeostatic proliferation. *Nat Med* **15**, 893-900 (2009).

14 Sallusto, F., Lenig, D., Forster, R., Lipp, M. & Lanzavecchia, A. Two subsets of memory T lymphocytes with distinct homing potentials and effector functions. *Nature* **401**, 708-712 (1999).

15 Archin, N. M. *et al.* Administration of vorinostat disrupts HIV-1 latency in patients on antiretroviral therapy. *Nature* **487**, 482-485 (2012).

16 Lehrman, G. *et al.* Depletion of latent HIV-1 infection in vivo: a proof-of-concept study. *Lancet* **366**, 549-555 (2005).

17 Sagot-Lerolle, N. *et al.* Prolonged valproic acid treatment does not reduce the size of latent HIV reservoir. *AIDS* **22**, 1125-1129 (2008).

18 Siliciano, J. D. *et al.* Stability of the latent reservoir for HIV-1 in patients receiving valproic acid. *J Infect Dis* **195**, 833-836 (2007).